Copyright

by

Xiaolei Li

2011

The Dissertation Committee for Xiaolei Li Certifies that this is the approved version of the following dissertation:

Transcriptional mechanisms that produce BK channel-dependent drug tolerance and dependence

Committee:

_____

Nigel S. Atkinson, Supervisor

_____

Richard W. Aldrich

_____

Ophelia Papoulas

_____

Jonathan T. Pierce-Shimomura

_____

Kimberly Raab-Graham

Transcriptional mechanisms that produce BK channel-dependent drug tolerance and dependence

by

Xiaolei Li, B. Med., M. S.

Dissertation

Presented to the Faculty of the Graduate School of

The University of Texas at Austin

in Partial Fulfillment

of the Requirements

for the Degree of

Doctor of Philosophy

The University of Texas at Austin

December, 2011

To my most beloved family

Acknowledgements

I would like to thank my mentor, Dr. Atkinson, and my wonderful committee members and wish to thank for their patience, suggestions and encouragement.

I want to thank the current and former members in the lab: Yan, Harish, Alfredo, Yazan, Rosie, Moon, Linda, Rudi, Jascha, Ben and Brooks. I also own thanks to Franky, Maiah, Mona, Ankur, Dorah, Nirja and Joey. They gave me much support and made the lab a fun place to be.

Transcriptional mechanisms that produce BK channel-dependent drug tolerance and dependence

Xiaolei Li, Ph.D.

The University of Texas at Austin, 2011

Supervisor: Nigel S. Atkinson

Tolerance to anesthetic drugs is mediated partially by homeostatic mechanisms that attempt to restore normal neural excitability. The BK-type Ca^{2+}-activated K^+ channel, encoded by the *slo* gene, plays an important role in this neural adaptation. In Drosophila, a single sedative dose of the organic solvent anesthetic benzyl alcohol induces dynamic spatiotemporal changes in histone H4 acetylation across the *slo* regulatory region and leads to *slo* induction and tolerance. Mutations ablating the expression of *slo* also block the acquisition of tolerance, whereas activating the expression of a *slo* transgene results in resistance to drug sedation. Moreover, artificially inducing histone acetylation with the histone deacetylase inhibitor causes similar acetylation changes, *slo* induction, and functional tolerance to the drug. Histone acetylation changes occur over two highly conserved non-coding DNA elements, 6b and 55b, of the *slo* control region. To investigate the function of these two elements, I generated individual knockout mutants by gene targeting. Both knockout alleles are backcrossed into the CS wild type background. The 6b element seems to repress *slo* induction after drug sedation, because the 6b knockout allele overreacts to the drug. Compared to the wild type, 6b knockout allele shows a much greater *slo* message induction after drug sedation, it also displays

stronger enhancements in seizure susceptibility and following frequency. In addition, the 6b deletion causes a persistent tolerance for at least a month, while tolerance only lasts about 10 days in wild type flies. My investigation also indicates that the 55b element limits basal *slo* expression in muscle. Finally, to investigate if the particular histone acetylation spikes are required for drug-induced *slo* induction and tolerance, I tether the histone-modifying enzymes, HDAC or HAT, to the 6b and 55b DNA elements, respectively. I observe that the positioning of an HDAC on these two elements blocks drug-induced *slo* induction and the development of tolerance. Therefore, histone acetylation across *slo* control region is required for the activation of *slo* and the acquisition of tolerance.

List of Figures

Chapter 1: General Introduction

ANESTHETIC TOLERANCE INVOLVES HOMEOSTATIC REGULATION OF NEURONAL ACTIVITY

We use *Drosophila melanogaster* as a model system to study the molecular mechanisms behind tolerance to anesthetic drug-induced sedation. Exposure to a sedating dose of anesthetic drugs, such as ethanol or benzyl alcohol, induces adaptations of the nervous system that modify the behavioral responses to subsequent drug exposures. These adaptations cause the duration of sedation to be significantly reduced, and tolerant animals recover more rapidly from sedation compared to naive animals. This behavior is called rapid tolerance to drug-induced sedation.

Drug tolerance

Drug tolerance refers to the reduction in the effect of a drug caused by prior exposure to the drug[1]. In humans, the acquisition of tolerance to the recreational effects encourages increased drug consumption in order to achieve the same effect that was previously experienced. Thus, tolerance promotes drug abuse and addiction, resulting in serious health and social problems. Anesthetic drugs cause changes in neural excitability, and the animal responds to these changes by adjusting its physiological processes to maintain its internal equilibrium in neural activity. Such homeostatic responses oppose drug effects and are thought to be responsible for drug tolerance, but the same homeostatic mechanisms persist during drug abstinence and lead to a dependence symptoms that is also used for the diagnosis of pharmacological drug dependence[2].

Tolerance is considered to be a key endophenotype of addiction[3], and genetic pathways responsible for tolerance may also underlie the changes leading to addiction. Drug addiction refers to the compulsive consumption of drugs with a loss of control in limiting intake, and it results in enormous problems in multiple areas, including health care, quality of life, economy, worker productivity, education and social security, etc. Compulsive consumption of drugs that leads to addiction is often motivated by severe social and psychological distress in humans[4], however, the great challenge in obtaining a comprehensive animal model that finely mimic human drug-taking behavior becomes an unavoidable barrier in addiction study. Therefore, research on the mechanisms behind tolerance holds the promise of enriching our understanding of drug addiction and could one day lead to an effective therapy.

Based on the timing of acquisition, tolerance can be grouped into three types. Acute tolerance appears during a single drug exposure. In contrast, rapid tolerance is acquired after a single drug exposure. This type of tolerance is usually assayed 24 h after the initial drug exposure. Chronic tolerance occurs in response to multiple or prolonged exposure to a drug.

Tolerance can also be mechanistically divided into metabolic and functional tolerance. Metabolic or pharmacokinetic tolerance is generated by an increase in the rate of drug clearance. In mammals, metabolic tolerance is often associated with the induction of liver enzymes that act to clear the drug[5]. On the other hand, functional or pharmacodynamic tolerance arises from homeostatic alterations at the cellular targets of

the drug that compensate for a drug-induced effect.

Our lab uses the following two drugs, the commonly abused drug ethanol and the volatile anesthetic benzyl alcohol, to study the mechanisms of rapid functional tolerance in Drosophila. Ethanol is one of the most prevalent and also one of the most well characterized substances in understanding the mechanisms of addiction. Although a moderate amount of alcohol is normally harmless, excessive alcohol consumption causes serious health and social problems. In 2005, alcohol caused 90,000 deaths from road traffic injuries, cancer, liver disease, alcohol use disorders, hemorrhagic stroke, arrhythmia and hypertensive disease in the United States[6]. According to a NIAAA report, alcohol related problems cost the US economy $185 billion every year[7].

Benzyl alcohol ($C_6H_5CH_2OH$) is a colorless organic compound with a mild pleasant aromatic odor. Due to its polarity, low vapor pressure and low toxicity, benzyl alcohol is widely applied in industry as a general solvent for paints, inks, lacquer and glues. In health care, this compound has also been used as a local anesthetic[8-10] and a bacteriostatic preservative in intravenous medications[11]. Exposure to high doses of benzyl alcohol causes toxic effects including respiratory failure, vasodilation, hypotension, convulsions, and paralysis in humans[12]. As the primary breakdown product of toluene, one of the most popular abused inhalant, benzyl alcohol elicits similar phenotypic responses as ethanol exposure in Drosophila[13]. Low doses of benzyl alcohol increase locomotor activity, whereas a higher dose of benzyl alcohol causes hyper-activity, followed by sedation within 10 minutes. Benzyl alcohol is well-tolerated by flies and can

be easily administered. It has been shown that flies develop tolerance to benzyl alcohol sedation after a single drug exposure[13]. Rapid tolerance manifests itself as a reduction in the duration of sedation during the second drug exposure. In this study, I use benzyl alcohol as a representative anesthetic solvent to study the neuronal basis of tolerance to drug-induced sedation.

The functional diversity of BK channels

The BK type voltage- and Ca^{2+}- activated K^+ channels (BK or MaxiK channels) have a large unitary conductance of 100-300 pS[14]. BK channels are prominently distributed to the axons and presynaptic terminals and usually co-located with voltage-gated Ca^{2+} channels, and they are also found in cell body and mitochondria[15,16]. The channels are activated by both membrane depolarization and increasing intracellular Ca^{2+} concentration. The opening of channels hyperpolarizes the membrane and inhibits voltage-gated ion channels, including Ca^{2+} channels, thus reducing Ca^{2+} influx.

The BK channel has a complex structure composed of four pore-forming α subunits, each of which contains seven transmembrane segments (S0-S6) and a big intracellular COOH-terminus that contains two regulators of K^+ conductance (RCK) domains[17]. Segments S1-S4 form the voltage sensor, while S5, S6 and their linker amino acids constitute the pore and selectivity filter. The tandem RCK domains of all the tetrameric subunits form a intracellular gating ring which contains four Ca^{2+} binding sites in RCK2 known as the Ca^{2+} bowl[18].

Functionally, BK channels play important roles in shaping action potential and

regulating neuronal excitability[19]. BK channels also affect smooth muscle tone[20,21], neurotransmitter release[22], endocrine secretion and electrical tuning in the inner hair cells[23]. Recently, BK channels have been shown to play a pivotal role in the regulation of responses of animals to anesthetic drugs[13,24].

It has been shown that the variety of alternative promoter activation and alternative splicing of BK channels contributes to their structural and functional diversity in different tissues or cell types. BK channels are encoded by the *slo* (a.k.a *slowpoke*) gene that was originally identified in fruit flies[25,26]. In Drosophila, the *slo* gene has a complex 7 kb transcription regulatory region including five tissue-specific promoters that control BK channel expression in neurons, muscles, embryonic and larval midgut and epithelial-derived tracheal cells[27-30]. In addition, *slo* has at least 14 alternative exons distributed among five alternative splicing sites[31]. Splicing variants of *slo* differ in essential features, such as unit conductance, calcium sensitivity and gating kinetics[32].

The functional diversity of BK channels is further modulated by β subunits, regulation by phosphorylation and alternative splicing. In mammals auxiliary β subunits (β1-4 or KCNMB1-4) regulate BK channel function in various tissues. β1 is the predominant regulatory subunit in smooth muscle specific expression[33] and the β2 subunit is enriched in kidney and pancreas, whereas β3 and β4 subunits are strongly expressed in the testes and brain, respectively[34,35]. In Drosophila, the Slowpoke channel binding protein (Slob) interacts with the carboxy-termianl domain of the BK channel, and has been shown to adjust BK channel activity and modulate synaptic transmission[36,37].

In addition BK channels are subject to regulation by phosphorylation by protein kinases, including protein kinase A (PKA), protein kinase C (PKC), protein kinase G (PKG), Ca^{2+}/calmodulin-activated protein kinase II (CAMKII) and Src tyrosine kinase[38-41]. Coupling of protein kinases and phosphatases to BK channel complexes allows for modulation of BK channels *in vivo*.

BK channels are required for the development of tolerance

BK channels are important anesthetic targets as well as pivotal modulators of behavioral responses to anesthetics. Acute ethanol exposure has been shown to potentiate BK channels in both mammals and *C. elegans*[42,43]. This potentiation is confined to specific cellular compartments and has been observed in neuronal terminals[44]. In contrast, low dose chronic ethanol exposure decreases ethanol potentiation of BK channels and channel density in a rat neuronal explant model system[45].

BK channels have been shown to be involved in the development of tolerance in mammals[24,45]. Recently the induction of neural transcription of the *slo* gene has been linked to the acquisition of tolerance to the anesthetic benzyl alcohol and to ethanol in flies. A single exposure to a sedative dose of the drug induces *slo* transcription, and the animals display tolerance to the subsequent drug exposure. A mutant that eliminates *slo* expression in the nervous system completely blocks the acquisition of functional tolerance to benzyl alcohol and ethanol, while transgenic induction of a neural isoform of *slo* phenocopies tolerance[13,46,47].

Generally speaking, the activation of a K^+ channel is assumed to hyperpolarize

neurons and repress excitability. However, the activity of BK channels has been positively correlated with neural excitability by reducing the refractory period while enhancing the firing rate of neurons[48-52]. The refractory period is the time it takes for the neuron to be ready to fire again. Using electrophysiological methods we have shown that benzyl-alcohol-induced BK expression enhances the following frequency of neurons, thereby increasing seizure susceptibility and neural excitability. This enables the animal to resist subsequent drug sedation[53].

Drug-induced epigenetic modifications regulate BK channel expression

In the nucleus of eukaryotic cells, DNA exists as a highly condensed structure known as chromatin that consists of DNA and packing proteins known as histones. Environmental factors cause changes of the chromatin structure that provide unique control over gene expression through gating access of transcription factors to DNA. By definition epigenetics is "the mechanism for the stable maintenance of gene expression that involves physically 'marking' DNA or its associated proteins"[54]. In other words, epigenetics refers to the structural adaptation of chromosomal regions that alters gene activity[55]. Epigenetic mechanisms are important for normal development and cell differentiation.

The basic unit of chromatin is the nucleosome that consists of a segment of 146 bp of DNA wound around a histone core. Histones are assembled as an octamer of two copies of H2A, H2B, H3 and H4. The structure of chromatin is highly condensed and is regulated by the methylation of DNA at CpG residues and by covalent post-translational

modifications of the amino or carboxy termini of histones that include acetylation, methylation, phosphorylation, ubiquitylation and sumoylation[56]. These modifications cause changes in the chromatin structure and the accessibility of transcription factors and RNA polymerase, thus influencing gene expression.

Most of the histone modifications identified to date are dynamic and potentially reversible, and are modified by specific enzymes that add or remove the modifications from their substrates. For example, histone acetyltransferases (HATs) add acetyl groups to lysine residues of histones, while histone deacetylases (HDACs) remove them. Histone methyltransferases (HMTs) and demethylases (HDMs) regulate the addition and removal of methyl groups.

Histone modifications play an important role in the regulation of transcription, DNA repair, replication and chromosomal condensation[56]. As the most well studied histone modification, histone acetylation occurs in both the nucleus and cytoplasm. The amino termini of histones are more accessible for modification by acetylation, and the well studied acetylation sites include K9, K14 and K18 of histone H3, and K5, K8, K12 and K16 of histone H4. Histone acetylation affects gene expression through two main mechanisms. First, acetylation of lysine residues decreases their positive charge and thus their electrostatic interaction to the negatively charged DNA. It has been shown that the amino terminal tail of H4 (residues 16-25) of one nucleosome interacts with an acidic pocket in a H2A-H2B dimer of the adjacent nucleosome. And neutralizing the positive charges of the H4 amino terminal tail by acetylation would break the interaction and

prevent the cross-linking between adjacent nucleosomes[57]. The physical relaxation of chromatin structure caused by histone acetylation stimulates gene transcription by increasing accessibility to the transcription apparatus. Second, acetylated histones are also attractive to transcription factors that contain the bromodomain, a ~110-amino-acid motif found in many chromatin-associated proteins[58]. For example, TAFII250 has two bromodomains that are capable of recognizing two neighboring acetylated lysines in partially acetylated inactive chromatin. TAFII250 together with its partners, the TATA-binding protein (TBP) and other TAFIIs, recruits other components of the transcriptional machinery to activate gene transcription[59]. Genome-wide acetylation analyses have shown that hyperacetylation in promoter regions are strongly correlated with gene activation, whereas hypoacetylation is correlated with gene repression[60,61]. Histone methylation marks are involved in the activation or repression of gene transcription, and transcriptional elongation[62,63]. For example, methylation of H3K4 is associated with gene activation, whereas H3K9 and H3K27 are associated with repression[64]. Histone phosphorylation is usually associated with activation of gene transcription[65].

Chromatin modifications have been shown to be involved in drug-related behaviors, such as addiction. Cocaine induces various histone modifications, including acetylation, phosphorylation and methylation, at specific gene promoters in the nucleus accumbens[66]. Inhibition of HDACs *in vivo* up-regulates histone acetylation and potentiates the rewarding effects of cocaine[66]. Moreover, CBP (a HAT) deficient mice show reduced histone acetylation and decreased sensitivity to cocaine[67]. The above

evidence suggests that gene specific histone acetylation affects behavioral sensitivity to cocaine.

In Drosophila, the activation of *slo* transcription contributes to the development of tolerance[13]. Moreover, a single sedative exposure of benzyl alcohol causes a dynamic histone H4 acetylation pattern within the transcriptional control region of the *slo* gene. The hyperacetylation changes are detected at neuronal promoters C0 and C1, as well as the evolutionarily conserved DNA elements 6b and 55b. Repression of HDACs with a universal inhibitor (sodium butyrate) causes hyperacetylation at the 6b element, induces *slo* transcription and phenocopies tolerance. Furthermore, the CREB transcription factor is required for all of these drug-induced changes. Activation of a CREB dominant-negative transgene blocks histone acetylation at *slo* promoter regions, induction of *slo* message and tolerance[68,69].

***Drosophila melanogaster* is a good model organism for the study of tolerance**

The fruit fly, *Drosophila melanogaster*, has been extensively used as a model organism for over 100 years since Morgan first worked on them to define the rules of genetics. Drosophila have many advantages as a model system. They are easy to culture and inexpensive to house. The life cycle is short (about two weeks), making it possible to study multiple generations in a few months.

In spite of the simplicity in genetics and anatomy, flies parallel many aspects of biology observed in so called "higher" organisms such as humans. As a well-studied model organism with a long established history, flies have powerful genetic and

molecular tools. The Drosophila genome has been completely sequenced and is well annotated, and mutants in most genes are available in the stock centers[70]. Drosophila and humans show conservation in synaptic vesicle release and recycling, signal transduction and neurotransmission[71,72]. Moreover, Drosophila and human genetics share similarities despite the difference in the genome sizes and quantity of genes. More than half of all Drosophila protein sequences share similarity with those of mammals, and sixty percent of human disease genes have counterparts or homologues in Drosophila[73]. Thus Drosophila has been increasingly used as disease models in drug studies because of its advantages in genetics[74].

Behaviorally fruit flies are capable of exhibiting many complex behaviors as do humans, e.g. circadian rhythm, drug responses, sleep, locomotion, courtship, fighting, aggressive behavior, learning and memory, cooperation and goal-driven behavior[75-78]. Drosophila and mammals also have conserved responses to anesthetics. For example, low doses of ethanol are excitatory and high doses cause incoordination, unresponsiveness and sedation. The volatile anesthetic benzyl alcohol and the abused drug ethanol cause similar responses in Drosophila[13,46].

DISSERTATION OVERVIEW

The overall goal of my work is to enrich the understanding of transcriptional regulation mechanisms involved in the development of rapid functional tolerance to the anesthetic benzyl alcohol in the *Drosophila melanogaster* model system. More specifically the investigation aims to explore the roles of the evolutionarily conserved

DNA elements 6b and 55b present in the promoter of the *slo* gene and their roles in the induction of *slo* expression in response to benzyl alcohol sedation and on the production of tolerance.

Chapter 2 focuses on the characterization of the 6b enhancer. This chapter first shows the generation of a 6b knock-out mutant $slo^{\Delta 6b}$, followed by the time-course analysis of $slo^{\Delta 6b}$ mutant with respect to behavioral tolerance, tissue-specific *slo* expression and histone H4 acetylation. It also covers investigation of other behaviors that have been associated with *slo*, such as seizure susceptibility and circadian rhythmicity.

Chapter 3 is the analysis of 55b enhancer. This chapter describes the generation of a 55b knock-out mutant $slo^{\Delta 55b}$ and the molecular and behavioral analyses of the mutant. The molecular analysis includes the study of the basal and drug-induced *slo* expression in different tissue and drug-induced histone H4 acetylation changes. This chapter also includes an extensive behavioral study of the mutant.

Chapter 4 shows the results of the analysis of the impact of endogenous histone acetylation levels on *slo* transcription and functional tolerance. It starts with the details of the construction of a two-part system in which a histone acetylation modifying protein such as an HDAC or a HAT is tethered to the 6b and 55b elements, respectively. The chapter also shows the effects of this approach on drug sensitivity, functional tolerance and *slo* expression under the influence of either an HDAC or a HAT.

An extensive discussion of the results and detailed descriptions of the methods are

included in the corresponding sections of Chapters 2-4. Finally, Chapter 5 presents a summary of the results of the study and suggestions about further directions.

Chapter 2: The 6b element regulates drug tolerance and withdrawal

INTRODUCTION

Functional tolerance is a reduction in the response to a drug caused by prior drug exposure. Drug tolerance and withdrawal have long been thought to have a common origin in the homeostatic changes that counter the effects of a drug. These changes which produce tolerance to subsequent drug exposure persist after drug clearance to generate withdrawal symptoms–a sign of physiological dependence[79,80]. In Drosophila, sedation with an organic solvent induces functional behavioral tolerance and a dependence phenotype (reduced seizure threshold) that have been shown to be caused by induction of the *slo* BK-type Ca^{2+}-activated K^{+} channel gene[53]. In response to a single sedation with the organic solvent anesthetic, benzyl alcohol, the excitability of the fly nervous system is altered, making the animal resistant to a subsequent benzyl alcohol sedation delivered on the following day. During the second benzyl alcohol exposure, the increased *slo* expression acts as a neural excitant that counters drug sedation. However, after drug clearance, the *slo*-induced increase in neural excitability persists, enhancing the susceptibility for seizures. Mutations that ablate neural *slo* expression block the acquisition of both the tolerance and withdrawal endophenotypes, while activating a *slo* transgene in the nervous system phenocopies tolerance when the flies are exposed to the drug but induces the withdrawal endophenotype in the absence of the drug[13,53].

The role of *slo* in response to organic solvents is highly conserved through

evolution. A single *slo* BK channel gene exists in Drosophila, Caenorhabditis, and mammals. BK channel activity has been shown to be modulated by organic solvents in both *C. elegans* and mammals and the behavioral response of *C. elegans* to ethanol sedation has been genetically linked to the gene[81-83]. The *slo* gene also contributes to the generation of similar neural responses in mammals. MicroRNA-regulated expression of *slo* BK channels have been shown to underlie physiological ethanol tolerance in the rat hypothalamo-neurohypophysial explant system[84]. The strong evolutionary concordance between invertebrates and vertebrates with regards to these responses means that invertebrate genetic model systems can be used to identify the general principles of how nervous systems homeostatically modulate their activity to become tolerant to organic solvent intoxication. Because tolerance and dependence have related origins, a description of the cellular mechanics underlying the production of tolerance is likely to help us understand cellular changes that lead to physiological dependence. Adult Drosophila are ideal for the study of functional tolerance because they do not develop metabolic tolerance to organic solvents (increased rate of clearance)[85].

The Drosophila *slo* gene has a complex 7 kb control region, containing at least five core promoters (transcription-start sites) that mediate developmental- and tissue-specific expression. Benzyl alcohol sedation activates the neural-specific core promoters (so-called Promoters C0 and C1, Fig 2.1) to induce *slo* expression in the nervous system. The identification of control elements that mediate this induction might be difficult because DNA regulatory elements are often small and function only in their native context[86]. To circumvent this obstacle, we used benzyl alcohol-induced changes in

histone acetylation to map the position of DNA elements that have a functional role in benzyl alcohol producing tolerance. The rationale for this approach is that histone acetylation is a common early step in the activation of transcription. Transcription factors acetylate histones to enhance the accessibility of the underlying DNA for protein binding and acetylated histones are also binding sites for bromodomain-containing transcription factors that stimulate transcription[58]. A survey of changes in histone modification can provide a record of recent transcription factor activity and is a reliable way to identify enhancers that regulate gene expression[87]. We have used the spatiotemporal pattern of histone H4 acetylation across the *slo* promoter region to identify a DNA element that is functionally important for the induction of the *slo* gene to benzyl alcohol and the resulting manifestation of benzyl alcohol tolerance and dependence. We focused our attention on DNA sequences underlying a discrete benzyl alcohol-induced histone acetylation spike across the 6b element. This highly conserved ~60mer situated between the two neural promoters was shown to underlie a strong and focused drug-induced histone H4 acetylation peak that coincided with induction of the neural promoters[68] (Fig 2.1). Furthermore, feeding flies the HDAC inhibitor, sodium butyrate, specifically enhanced 6b acetylation, induced *slo* neural expression and phenocopied functional benzyl alcohol tolerance in a *slo*-dependent manner. Here we show that element 6b plays a specific role in limiting the response of the *slo* gene. Removal of the 6b element, by homologous end-outs gene targeting[88], produces a *slo* allele hypermorphic with respect to drug sedation; increasing gene induction to produce functional tolerance that lasts for an inordinately long period of time and which also enhances susceptibility to seizure, a dependence endophenotype.

RESULTS

Removal of the 6b element from the *slo* promoter region.

In order to investigate the function of the 6b element in the regulation of the *slo* gene and in the development of tolerance to drug-induced sedation, mutations that abolish the element were generated through homologous recombination-based ends-out gene targeting (Fig. 2.2). Correct targeting events were verified by Southern blotting analysis (Fig. 2.3), genetic linkage and DNA sequencing. The derived $slo^{w\Delta 6b}$ strain was unable to acquire tolerance to benzyl alcohol (data not shown). However it still carries a 4.5-kb $white^{+}$ gene between the neural promoters C0 and C1 and this may disrupt *slo* transcription by interfering the alternative promoter activation or RNA splicing. Therefore the $white^{+}$ marker gene was removed by cre-lox recombination to obtain the $slo^{\Delta 6b}$ allele that was subsequently backcrossed to the wild type Canton S background for six generations to minimize genetic difference between the mutant and wild type lines. The $slo^{\Delta 6b}$ homozygotes are healthy with no obvious physical abnomalities or deficiencies in growth rate or development (data not shown). Because loxP sequences have not been reported to be transcriptionally active and because two other loxP insertions into the *slo* transcriptional control region had none of the consequences attributed to the $slo^{\Delta 6b}$ allele (data not shown), we ascribe the changes described below to the removal of element 6b.

All of the original seven *slo* mutant alleles are believed to be null mutations, either failing to express protein or producing a protein that fails to assemble into a functional channel[25]. These mutant alleles manifest extremely similar changes in behavior. Without

any sort of pretreatment, null mutations in *slo* moderately impair rather simple behaviors, reducing the rate of walking, the ability to climb, and the capacity for flight. All also display the so-called "sticky-feet" phenotype in which a short stimulation with heat, followed by a return to ambient temperature causes the flies to behave as if their feet are stuck to the surface upon which they stand. In addition, *slo* null mutants have been shown to almost completely lack circadian rhythms and to be unable to acquire behavioral tolerance to sedation by benzyl alcohol[13,25,89]. With regard to all of these behaviors, $slo^{\Delta 6b}$ mutants are behaviorally indistinguishable from wild type animals (Fig. 2.4, 2.12A, B, D).

A single drug sedation induces abnormal long-term tolerance in $slo^{\Delta 6b}$.

At first, the mutant was assayed for resistance to anesthetic benzyl alcohol. Age-matched female flies of CS and $slo^{\Delta 6b}$ were sedated by a single benzyl alcohol exposure. I found that both $slo^{\Delta 6b}$ and CS flies recovered at the same rate (Fig. 2.5), suggesting this mutation did not affect intrinsic sensitivity for sedation with benzyl alcohol. Next, the mutant was subjected to a tolerance time-course assay to investigate if the 6b element is related to the acquisition or the duration of tolerance. The interval between the first drug sedation and the tolerance assay was 1 d, 4 d, 7 d, 14 d, 21 d and 28 d, respectively. As shown in Fig. 2.6, tolerance in CS strain persisted for about 1 week, whereas the $slo^{\Delta 6b}$ still showed strong tolerance even 28 days after the first drug exposure. I did not further extend the tolerance time-course beyond 28 days because after a month, the flies were weak and a large fraction of them could not survive the drug sedation. The prolonged

tolerance is a unique phenotype that has only been detected in *slo*$^{\Delta 6b}$ mutants. The same prolonged tolerance is also observed for ethanol-induced sedation in the 6b mutant (data not shown).

THE SLO$^{\Delta 6B}$ MUTANTS SHOWS AN AMPLIFIED TRANSCRIPTIONAL RESPONSE TO DRUG SEDATION.

Induction of neural *slo* transcription and tolerance are closely connected. I used RT-PCR to quantify the relative abundance of mRNA expressed from the neural promoters before and after benzyl alcohol sedation. In animals that had never been sedated, the mutant displayed the same relative abundance of neural *slo* mRNA as did the wild type (CS) fly (Fig. 2.7A), suggesting the deletion of the 6b element did not affect basal *slo* transcription. However benzyl alcohol sedation caused a 150% transient neural *slo* message induction in *slo*$^{\Delta 6b}$, whereas the induction in CS was only 50-60% (Fig. 2.7B, C). The transcription of *slo* returned to normal in both strains 24 h after sedation (Fig. 2.7D, E).

Prolonged tolerance might be caused by a pulsatile reactivation of the gene that maintains an elevated level of BK channel activity. In mammals a single kainate injection has been shown to cause a chronic behavioral change that involves multiple gene inductions, including a short acute induction and a delayed induction persisted for several weeks[90]. To explore if the chronic tolerance in *slo*$^{\Delta 6b}$ also derives from subsequent *slo* transcriptional inductions, I carried out a time-course analysis that monitored *slo* mRNA abundance in the nervous system from 6 h to 28 d after a single benzyl alcohol sedation

(6 h, 1 d, 4 d, 7 d, 14 d, 21 d and 28 d). However, the time-course analysis did not show evidence of an additional round of *slo* induction. It appears that the abnormal longevity of tolerance is the product of single burst of *slo* expression. (Fig. 2.8).

Quantification of histone H4 acetylation across the *slo* control region.

Histone acetylation at H4 has been connected to *slo* induction and the development of tolerance. The drug induced histone acetylation pattern in $slo^{\Delta 6b}$ was investigated by chromatin immunoprecipitation (ChromIP) assay with anti-H4Ac antibody, and real-time PCR was performed to quantitate the amount of DNA precipitated in the assay. The regions assayed for histone acetylation includes tissue specific promoters (neural promoters C0 and C1, midgut promoters C1b and C1c, and muscle promoter C2), two putative CRE sites and evolutionarily conserved DNA elements 4b, 6b and 55b (Fig. 2.9A). The *Glycerol-3-phosphate dehydrogenase* (*Gpdh*) gene was chosen as the internal control because its transcription and acetylation levels are independent of benzyl alcohol sedation[68].

Histone acetylation was finely focused at neural promoter C0 6 h after sedation (Fig. 2.9B), meanwhile neural *slo* transcription was remarkably induced. However, at this time point drug sedation also caused acetylation spikes across 6b and C1 in CS wild type flies. Therefore the 6b deletion also blocked the hyperacetylation across C1. By 24 h, acetylation level returned to the baseline level and the peak over C0 disappeared (Fig. 2.9C), meanwhile the *slo* transcription returned to normal levels. A no-antibody control was included in each ChromIP assay to confirm the specificity of the antibodies and to

validate the assay. It shows the amount of DNA non-specifically bound to protein G beads (noise). In the assay it is poorly amplified in the real time PCR compared with co-immunoprecipitated samples (signal), indicating that the abundance of DNA in the no-antibody control is either undetectable or negligible.

Sedation caused a greater enhancement in seizure susceptibility in *slo*$^{\Delta 6b}$.

Previously, *slo* induction caused by prior benzyl alcohol sedation and the overexpression of *slo* have been shown to reduce the seizure threshold of flies[53]. The seizure susceptibility assay was performed to investigate the effect of the *slo*$^{\Delta 6b}$ mutation on this response. Seizures are symptoms caused by transient, abnormally excessive electrical activity in the brain. Clinically, seizures have been related to alcohol acute intoxication and withdrawal[91]. In Drosophila, drug-induced *slo* expression is both necessary and sufficient for the enhancement of seizure susceptibility[53]. In the study, the seizure phenotype was triggered by a train of high-frequency electroconvulsive shock at escalating voltages and the seizure phenotype was identified as a high-frequency spontaneous initial discharge followed by a failure period to response and a delayed secondary discharge (Fig. 2.10A). Seizure susceptibility was represented by seizure threshold, which was determined as the lowest voltage that induces the behavior successfully.

The average seizure stimulus voltages in CS and *slo*$^{\Delta 6b}$ was measured before and after BA sedation. In CS flies, the seizure threshold was 34.4 ± 6.3 V before sedation, and 24.4 ± 2.4 V after sedation. Before sedation, the *slo*$^{\Delta 6b}$ flies exhibited an average

seizure threshold of 26.1 ± 4.1 V, while the stimulating voltage dropped to 12.8 ± 1.2 V one day after benzyl alcohol sedation (Fig. 2.10B). The $slo^{\Delta 6b}$ mutant exhibited a significant lower seizure threshold compared with wild type flies before and after benzyl alcohol sedation.

To more clearly illustrate the effect of the mutation on benzyl alcohol-induced change in seizure threshold, the percentage change in seizure threshold was calculated by normalizing the reduction in the seizure threshold voltage by the control voltage. Benzyl alcohol induced a bigger percentage change in the seizure threshold voltage in $slo^{\Delta 6b}$ flies than in the wild type. The CS flies showed a reduction of 29.0 ± 3.2 percent in seizure voltage, whereas the percentage was 51.0 ± 4.2 in $slo^{\Delta 6b}$ (Fig. 2.10C). I also tracked the seizure susceptibility at 7 d and 14 d post benzyl alcohol sedation. No seizure susceptibility difference was detected between the sedated and control flies, or between the wild type and mutant flies (Fig. 2.10D, E).

$slo^{\Delta 6b}$ exhibited a larger increase in the neuronal following frequency after drug exposure.

The following frequency profile of the giant fiber pathway was explored to demonstrate the effect of the 6b element deletion on neural excitability. Flies were given trains of stimuli with a frequency ranging 40 to 220 Hz. As the frequency increases, the interval between two adjacent stimuli reduces. Animals fail to respond to the stimuli when the interval reaches the refractory time. Therefore the magnitude of following frequency shows how fast the neuron can fire. The following frequency with 50%

response rate (FF50) was determined and data were plotted in Fig. 2.11. The average FF50 was increased in both mutant and wild type by 24 h after benzyl alcohol sedation. The induction was approximately 24.4% in CS and 46.8% in the mutant. Again, the $slo^{\Delta 6b}$ mutant displayed a two-fold change in response compared to wild type.

The $slo^{\Delta 6b}$ mutants were more rhythmic than wild type animals.

Circadian patterns of activity and sleep of CS, $slo^{\Delta 6b}$, and slo^{4} flies were compared using recently eclosed flies that were entrained in LD for 3 days before being transferred to DD and monitored for 6 days. The CS wild type showed rhythmic oscillations in both activity and sleep while the slo^{4} loss-of-function mutants were behaviorally arrhythmic (Fig. 2.12A) with regard to both parameters. The overall activity levels of slo^{4} animals were much higher than the wild type. With regard to these measures the $slo^{\Delta 6b}$ mutant closely resembled wild type in terms of general level of activity and the periodicity of circadian oscillations (Fig 2.12B, D). Intriguingly, the $slo^{\Delta 6b}$ strain had a higher index of rhythmicity than even the wild type (Fig. 2.12C).

The *slo* gene has been shown to be under circadian regulation, and its expression is found to cycle along with a *slo* binding protein[89]. It is possible that the increase in the behavioral rhythmicity index, described above, is caused by more robust cycling of *slo* gene expression. To find out if the 6b deletion mutation causes the expression of *slo* to be more regular, I performed a time-course analysis of the circadian pattern of neural *slo* expression for two days under free-running conditions. I assayed neural *slo* mRNA abundance, with RT-PCR, at time points associated with the peak and valleys of *slo*

expression as described in the literature[89]. As shown in Fig. 2.13, both wild type and the mutant exhibited a rather "flat" expressing pattern. No significant difference was detected between the two circadian patterns of expression.

DISCUSSION

This work represents a novel discovery, a cis-acting DNA regulatory element that specifically modulates a complex behavioral response to a drug. The *slo* gene encodes the BK type calcium-activated potassium channel that is expressed in all or most neurons in the central nervous system[28]. In accordance with this broad expression pattern, loss-of-function mutations in slo are behaviorally pleiotropic. These animals are uncoordinated, fly poorly, lack circadian rhythms, exhibit sticky feet paralysis in response to overstimulation, are slightly resistant to seizures and fail to acquire rapid tolerance to sedation with organic solvents such as benzyl alcohol[13,89,92]. The 6b element, which is positioned between the two neural core promoters of the *slo* gene, appears to be specifically involved in the homeostatic regulation of neural expression. While we cannot easily visualize changes in expression in different structures within the brain, the determination by RT-qPCR that $slo^{\Delta 6b}$ homozygotes have the same relative abundance of *slo* neural-specific transcripts and the fact that the mutant animal lacks non-drug related *slo* phenotypes is consistent with the interpretation that the effect of the mutation on basal expression from the gene is minimal. The $slo^{\Delta 6b}$ mutation disrupts only the drug-related phenotypes–seizure threshold and functional tolerance but does not generate any of the other phenotypes caused by loss-of-function mutation in *slo*.

Wild type animals respond to benzyl alcohol sedation with a 24 h increase in the *slo* expression that has been directly linked to the production of functional tolerance to sedation[13]. Functional tolerance, however, outlasts the period of *slo* induction by about 9 days. The $slo^{\Delta 6b}$ mutant over-reacts to drug sedation producing a greater induction of *slo* expression although the duration of induction appears to be unchanged. This overreaction at the molecular level appears to precipitate a rather substantial increase in the behavioral response. The mutation vastly exaggerates the duration of functional tolerance from ~10 days to at least 28 days. Technical limitations prevent us from assaying tolerance after this point therefore, twenty-eight days is the lower limit on the duration of tolerance in the mutant.

While transient drug-induced induction of *slo* must produce channels that outlive the window of increased gene expression, it seems improbable that in 24 h the mutant allele could produce a sufficient superabundance of BK channels to maintain tolerance for at least 28 days. We cannot directly measure the abundance of the BK channel protein because antibodies specific for the Drosophila protein no longer exist and the gene has not yet been epitope tagged. However, the time-course of another *slo* dependent behavior suggests that the increase in channels is short lived.

Previously, it has been shown that the seizure threshold of flies is inversely related to the neural expression of the *slo* BK channel gene[53]. Electroconvulsive stimulation of fly brain, through electrodes placed on the eyes, generates a seizure. This patterned seizure is characterized by an initial electrical seizure, a refractory period

during which the animal is unresponsive to stimulation, and a secondary spontaneous seizure after which the nervous system once again becomes responsive to stimulation. Null mutations in *slo* make the animals seizure resistant while increased gene expression results in seizure sensitization (reduction in the seizure threshold)[53]. The increase in BK channel activity reduces the seizure threshold by shortening the neuronal refractory period. By definition, this response is a withdrawal phenotype since it is precipitated by drug exposure but is apparent after drug clearance. Here we show that there is a clear lack of correspondence between the duration of the reduction in seizure threshold and the duration of functional tolerance. This strongly suggests that a global increase in BK channel density does not persist for the entire 28 d period.

The difference in the time-course of tolerance and the seizure response suggests that tolerance must be produced by a structure in the brain that does not contribute to the seizure phenotype and that in this structure that the dysregulation of $slo^{\Delta 6b}$ allele extends to the duration of expression. In this proposed neural structure, the $slo^{\Delta 6b}$ allele must become persistently active following benzyl alcohol sedation.

The 6b element was identified as a candidate element because it underlaid a drug-induced histone acetylation spike. In wild type, increased histone acetylation persisted over 6b for 24 h after benzyl alcohol sedation. Furthermore, the HDAC inhibitor sodium butyrate induced *slo* expression, phenocopied tolerance, and generated a single acetylation spike over element 6b. This led us to hypothesize that a histone deacetylase was chronically active at 6b and that perhaps the regulation of this deacetylase

contributed to *slo* induction. The response of the $slo^{\Delta 6b}$ mutants to benzyl alcohol sedation suggests that this interpretation is correct. That 6b is a negative regulator of *slo* expression.

We used the drug-induced H4 acetylation profile as a convenient indicator of transcription factor activity. While we do not know which transcription factor, or how many are acting, we know where and when they act. Acetylation in the vicinity of transcriptional promoters is usually associated with an increase in promoter activity[93]. The histone acetylation profile of the $slo^{\Delta 6b}$ mutant suggests that the 6b element differentially regulates the neural-specific core promoters C0 and C1. After sedation, the acetylation over Promoter C0 is augmented while the drug-induced acetylation at C1 is suppressed. Thus in the wild type, we propose that the 6b element limits the activation of core promoter C0 and enhances activation of core promoter C1.

BK channels expressed from the *slo* gene have been shown to underlie a form of ethanol functional tolerance described in the the rat hypothalamic-neurohypophysial explant system[24]. In this system, ethanol potentiates BK channels activity which leads to an increase in firing and a suppression of hormone release. However, chronic ethanol exposure leads to tolerance. Tolerance is produced by the internalization of preexisting channels. Activation of a microRNA (mir9) targeting slo transcripts encoding ethanol sensitive channels shifts expression to the production of ethanol resistant BK channels in both the HNS and medium spiny neurons of rats[84]. In mammalian model systems of slo dependent ethanol tolerance, transcriptional regulation has not been identified as a key

factor, nor has post-transcriptional regulation been identified as important in the Drosophila model of organic solvent tolerance. This may however be a product of the different properties and experimental advantages offered by each model system although it is also possible that different organisms emphasize different regulatory regimens.

This study demonstrates the profound utility of epigenetic histone modifications to map the position of DNA elements that mediate specific regulatory responses. Histone modifications serve as molecular footprints that visualize the action of transcription factors. Such a method preselects for regulatory elements that are of functional importance and narrows the field of elements that must be functionally tested in order to understand how the genome senses and responds to the environment.

The 6b element, as the key part of our working model for drug-responsive *slo* induction, possibly acts as a repressive control element of the *slo* gene. The chromatin within *slo* regulatory sequences has a dynamic structure varying between the active, loose state and an inactive, tight status. Before drug sedation, an HDAC is probably docked in close proximity to the 6b element and inhibits histone acetylation, thus the *slo* regulatory region is in the inactive state and gene expression repressed. When drug sedation activate histone acetylation and turn the chromatin into an active state, *slo* expression is induced.

Examination of the 6b element shows that it contains transcription factor binding site motifs that might account for this mutant phenotype. Within 6b there is an HSE motif that could be recognized by the heat shock regulatory transcription factor (HSF). HSF has been shown to regulate histone acetylation levels in the mammals through its association

HDAC1 and HDAC2[94]. The drug-induced stress may induce transcription factor HSF, which might help to position HDACs at 6b to deacetylate histone and compact chromatin, thus repressing transcription. Deletion of the 6b element might permanently prevent the positioning of regulatory HDACs that are used to limit or terminate homeostatic activation of the slo gene and thereby the mutant over-responds to induction by benzyl alcohol.

Last but not least, $slo^{\Delta 6b}$ demonstrated a more regular rhythmic activity cycle compare with CS wild type. The Drosophila *slo* gene has been shown to be under circadian regulation, as the expression of the gene is found to be cycled along with a *slo* binding protein[89]. In this study, both wild type and the mutant exhibited a rather "flat" expressing pattern, and no significant difference was detected between them. However, the results do not necessarily disprove the causation between the *slo* expression cycle and the rhythmicity enhancement of activity. It is also possible that the enhancement of cell specific *slo* cycling leads to this behavior.

Figure 2.1. Map of the *slo* transcriptional control region and areas showing enhanced histone acetylation after drug sedation. The graph shows the 7-kb control region of *slo* includes five tissue-specific promoters. They are neuronal promoters C0 and C1; midgut promoters C1b and C1c; muscle and tracheal cell promoter C2. The transcriptional start sites are indicated by arrows. Boxes below the line identify exons. lines connecting exons represent their splicing pattern. Black boxes below the line denote the position of non-coding evolutionary-conserved DNA elements. The table shows the time-course of histone H4 hyper-acetylation for 48 h after benzyl alcohol sedation (column H4 Acetylation) for each of the conserved elements and correlates this with increased accumulation of *slo* mRNA in the nervous system (column RNA) and the appearance of functional tolerance (column Tolerance). The number of plusses and arrows corresponds to the histone H4 hyperacetylation level and the relative abundance of *slo* mRNA, respectively. Checks identify when behavioral tolerance can be detected. Behavioral tolerance to benzyl alcohol persists for about 10 days (this study). Data in the table are from Wang et al.[68].

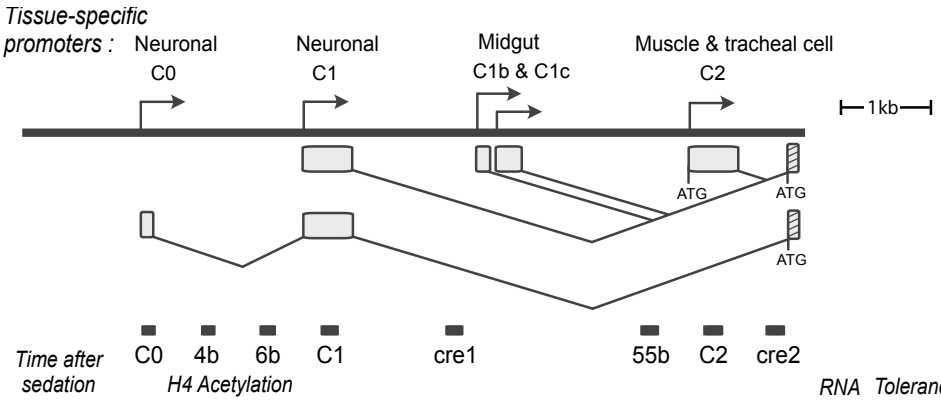

Time after sedation	H4 Acetylation	RNA	Tolerance
4h	++		
6h	+ + ++	↑↑	✓
24h	++	↑	✓
48h			✓

Figure 2.2. Deletion of the 6b element by ends-out gene targeting. A) The targeting scheme. The donor construct contains two pieces of inserts (white boxes) homologous to the flanking sequences of the 6b element (grey boxes). The homologous recombination between the two inserts and their chromosomal counterparts resulted in the replacement of the 6b element by a *white*$^{+}$ gene. A Cre recombinase is used to hop out the *white*$^{+}$ that has lox sites on both ends. In *slo*$^{\Delta 6b}$ allele the 6b element is substituted by a lox site. B) The outline of crossing scheme for 6b targeting. The donor transgenic DNA on the second chromosome is used to target *slo* on the third. Linearized extrachromosomal donor fragment derived from two transgenes: FLP pops out the donor DNA from the second chromosome as a circular fragment; I-*Sce*I restriction enzyme cuts and linearizes the donor fragment.

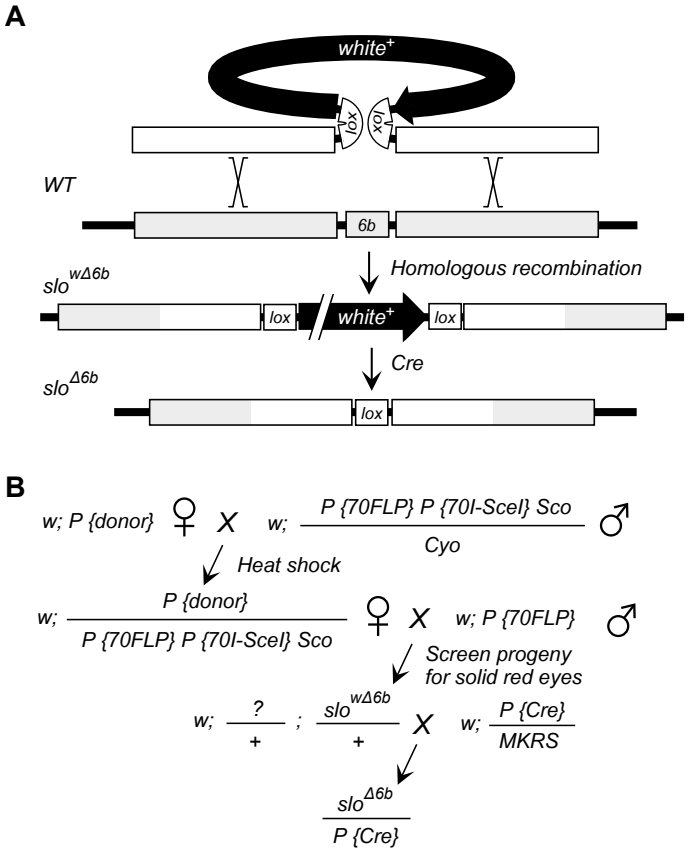

Figure 2.3. Southern blotting analysis of targeting events confirm homologous recombination into the *slo* locus. Panel A shows the Southern blot and panel B shows the corresponding restriction map. The source of the *Bso*BI-disgested genomic DNA is marked above each lane in panel A. WT refers to the w^{1118} recipient line which produces a 8.5 kb band. The $slo^{w\Delta 6b}$ / + heterozygote produces two bands that match the predicted size of 8.5 and 4.7 kb. The $slo^{w\Delta 6b}/slo^{w\Delta 6b}$ homozygotes produce only the 4.7 kb band predicted to be produced by correct targeting of the transgene. $slo^{w\Delta 6b}$ contains a mini-w+ transgene flanked by loxP sites. Removal of mini-w^{+} by Cre-LoxP recombination generated allele $slo^{\Delta 6b}$ in which 6b has been replaced by loxP. $slo^{\Delta 6b}/slo^{\Delta 6b}$ homozygotes produce a *Bso*BI band of 8.5 kb. The DNA fragment used as the probe and he expected fragments from *Bso*BI digestion are indicated in panel B.

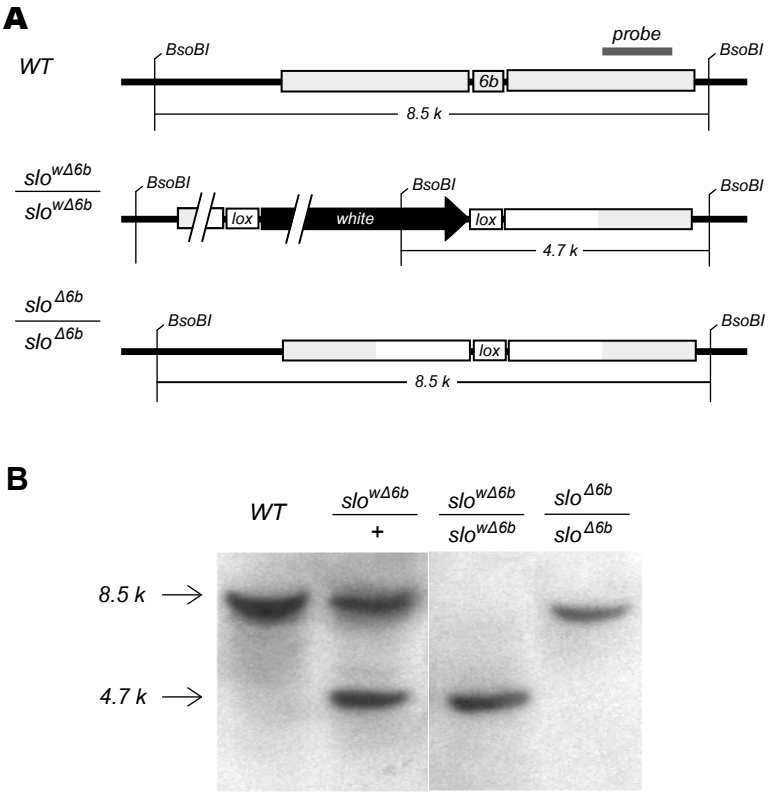

Figure 2.4. The $slo^{\Delta 6b}$ fly showed normal locomotor activities. A) $slo^{\Delta 6b}$ showed normal walking distance in a 10 min free walking test. B) The $slo^{\Delta 6b}$ flies showed normal climbing ability. Flies that climbed beyond 10 cm within 10 sec were considered as passing the climbing assay. Over 95% of CS and $slo^{\Delta 6b}$ flies passed the climbing test, whereas the percentage of slo^{4} stock was only around 30%. C) The 6b deletion did not affect flight capacity. Flies were dropped into a 15 × 62 cm pipette jar through a funnel at the top. The falling flies flew toward the wall and were stuck in the mineral oil pre-coated on the wall. Wild type and $slo^{\Delta 6b}$ animals flew well, and most of them were found within 10 cm to the top. In contrast slo^{4} animals flew poorly and were evenly distributed along the wall. Student's *t*-test and one-way ANOVA with Dunnett's post hoc test, $*P \leq 0.05$; $**P \leq 0.01$. Error bars represent SEM.

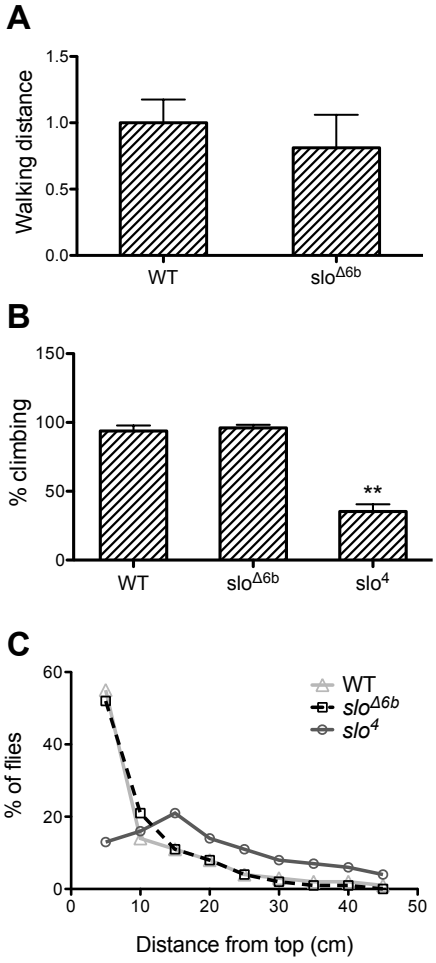

Figure 2.5. The deletion of the 6b element did not affect drug resistance. Recently eclosed female flies were sedated by BA and then transferred to clean vials to recover. The recovery curves were plotted as the percentage of flies that have been returned to climbing from sedation. The difference between recovery curves of wild type fly (black) and *slo*$^{\Delta 6b}$ (grey) are not significant. The *slo*$^{\Delta 6b}$ strain had been backcrossed to CS wild type for six generations. The statistical significance between the two recovery curves was determined by log-rank test. Error bars represent SEM (standard error of the mean).

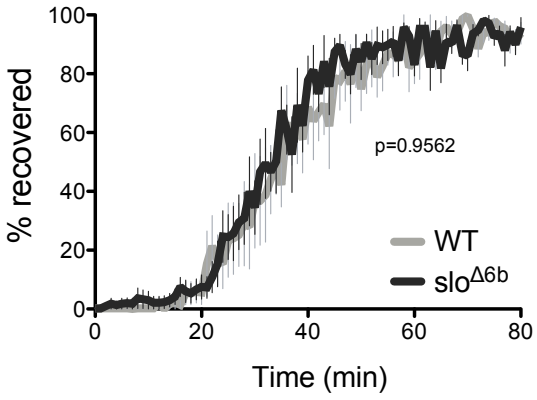

Figure 2.6. Benzyl alcohol caused long-term tolerance in *slo*$^{\Delta 6b}$ flies. The recovery curves describes the percentage of flies that have been recovered from the first sedation (gray) and the second sedation (black). Tolerance lasts for at least 28 d in *slo*$^{\Delta 6b}$, however, it is detected in wild type for only a week. Log-rank test. *$P \leq 0.05$. Error bars represent SEM.

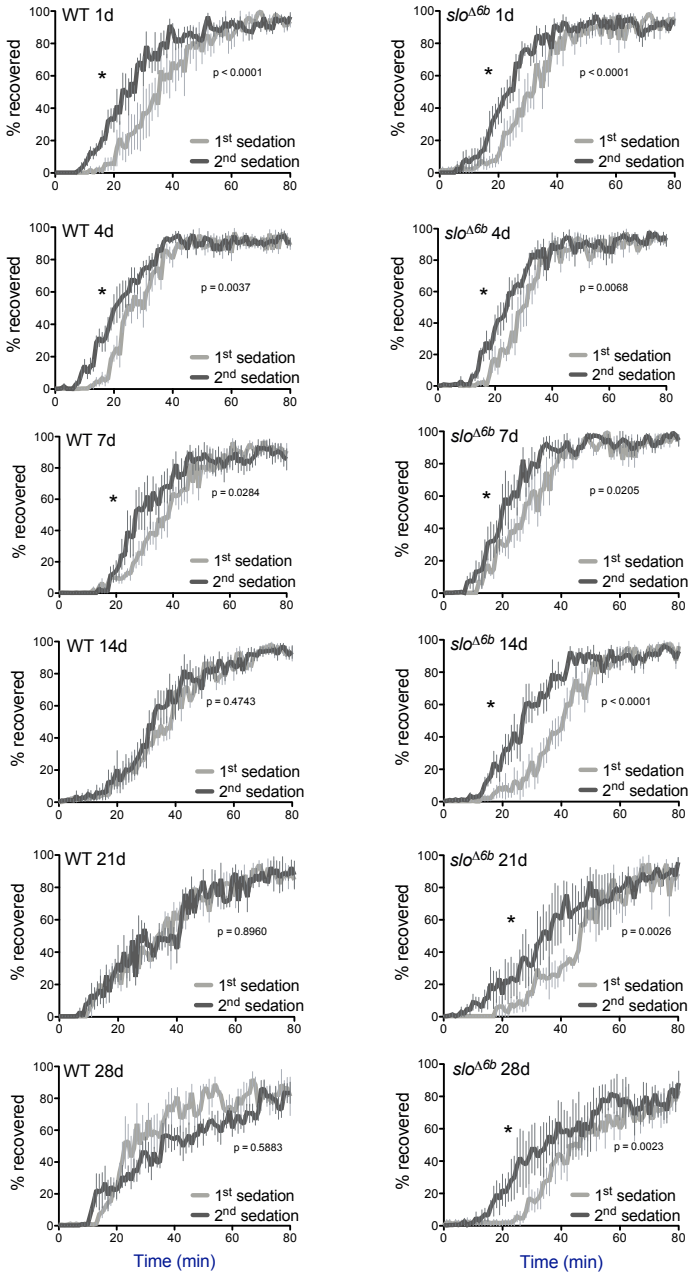

Figure 2.7. The analysis of *slo* transcription in $slo^{\Delta 6b}$ flies. The mRNA levels of *slo* were determined by real-time RT-PCR using primers that only amplify neural *slo* transcripts. A) The 6b ablation did not affect the basal *slo* expression (P = 0.859). B) Benzyl alcohol induced neural *slo* transcription in WT at 6 h after sedation (**P = 0.0012). C) The transcription of *slo* was induced in the mutant 6 h after benzyl alcohol (BA) sedation (***P = 0.0003). D) The *slo* transcription in WT returned to baseline 24h after sedation (P = 0.4689). Unpaired t-test, n = 3. Error bars represent SEM. E) The transcription of *slo* returned to normal in $slo^{\Delta 6b}$ 24h after sedation (P = 0.3041).

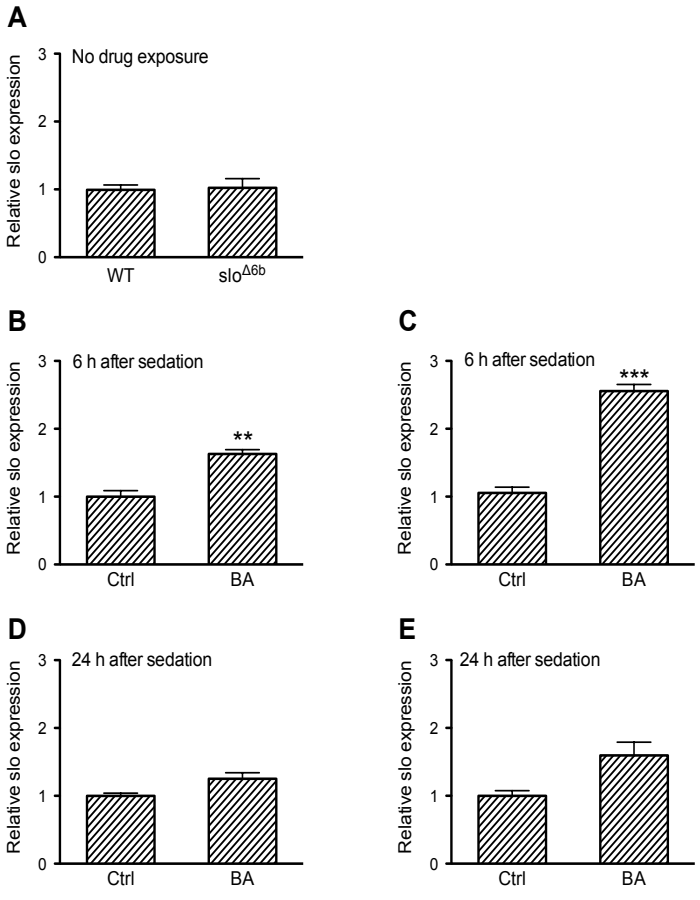

Figure 2.8. The time-course analysis of *slo* transcription in $slo^{\Delta 6b}$. The mRNA levels of *slo* were determined by real-time RT-PCR using C1 primers that only amplify neural *slo* transcripts. Unpaired *t*-test, n = 3-6, **, $P \leq 0.01$. Error bars represent SEM.

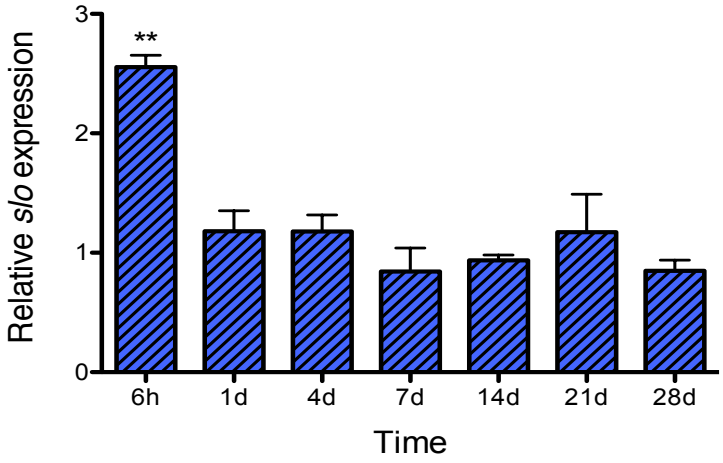

Figure 2.9. Patterns of histone H4 acetylation across *slo* transcriptional control region in $slo^{\Delta 6b}$ after benzyl alcohol sedation. A) Map of the *slo* transcriptional control region and areas assayed in ChromIP. Arrows identify the position of the tissue-specific slo core promoters and open boxes on the line represent exons. The black boxes below the line show the conserved elements tested in the ChromIP assay. In $slo^{\Delta 6b}$ the 6b site was replaced by a loxP element. B) H4 acetylation levels 6 h after BA sedation detected in wild type and $slo^{\Delta 6b}$. The fold change of acetylation was the ratio of the acetylation levels of drug sedated flies over untreated ones. C) Acetylation state surveyed 24 h after BA sedation. One-way ANOVA with Dunnett's comparison post tests, n=3, $*P \leq 0.05$, $**P \leq 0.01$. Error bars represent SEM.

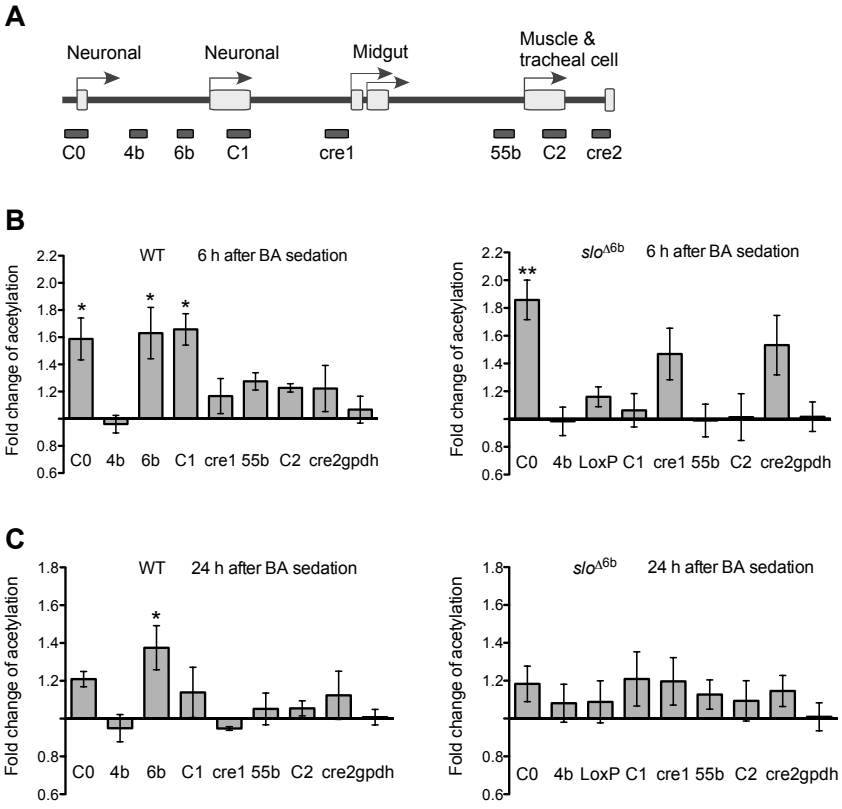

Figure 2.10. Drug sedation caused a much greater transient enhancement of seizure susceptibility in $slo^{\Delta 6b}$. Electroconvulsive stimuli (ES) of varying voltages ranging 5-50 V were utilized to determine the seizure susceptibility, which is represent by the minimum stimulus voltage to trigger seizure. A) The seizure phenotype was identified as a high-frequency spontaneous initial discharge (ID) followed by a failure period to response and a delayed discharge (DD). B) The average stimulus voltages in CS and $slo^{\Delta 6b}$ measured one day after BA sedation. The $slo^{\Delta 6b}$ mutant exhibited a significant lower average stimulus compared with wild type flies. BA sedation reduced stimulus voltage in both stocks. C) The percentage of stimulus voltage reduction in CS and $slo^{\Delta 6b}$. D) The average seizure stimulus voltages of CS and $slo^{\Delta 6b}$ 7 d after sedation. E) The average seizure stimulus voltages 14 d after sedation. Student's *t*-test, $*P \leq 0.05$; $**P \leq 0.01$. Error bars represent SEM.

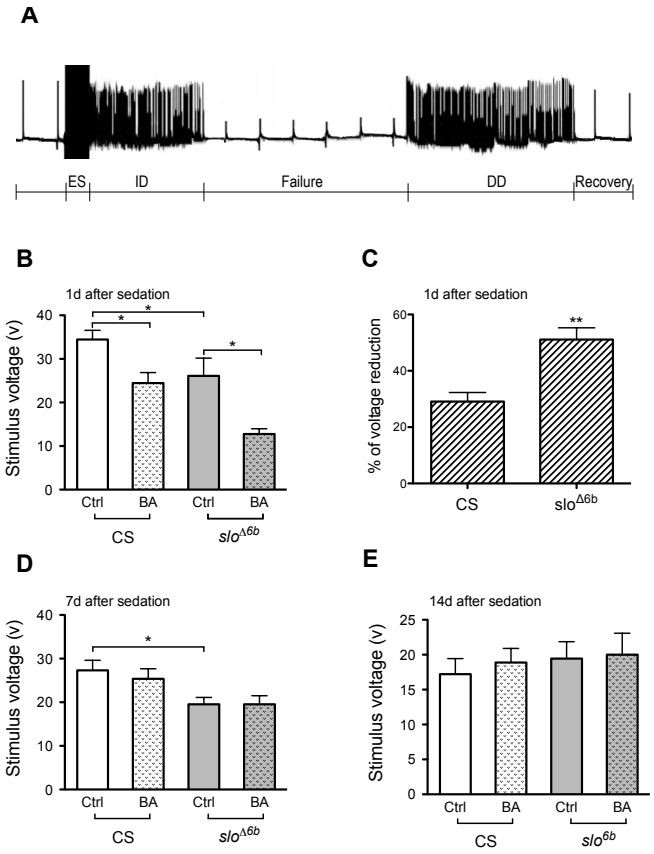

Figure 2.11. Following frequency analysis of CS and *slo*$^{\Delta 6b}$ stocks. The following frequency (FF) of the giant fiber pathway was determined using stimuli sets consisting of three trains of 10 suprathreshold pulses (5 V over the short-latency threshold) at 40-220 Hz. A) Representative traces of short-latency recordings from the flight muscle DLM after 100 Hz and 160 Hz stimuli. B) The average FF50 was induced by BA sedation in both strains. C) The mutant showed a bigger drug-induced FF50 enhancement. Student's *t*-test, $*P \leq 0.05$; $**P \leq 0.01$. Error bars represent SEM.

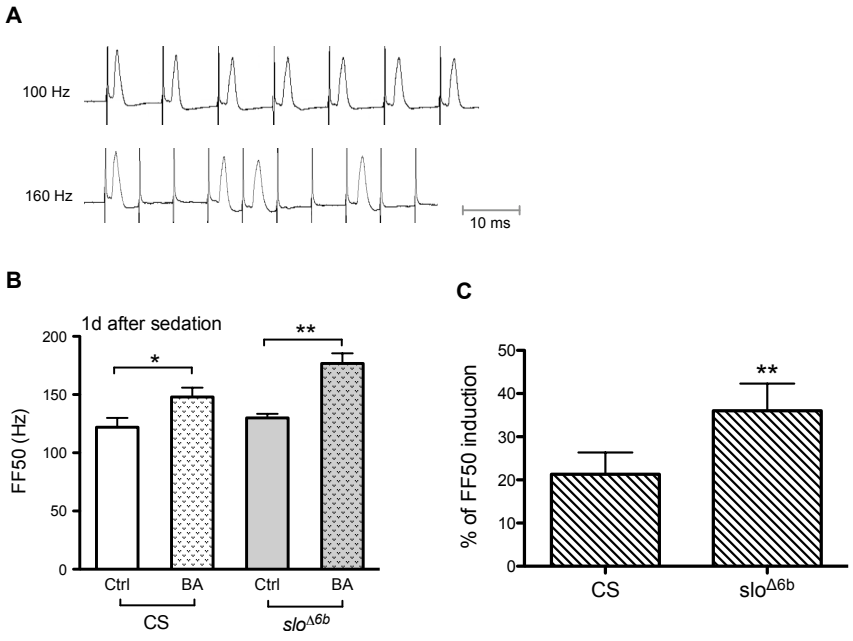

Figure 2.12. Rhythmicity of the $slo^{\Delta 6b}$ allele was strengthened. A) Rhythmic activity of CS, $slo^{\Delta 6b}$ and slo^{4} flies. Recently eclosed flies were entrained in LD for 3 days before being transferred to DD and monitored for 6 days. Both CS and $slo^{\Delta 6b}$ flies demonstrated rhythmic oscillation in activity and sleep. The $slo^{\Delta 6b}$ mutant demonstrated higher peak activity compared to CS. However the loss-of-function mutant of slo^{4} was behaviorally arrhythmic. B) The $slo^{\Delta 6b}$ strain displayed similar average daily activity as CS, however, the loss-of-function mutant slo^{4} showed enhanced activity. C) The percentage of flies that were identified as rhythmic. D)The $slo^{\Delta 6b}$ mutation did not affected the length of period. Student's *t*-test and one-way ANOVA with Dunnett's post hoc test, $*P \leq 0.05$; $**P \leq 0.01$. Error bars represent SEM.

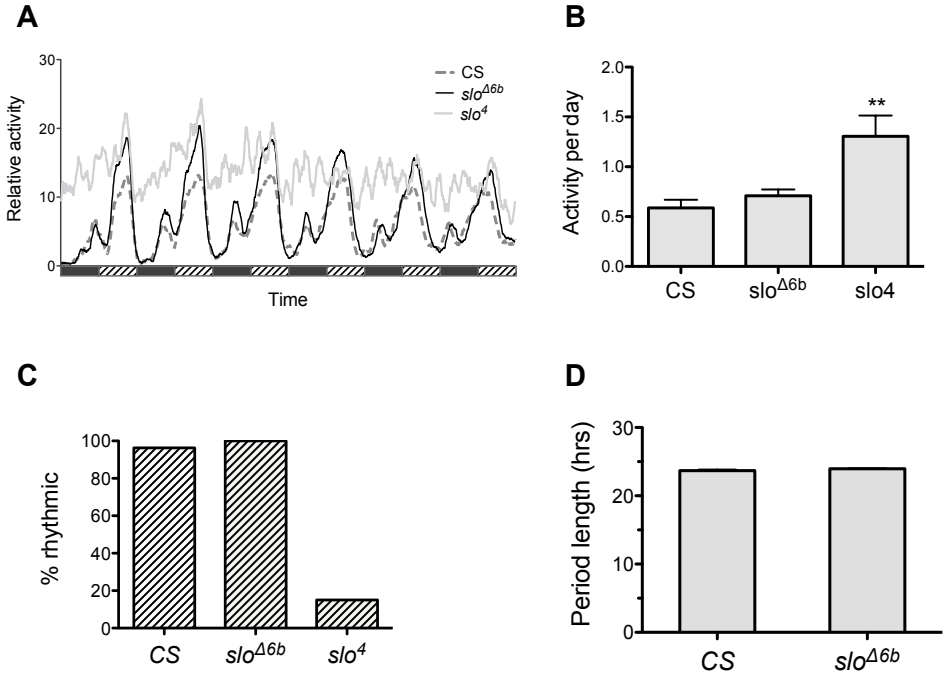

Figure 2.13. Cycling of neural *slo* message in $slo^{\Delta 6b}$ and CS. The graph shows the circadian pattern of relative neural *slo* expression within two days under free-running conditions. These time points have been shown to be associated with highest or lowest neural transcription of slo^{89}. Relative *slo* mRNA abundance of CS (blue) and $slo^{\Delta 6b}$ (red) was determined by RT-real time PCR and was plotted as mean ± SEM. Statistic significance was determined by two-way repeated measures ANOVA, n = 3.

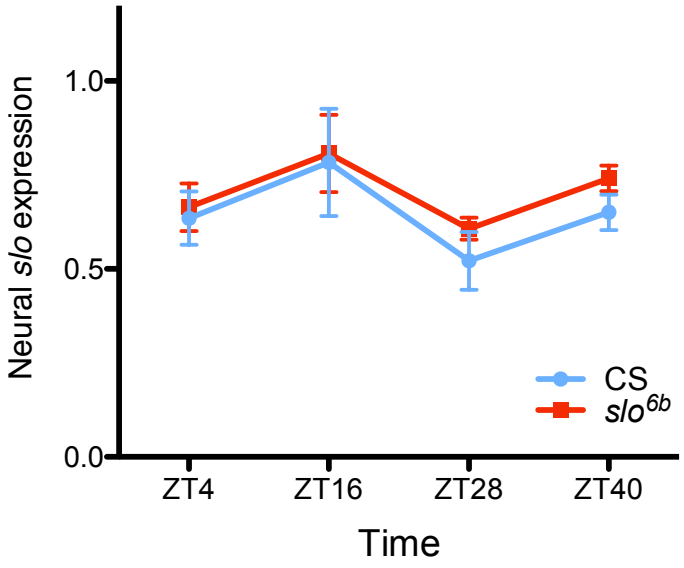

METHODS

Fly stocks

Drosophila stocks were Canton S (wild type), $slo^{\Delta 6b}$ and slo^{4}. Flies were raised on standard cornmeal medium in a 12/12 light/dark cycle at 22°C. Newly eclosed flies collected during a 2 d time period were studied 4-5 days after eclosion.

Ends-out gene targeting of the 6b element

The 6b deletion construct

The two flanking DNA fragments of the *slo* 6b element were amplified by PCR with Canton S genomic DNA template and proofreading *PfuTurbo* DNA polymerase (Stratagene CA) and inserted into the ends-out vector pW25[95]. Primers 5'-GCGGCCGCGAGGGATGCTGCTGCTTTAC-3' and 5'-GCGGCCGCATTCTCGCCG TTTTTAAATTCTCAG-3' were used in the PCR to amplify and add *Not*I sites to both ends of a 3.26-kb DNA fragment upstream of the 6b element, while primers 5'-GGCGCGCCTTGACACGCTTGCTTTTCCGGCTA-3' and 5'-GGCGCGCCAAGTT GGCCCAGTTTGTTTG-3' were designed to amplify and add *Asc*I termini to a 3.03-kb DNA fragment downstream of 6b. These two donor fragments were then inserted into the corresponding sites of pW25 with the same orientation. The pW25 vector also contains a $white^{+}$ gene between the two inserts.

Generation of the donor insertion lines

The 6b deletion construct was introduced into white background by standard *P*

element germline transformation. All the insertion lines are mapped for the location of the donor transgene, and lines with the donor transgene on the first or the second chromosome were utilized to induce targeting.

Crosses and heat shocks

The scheme of 6b targeting was shown in Fig. 2.1. To induce targeting, donor insertion lines are crossed to the *P{hsp70FLP}P{hsp70I-SceI}* strain (Bloomington # 6934). The progeny were heat-shocked during the first 3 days of development to induce transgenic FLP and I-SceI . The heat shock was conducted by submerging fly vials into a water bath kept at 38°C for 1 h. Virgin females with donor and *P{hsp70FLP}P{hsp70I-SceI}* are collected and crossed to male FLP flies (Bloomington # 6938), and the progeny are screened for solid red eyes. The *white*$^{+}$ gene was mapped to identify targeting events in which *white*$^{+}$ was relocated to the target chromosome 3. And Southern blotting was carried out to confirm targeting events occurred exactly in the designed position. Finally, the targeted strain was crossed to *P{Cre}* line (Bloomington # 1501) to remove the *white*$^{+}$ maker and obtain the 6b deletion mutant *slo*$^{\Delta 6b}$.

Southern blot analysis

Southern blot analyses were performed to verify the ends-out targeting events using a DIG kit (Roche Diagnostics, IN) as recommended by the manufacturer. Genomic DNA was prepared from targeted allele and wild type, followed by overnight digestion with BsoBI (NEB, MA), agarose gel electrophoresis and nylon membrane transfer as described[96]. The probe DNA in use was a 0.6 kb fragment in the 3' inert prepared by PCR

with primers 5'-GCGACCACAAATCGTCCAAACACA-3' and 5'-TAGCACTGCGAAC TATCGCTGGAA-3'. The blot was hybridized to the digoxigenin (DIG) labeled probe and was detected by DIG antibody and chemiluminescence signal.

Benzyl alcohol exposure

Recently eclosed female flies were distributed into multiple groups of 10. The 30 ml glass vials were coated with 200 µl of 0.4% benzyl alcohol in acetone, followed by constant rotation for 20 min to evaporate the highly volatile acetone and leave a finely distributed thin layer of less volatile benzyl alcohol on the wall. In contrast the vials for controls were coated with acetone only, which was completely evaporated after 20 min. Animals were transferred into the either the benzyl alcohol vials or the control vials until all the flies in the drug vials were completely sedated (usually 5-10 min). After exposure, flies were moved back to food vials for recovery.

Tolerance assay

Tolerance assay was performed as described before with minor modifications [13]. Recently eclosed female flies were divided into 12 groups of 10. In the first exposure, six groups were sedated with 0.4% BA, and the others were mock sedated with acetone. On the day of assay, all groups were sedated with 0.4% BA, and then were transferred to fresh vials to recover. Flies were scored as recovered when they resumed climbing. The whole course of recovery was analyzed by a computer controlled automated movement detection system developed in our lab[97]. The recovery curves were plotted according to the percentage of recovered flies against time. The log-rank test was used to determine

significance between curves. Error bars represent the SEM for each individual data point.

Log-rank test

The log-rank test for equality of survival was used to determine the significant difference between two recovery curves from the tolerance assay. The log-rank test, also named the Mantel-Cox test, is a nonparametic hypothesis test to compare the survival distributions of two groups at each observed event time. The analysis bases on the times of events. For each observed event time point, the expected number of events were calculated based on the observed number of events given there is no difference between the two recovery curves, and then were added up to obtain the overall number of estimated events. The statistic of log-rank test is the sum of $(O-E)^2/E$ for each group, where O and E represent the total number of the observed and expected events, respectively. The test statistic was compare with a χ^2 distribution with 1 degree of freedom to obtain the significance[98,99].

Chromatin immunoprecipitation assay

About 1,500 *slo*$^{\Delta 6b}$ flies were either benzyl alcohol sedated or mock sedated for 6-8 minutes and were allowed to recover in a drug free environment. Six and twenty-four hours after sedation, flies were frozen in liquid nitrogen, and fly heads were harvested by vortex decapitation and sieving. Heads were cross-linked with 2% formaldehyde for 3 min and chromatin was solubilized and sonicated on ice by 5 sections of 25 s sonication bursts to produce fragments of ~600 bp using a sonic Dismembrator 250 (Fisher

Scientific).

The chromatin immunoprecipitation (ChromIP) assays were performed as described[68]. The polyclonal antibodies against acetylated histone H4 at K5, K8, K12 and K16 (Upstate Biotechnology catalog # 06-866) was used to precipitate DNA. Chromatin immunoprecipitation assays were performed more than three times with independent chromatin samples.

Real time PCR analysis

Real time PCR was performed using the ABI SYBR Green PCR Master Mix. Primers were designed to amplify 100~200 bp fragments at specific regions of the *slo* transcriptional control region, including the two neural promoters (C0, C1), muscle promoter (C2) and five evolutionarily-conserved areas (4b, 6b, cre1, 55b, cre2). Genes *Gpdh* and *Cyp1* were used as internal controls because neither of their expression was affected by benzyl alcohol sedation[68]. Primers are: C0 (5'-ATCGAACGAAGCGTC CAG-3', 5'-CGACGCGCTCAAACG-3'); 4b (5'-GACCCGATGATAAAGTCGATGT-3', 5'-GCCAGTGACTGACTGACACACA-3'); 6b (5'-CCAGCAGCAATTGTGAGAAA-3', 5'-CGAAGCAGACTTGAAAGCAA-3'); lox (5'-AAACGGCGAGAATGCGGC-3', 5'-TCAAGGCGCGCCCTAGACT-3'); C1 (5'-ACAAACCAAAACGCACAATG-3', 5'-AATGGATGAAGGACTGGGAGT-3'); cre1 (5'-GATGGGAAAGCGAAAAGACAT-3', 5'-CATGTCCGTCAAAGCGAAAC-3'); 55b (5'-TACCCAATTGAATTCGCCTTGTCT T-3', 5'-CCCACTCTCCGGCCATCTCT-3'); C2 (5'-GCACTCGACTGCACTTGAAC-3', 5'-AATGAAAAAGTTCTCTCTGTGCAT-3'); cre2 (5'-TGGATTGCGACCGAGTGTCT

-3', 5'-ATCAATACGATAACTGGCGGAAACA-3'); *Gpdh* (5'-GCATACCTTGATCTT GGCCGT-3',5'-GCCCTGAAAAGTGCAAGAAG-3'); *Cyp1* (5'-TCTGCGTATGTGTG GCTCAT-3', 5'-TACAGAACTCGC GCATTCAC-3').

Real time PCR amplifications were run in duplicate, and the dissociation/melting curves were used to detect nonspecific amplifications. The relative amount of the DNA precipitated by the H4Ac antibody was determined by ΔΔCt method. Fold enrichment of H4 acetylation of drug-sedated group equals $2^{(\Delta Ct_{ctrl} - \Delta Ct_{BA})}$, where $\Delta Ct = Ct_{IP} - Ct_{Input}$. The entire protocol has been repeated at least three times and the mean and SEM were calculated. Statistical significance was determined by the one-way ANOVA test.

Quantitative RT-PCR analysis

RNA was extracted from heads as described[13]. Reverse transcription and real time PCR were performed in triplicate with *slo* exon C1, C2 and *Cyclophilin 1* (*Cyp1*) primers[47]. Relative RNA quantity was calculated using the standard curve method (Applied Biosystems manual). Significance was calculated using the Student's *t* test.

The primers used are shown as follows: *slo* exon C1 forward primer 5'-AAACAAAGCTAAATAAGTTGTGAAAGGA-3'; *slo* exon C1 reverse primer 5'-GATAGTTGTTCGTTCTTTTGAATTTGA-3'; *Cyp1* forward primer 5'-ACCAACCAC AACGGCACTG-3; *Cyp1* reverse primer 5'-TGCTTCAGCTCGAAGTTCTCATC-3'.

RNA time-course

To survey the cycling of *slo*, Newly eclosed CS and $slo^{\Delta 6b}$ flies were entrained for

5d in a 12/12 light/dark cycle at 22°C. Animals were collected and immediately frozen in liquid nitrogen at the following Zeitgeber time: ZT4, ZT16, ZT28 and ZT40. These time points have been shown to be associated with highest or lowest neural transcription of *slo*[89]. RNA was purified from fly heads and the relative amount was determined by quantitative real-time RT PCR.

Climbing assay

The climbing assay was conducted as described to measure relative activity of flies[100]. Three groups of 12 flies each were placed in a 20 × 150 mm glass test tube, and gently tapped to the bottom. The number of flies that climbed beyond 10 cm within 10 sec was counted. The experiment was repeated three times. Statistical significance between percentages of flies passed the test was calculated using the Student's *t* test.

Flight assay

The flight capacity of animals was determined with minor modifications as described[101]. Approximately 500 flies were dumped into a 15 × 62 cm pipette jar through a funnel at the top. The falling flies flew toward the wall and were stuck in the mineral oil pre-coated on the wall. The position of each fly was marked and its distance from the top was measured. Flies with good flight capacity clustered near the top of the jar, where flies flew poorly stayed close to the bottom.

Sticky-feet behavioral assay

The sticky-feet behavioral test was performed as described with minor

modifications[101]. Flies of 4-5 days old were heat-shocked in a glass vial incubated at 37°C for 7 min. After that, animals were gently transferred to the benchtop and left undisturbed for about 10 sec. And a flat toothpick was used to poke flies on the side. The sticky-feet phenotype is identified when a fly hold onto the surface instead of flying/moving away.

Circadian rhythm analysis

Flies were raised in a rhythmic 12:12 light:dark cycle. Male flies (aged 4-6) were individually loaded, without anesthesia, into 5 mm × 65 mm glass tubes with 5% sucrose 2% agar food at one end. These tubes were then loaded into DAM2 *Drosophila* Activity Monitors (Trikinetics, Waltham MA) that have infrared beams that detect when a fly crosses the middle of the tube. The monitors are then placed into an incubator kept at 24°C. At the end of the light cycle after the flies are placed into the incubator, the lights are permanently turned off to observe free-running rhythms. Flies were monitored in 5-min bins for 14 days. At the end of this time period, any fly that did not move for any 24-hour period in the first ten days was discarded from analysis. Circadian analysis was analyzed using a Matlab software[102]. Only the first week of activity was analyzed. Plots showing movement over time are created by averaging movement from flies from each genotype. Period and rhythm indices are generated by the autocorrelation component of the software. Sleep bouts were assumed to be when a fly did not cross the beam for five minutes.

Electrophysiology analysis

An adult female fly was fixed on wax mount on a stereoscope stage. Tungsten

wire electrodes (FHC Inc) sharpened to approximately 5-µm diameter were inserted in the fly using micromanipulators (Narishige). Two 200-µm diameter insulated tungsten wire electrodes was inserted through each of the compound eyes. A 75-µm diameter recording electrode was pierced through the dorsal cuticle into the upper DLM. A 200-µm diameter reference electrode was placed on the abdomen. Stimuli were generated using a S48 square pulse stimulator, isolated with a SIU5 Stimulus Isolation Unit (Grass-Telefactor). Responses from the DLM muscles were amplified with a Microelectrode Amplifier Model 1800 (A-M Systems), digitized by a DigiData 1200 (Axon instruments) and recorded in a PC using FETCHEX, pCLAMP 6 software (Axon instruments).

Seizure susceptibility measurement

Seizure threshold was measured utilizing the giant fiber (GF) pathway as described[53]. A 1.5-s long 200 Hz ECS pulse of various voltage was used to trigger seizure in the animal. A seizure was recognized as a high frequency initial discharge, followed by a prolonged failure period and a delayed secondary pulse. The minimum voltage of stimulation to trigger seizure was determined as seizure voltage threshold of the fly.

Determination of neuronal following frequency

The following frequency of the giant fiber pathway was determined as described[53]. To determine the threshold of giant fiber pathway, a fly received single 0.1-µs pulses of increasing voltage at 5-s intervals to induce DLM response. Then the latency to the responses after the stimulation was measured. The voltage amplitude of the stimuli was increased until a response with a constant short latency of 1.4 ms was detected. The

following frequency was determined using stimuli sets consisting of three trains of 10 suprathreshold pulses (5 V over the short-latency threshold) at 40-220 Hz. Flies were allowed to rest for 5 s between each stimulus train and 15 s between each train set to protect animals from exhaustion. The number of responses detected in the muscle were plotted against frequency to generate a frequency-response curve. Statistical significance was determined by two-way repeated measures ANOVA.

Chapter 3: 55b regulates muscle-specific *slo* expression

INTRODUCTION

The *slo* gene encodes the BK-type voltage- and Ca^{2+}-activated K^+ channel that plays important roles in shaping action potential and regulating neuronal excitability, in regulating firing pattern and synaptic transmission, and in the control of smooth muscle tone[19-22]. Recently *slo* has been implicated in the homeostatic response after anesthetic drug sedation that enhances the activity of the nervous system to balance out drug effects and thus lead to the development of functional tolerance (reduced responsiveness to an effect of a drug caused by prior drug exposure). However, after drug clearance, the same enhancement in BK channel activity persists, thus producing withdrawal symptoms, including enhanced seizure susceptibility[53]. Flies are ideal for the study of functional tolerance as they do not develop metabolic tolerance to organic solvents (increased rate of clearance)[53,85]. We have shown that the upregulation in neural *slo* expression is both necessary and sufficient for the development of drug-induced tolerance in Drosophila[13,46]. The *slo* gene and its role in the response to anesthetic solvents are highly conserved between flies and other eukaryotes, such as *C. elegans* and mammals[81-83]. For example, microRNA-regulated expression of *slo* BK channels has been shown to underlie physiological ethanol tolerance in the rat hypothalamo-neurohypophysial explant system[84].

The Drosophila *slo* gene is regulated by alternative promoter activation and alternative RNA splicing, which altogether, allow cells to customize BK channels with

fine-turned conductance and calcium sensitivity to meet their particular needs. The *slo* gene has a complex 7 kb transcriptional control region, containing at least five promoters that mediate developmental and tissue-specific expression. It also contains 14 alternative exons distributed among five alternative splicing sites[27,29-31,103].

The DNA elements 6b and 55b are short evolutionarily conserved DNA elements of *slo* identified by sequence homology analysis among multiple Drosophila species[27,103]. A single anesthetic benzyl alcohol sedation has been shown to induce dynamic spatiotemporal changes of histone H4 acetylation across the *slo* transcriptional control region. The earliest histone acetylation peak is identified over the 55b element 4 hr after drug exposure. Six hours after sedation, the 6b element and the two neural promoters (C0 and C1) are associated with enhanced histone acetylation. This correlates with induction of neural *slo* message and behavioral tolerance. By 24 hr, enhanced acetylation is only observed at the 6b element. By 48 hr, both histone acetylation level and *slo* message abundance have returned to baseline. In addition, administration of a universal HDAC inhibitor sodium butyrate causes hyperacetylation across the *slo* control region, induces *slo* transcription and phenocopies tolerance[68]. Histone acetylation is a common early step in gene activation and plays an important role in drug addiction[104,105]. These data suggest the potential role of the 55b element as a key element that initiates the activation of the *slo* gene after drug sedation.

RESULTS

Generation of the 55b deletion mutant

To address the *in vivo* role of 55b, we created a knockout mutant of this DNA element by homologous recombination based ends-out gene targeting[106]. In brief, the 55b element was substituted by a mini-*white*$^{+}$ marker from a donor transgene through homologous recombination to obtain the *slo*$^{w\Delta 55b}$ allele. To verify targeting events, Southern blot analysis was performed using a DIG labeled probe specifically recognizing the 3 kb upstream DNA sequence of 55b. As shown in Fig. 3.1, DNA from wild type (lane 1) showed a 5.6 kb fragment; while DNA from *slo*$^{w\Delta 55b}$ homozygotes (lane 2-5) exhibited a 4.3 kb band. The mini-*white*$^{+}$ marker gene was later excised through Cre/lox recombination to eliminate the transcriptional effects of the transgene, and the derived *slo*$^{\Delta 55b}$ allele was backcrossed to wild type (CS) flies for six generations for a more isogenic background. The *slo*$^{\Delta 55b}$ homozygotes are healthy animals showing normal growth rate and development.

slo$^{\Delta 55b}$ did not affect drug-induced epigenetic responses.

The 55b element has the earliest benzyl alcohol-induced histone H4 acetylation peak[68]. We hypothesized that the *cis*-acting element 55b is an important regulator of the *slo* gene, probably by acting as the initiator of drug-induced histone acetylation modifications across the *slo* regulatory region. If this hypothesis is correct, then loss of 55b should prevent *slo* induction, the post-sedation histone acetylation pattern associated

with drug induction of *slo*, and the production of behavioral tolerance. The abundance of *slo* message in $slo^{\Delta 55b}$ flies was quantified by real-time RT-PCR using primers specifically recognizing all the neural splicing variants. In contrast to our expectation, we found that the 55b deletion did not affect the magnitude and time-course of neural *slo* induction after drug sedation nor did it affect the basal level of neural *slo* expression. Furthermore, in both the mutant and wild type lines, the induction of *slo* transcription had a normal time-course. Induction was detected 6 h after drug sedation and had disappeared by 24 h post sedation (Fig. 3.2).

To investigate if 55b is responsible for the subsequent acetylation changes of the *slo* transcriptional control region, ChromIP was performed in $slo^{\Delta 55b}$ using an antibody specific for histone H4 acetylation to separate chromsosomal fragments with H4 histone highly acetylated, and real-time qPCR was utilized to quantitate those fragments. In the wild type, we detected enhanced histone acetylation at neural promoter C1, the DNA elements 6b and 55b four hours after benzyl alcohol sedation, while promoter C0 showed mildly increased acetylation (not significant). In the $slo^{\Delta 55b}$ mutant hyperacetylation was found at C0, C1 and 6b at 4 h post sedation. By 6 h, acetylation peaks were found at C0, 6b and C1 in both the wild type and the mutant. By 24 h, only the 6b element showed a significant histone acetylation spike in the wild type, whereas in mutant histone acetylation levels had returned to the baseline level (Fig. 3.3). Based on these data, it seems that the 55b element is not required for subsequent drug-induced histone acetylation across the *slo* promoter region. These data indicates that the 55b element is

not a trigger for the later histone modifications.

$slo^{\Delta 55b}$ did not affect drug-induced tolerance and withdrawal phenotype.

Induction of a neural-specific *slo* splice variant has been shown to produce resistance to benzyl alcohol and ethanol[13,47], suggesting that the expression of *slo* in the nervous system is essential for drug resistance. Our lab has also shown that the increased expression of *slo* leads to the reduction of the neural refractory rate and the enhancement of seizure susceptibility that are believed to lead to withdrawal symptoms[53]. However, it is possible that drug resistance and tolerance are controlled by specific brain region and the 55b mutation could only affect the small subset of neurons that regulate these behaviors. Therefore, the mutant was subjected to different drug-related behavior tests. Here resistance and tolerance describe different drug phenotypes. The former demonstrates the baseline magnitude of drug responsiveness that affects drug consumption and contributes to drug addiction[107], while tolerance is believed to be a homeostatic response of the nervous system that enhances neuronal activity to counteract the sedative effect of the drug[13].

At first, the mutant was assayed for resistance to anesthetic benzyl alcohol. Age-matched female flies of CS and $slo^{\Delta 55b}$ were exposed to a sedating dose of benzyl alcohol for the first time. These animals became hyperactive, uncoordinated and eventually sedated. Then animals were allowed to recover in a drug-free environment, and the rate of recovery was used as an indicator of drug resistance. Both the mutant and wild type flies recovered at the same rate, suggesting the $slo^{\Delta 55b}$ mutation did not affect resistance to

benzyl alcohol (Fig. 3.4). Next, the mutant was assayed for the capacity to acquire tolerance. Age-matched CS and $slo^{\Delta 55b}$ flies (4 days post-eclosion) were sedated with benzyl alcohol, allowed to recover and then stored on food for 1 d, 7 d and 14 d before being tested for the functional tolerance. To test for functional tolerance, the flies were then sedated a second time and their period of sedation measured. Stocks were recognized to be capable of acquiring tolerance if they recovered more rapidly from the second sedation than from the first sedation. As shown in Fig. 3.5, $slo^{\Delta 55b}$ acquired tolerance to benzyl alcohol (left shifted recover curve), and tolerance in the mutant lasted for 7 days, as in the wild type. These results suggest 55b does not affect the acquisition or the duration of tolerance to benzyl alcohol sedation.

Resistance and tolerance describe different drug phenotypes. The former demonstrates the baseline magnitude of drug responsiveness, while tolerance indicates the drug-induced reduction in responsiveness. Resistance to the sedating/intoxicating effects of anesthetic drugs affects drug consumption and contributes to drug addiction[107]. Induction of a neural-specific *slo* splice variant has been shown to produce resistance to benzyl alcohol and ethanol[13,47], suggesting that the expression of *slo* in the nervous system is essential for drug resistance. Ablation of the 55b element did not affect resistance to benzyl alcohol or change the basal neural *slo* expression.

Drug-induced *slo* expression acts as a neural excitant that accelerates neural excitability to counter the sedative effects of the anesthetic. However, after drug clearance, the *slo*-induced increase in excitability persites to generate withdrawal-related

behavioral changes. These include increased capacity for repetitive neuronal firing and enhanced seizure susceptibility[53]. Here we looked at these drug withdrawal-related phenotypes utilizing the giant fiber (GF) preparation. To investigate whether the mutation alters drug-induced effects on the refractory period of the giant fiber pathway, we measured the giant fiber following frequency. Trains of stimuli at various frequencies ranging from 40 to 220 Hz were delivered to the brain and responses in the flight muscle were recorded. The giant fiber circuit fails to respond when the interval between the individual stimuli is less than the refractory period of the GF neurons. We found that the FF50 (the frequency with 50% response rate) of GF pathway of the mutant and wild type had the same baseline levels, and both were significantly increased 24 h after benzyl alcohol sedation (Fig. 3.6A).

To further characterize the neural excitability of the flies, trains of high frequency electroconvulsive shocks (ECS) of various voltages were delivered to the brain to trigger a seizure-like electrical response, and the minimum triggering voltage was recorded as the seizure threshold. The seizure-like phenotype was characterized as a high-frequency spontaneous initial discharge followed by a failure period to the response and a delayed secondary discharge (Fig. 3.6B). The average seizure stimulus voltages in the mutant and wild type flies were measured before and after BA sedation. Without drug exposure, the $slo^{\Delta 55b}$ flies exhibited an average threshold of 33.18 ± 3.182 V, while the stimulating voltage dropped to 21.88 ± 2.98 V one day after benzyl alcohol sedation. The wild type showed similar responses, suggesting that the mutation does not affect basal seizure

susceptibility or drug-induced seizure susceptibility enhancement.

The 55b mutation enhanced basal mobility and the muscle expression of *slo*.

In Drosophila, the muscle-specific expression of BK channels is regulated by the C2 promoter that is only 300 bp downstream of the 55b element, thus the 55b element might play a role in the regulation of *slo* expression in muscle. To test this hypothesis, we conducted real-time RT-PCR using primers specific recognizing the muscle splice variant. We found that the $slo^{\Delta 55b}$ mutant exhibited significantly enhanced basal muscle *slo* expression compared to wild type (Fig. 3.2D). However, in contrast to the transcriptional regulation of *slo* in the nervous system, drug exposure did not further induce muscle *slo* expression in both lines (Fig. 3.2E-F).

Basal mobility is an important indicator of normal physiological performance, and is affected by genotype, age, gender, nutrition, temperature and circadian factors, etc. Here we conducted a ten minute walking test to determine if the $slo^{\Delta 55b}$ mutation increased mobility. As shown in Fig. 3.7A, the walking distance was significantly induced in $slo^{\Delta 55b}$ mutant, while another *slo* DNA element deletion mutant ($slo^{\Delta 6b}$) traveled the same distance as the wild type, suggesting the change of basal mobility is specific to the 55b element.

However, the $slo^{\Delta 55b}$ mutation did not affect all the locomotor activities we tested. The 55b deletion did not affect climbing and flight capacity, while the null mutant slo^{4} showed disturbed activity in both tests (Fig. 3.7B, C). Like the wild type CS, The $slo^{\Delta 55b}$

line also displayed rhythmic behaviors in locomotor activity. However, the null mutant *slo*^{4} was completely arrhythmic (Fig. 3.7D).

DISCUSSION

Recent studies have shown that histone acetylation of the *slo* promoter region is involved in drug-induced *slo* gene up-regulation and the development of tolerance. The evolutionarily conserved DNA element 55b is the region associated with the enhanced acetylation peak as measured in a ChromIP time-course assay 4 h after benzyl alcohol sedation[68]. However, in our measurement, promoter C1 and the 6b region were also recognized as hyper-acetylated at the same time point (Fig. 3.3B). This difference may result from the variability between wild type stains being utilized, or from changes in experimental conditions such as age and batch of reagent. As to the other two time points being examined, 6 h and 24 h after sedation, our results are in great agreement with previous observations[68]. These conserved results prove the ChromIP-qPCR to be an effective and robust method to capture the epigenetic properties in Drosophila.

The *slo* transcriptional control region also contains two putative cAMP responsive element (CRE) binding sites, which are indicated as cre1 and cre2. Moreover, a putative AP-1 binding site is present in the 55b element. The CRE sites and AP-1 sites share consensus DNA sequences, and their specific recognizing proteins, CREB and c-jun, have been shown to be able to dimerize and bind to the AP-1/CRE-like binding site[108]. Furthermore, the CREB transcription factor has been shown to be responsible for these drug-induced changes. It has been shown that benzyl alcohol sedation enhances the

occupancy of activated CREB in the *slo* regulatory region, while activation of a CREB dominant-negative transgene blocks hyperacetylation at *slo* regulatory regions, prevents *slo* message induction and ablates tolerance[68,69].

The $slo^{\Delta 55b}$ mutation enhanced basal muscle *slo* expression, thus leading to an increased mobility relative to wild-type background. However, benzyl alcohol sedation did not further induce muscle *slo* expression. Based on these results, the 55b element is likely to be a transcriptional repressor for muscle specific *slo* expression and furthermore, this repressor is not affected by drug exposure. Interestingly, the mutation did not affect other locomotor activities, including climbing, flying, and circadian rhythmicity. Also these flies did not exhibit the "sticky-feet" phenotype. However, a *slo* null mutation results in reduced flight capacity, loss of circadian rhythmicity and a "sticky-feet" phenotype[89,92]. These results suggest walking activity is more sensitive to muscle *slo* expression.

The 55b element contains multiple putative transcription factor binding sites, including a TGIF binding site (Fig. 3.8). TGIF is a DNA-binding homeodomain protein that acts as a multifunctional transcriptional repressor, and the transcriptional repression by TGIF in part depends on the activity of HDAC[109]. TGIF has been shown to compete with p300 for interaction with Smad2 that forms a complex with Smad4 upon TGFβ receptor activation. The Smad2-Smad4 complex binds to target promoters and recruits co-activators such as p300/CBP or co-repressors such as TGIF[110]. The 55b element also contains a putative site for StuAp that is a transcriptional repressor characterized in

Aspergillus nidulans[111]. These binding motifs may contribute to the repressing effects of the 55b element.

Two putative AP-1 sites are also detected in the 55b region. AP-1 (activating protein-1) family of transcription factors consists of homodimers or heterodimers of subunits from Jun (c-Jun, v-Jun, JunB and JunD), Fos (c-Fos, v-Fos, FosB, Fra1 and Fra2) or ATF (ATF2, ATF3/LRF1 and B-ATF) that interact through a leucine zipper motif and bind to the recognition DNA element via a basic DNA contact region[112]. Both AP-1 and CREB transcription factors transduce environmental signals into alteration in expression of specific target genes. AP-1 and CREB also share similarities in molecular properties and activation mechanisms, and CBP is required for the activation of both of them[113,114]. Moreover, it has been shown that members from the two families can form cross-family heterodimers[115], and cross-talk between the two families can occur as CREB has been shown to bind to AP-1 sites[116].

Our lab has shown the occupancy of CREB at the 55b element and two CRE sites is enhanced by benzyl alcohol sedation[68]. However, the 55b element does not contain any CRE sites, thus CREB protein is thought to interact with the 55b element via the AP-1 site. Upon binding to these DNA elements, CREB may stimulate *slo* expression via recruiting the co-activator CBP that has intrinsic HAT activity[117]. By activating histone acetylation, CBP induces chromatin accessibility and facilitates the docking of transcription machinery. CREB has been shown to be required for the induction of *slo* and for the development of tolerance[68]. However, ablation of 55b did not abolish *slo*

induction or tolerance, suggesting that the occupancy of the two CRE sites by CREB is critical for drug-induced *slo* regulation and tolerance. Thus the 55b element is not required for drug-induced *slo* activation and the development of tolerance.

Figure 3.1. Southern blot analysis of the 55b targeting event. A) The digestion map of *slo* regulatory region in wild type and the targeted mutant. Genomic DNA was digested with *Hind*III and blotted to a membrane that was detected with a 3.1 kb probe shown as the 5'-homologous fragment. A 5.6 kb fragment was recognized in the wild type, while a 4.3 kb band was recognized in the $slo^{w\Delta 55b}$ targeted mutant. B) The Southern blot analysis. Lane 1, DNA from the wild type fly showing a 5.6 kb fragment; lane 2-5, DNA from homologous targeted alleles showing a 4.3 kb band; land 6, DNA from a heterozygous targeted allele $slo^{w\Delta 55b}$/+.

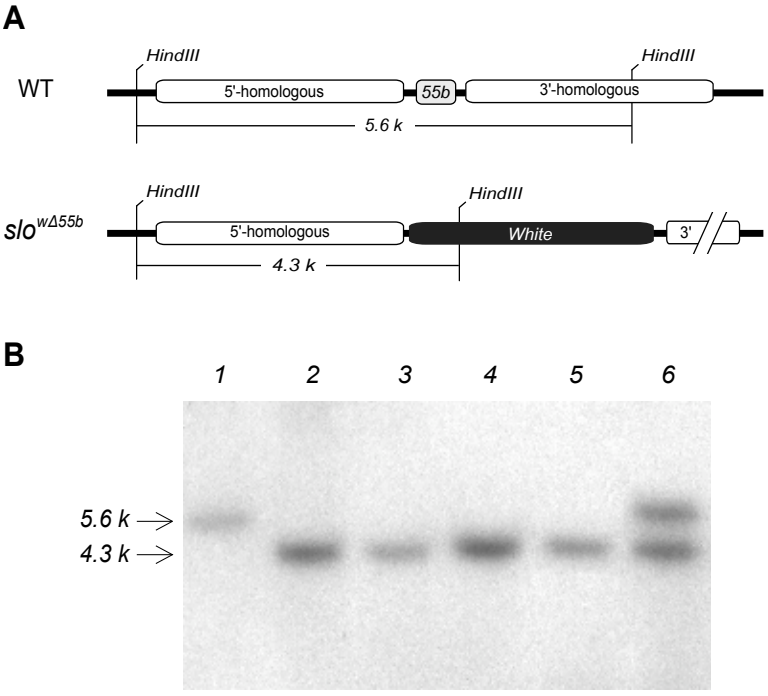

Figure 3.2. Analysis of *slo* transcription in the nervous system and muscle. A) Relative neural *slo* expression levels in $slo^{\Delta 55b}$ and wild type, determined by real-time RT-PCR using C1 primers that only amplify neural *slo* transcripts. B-C) The ratio of *slo* message abundance after drug sedation over untreated control. D) The $slo^{\Delta 55b}$ flies displayed enhanced basal muscle *slo* message expression compared to the wild type. The *slo* mRNA levels of the muscle were determined by real-time RT-PCR using C2 primers that only amplify muscular *slo* transcripts. E-F) The muscle *slo* transcription in both mutant and wild type were not altered by drug sedation. Statistical significance was determined by Student's *t*-test; $*P \leq 0.05$. Error bars represent SEM.

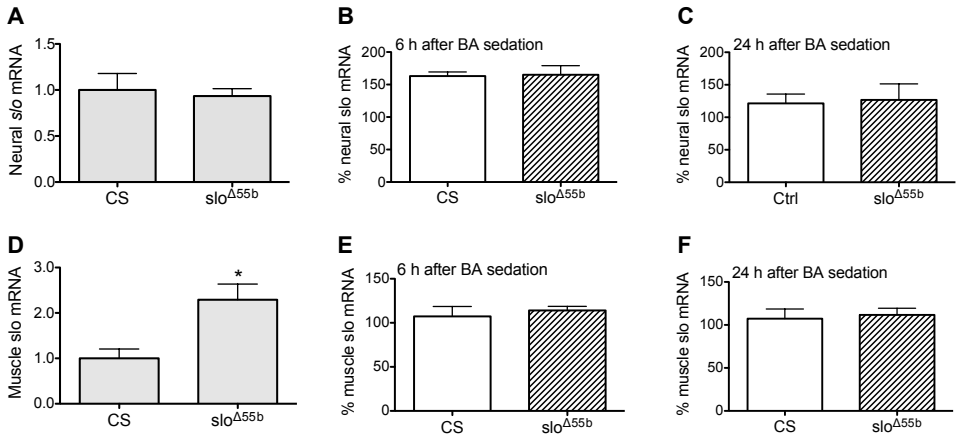

Figure 3.3. Patterns of histone H4 acetylation across *slo* transcriptional control region in *slo*$^{\Delta 55b}$ after benzyl alcohol sedation. A) Map of *slo* control region. B) H4 acetylation levels at 4 h after BA sedation detected by ChromIP and real-time PCR. Fold change of acetylation was the ratio of the acetylation levels of drug-sedated flies over untreated ones. C) Acetylation levels at 6 h after BA sedation. D) Acetylation levels at 24 h after BA sedation. Statistical significance was determined by one-way ANOVA with Dunnett's comparison post tests (n = 3, $*P \leq 0.05$). Error bars represent standard error of the mean (SEM).

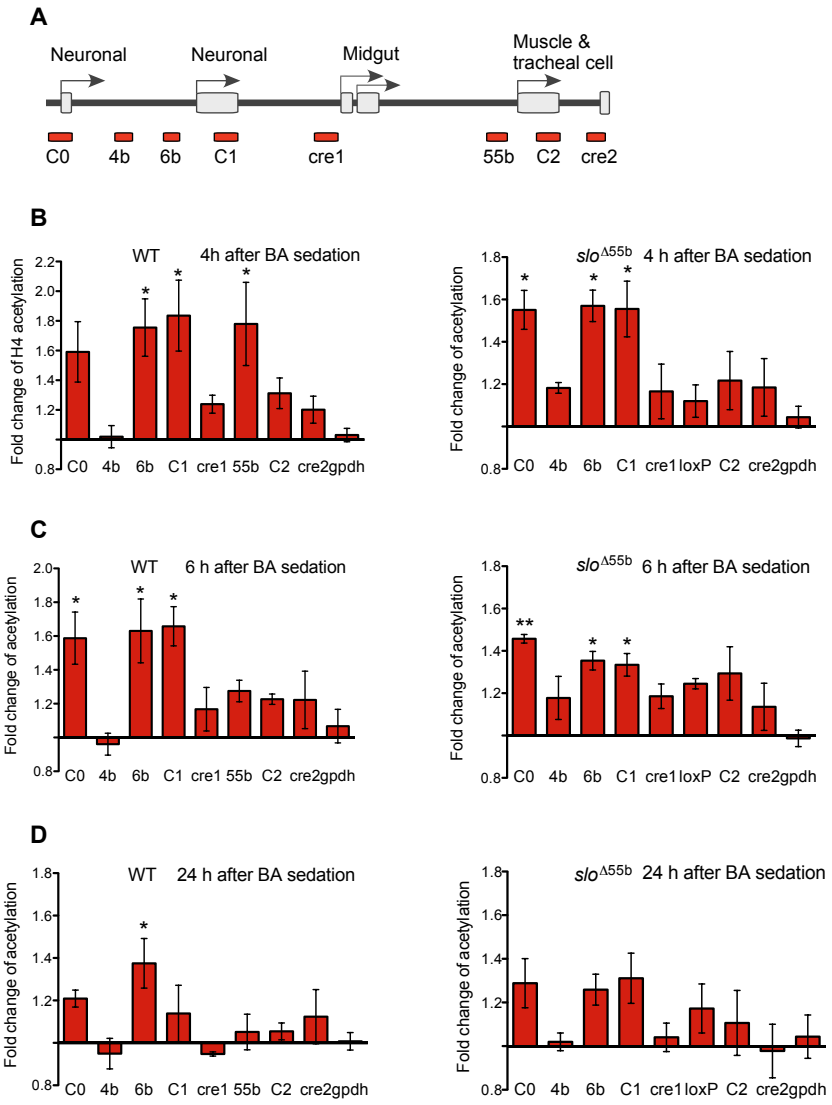

Figure 3.4. The 55b deletion mutation did not affect resistance to benzyl alcohol sedation. To test the resistance to anesthetic benzyl alcohol, age-matched female flies of both CS and $slo^{\Delta 55b}$ were exposed to a single sedating dose of benzyl alcohol. After that flies were transferred to fresh vials to recover. The percentage of recovered flies over time was plotted. Both CS and $slo^{\Delta 55b}$ flies recovered at the same rate. The statistical significance between the two recovery curves was determined by log-rank test and error bars represent SEM.

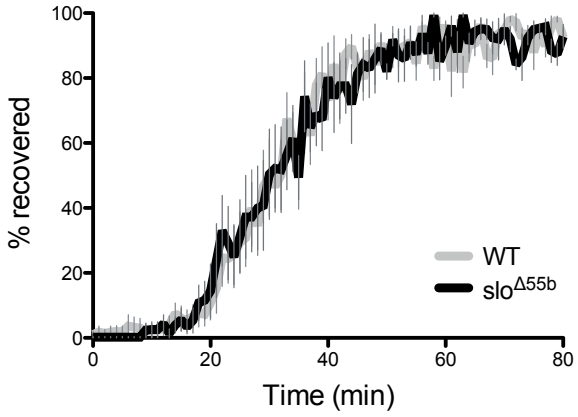

Figure 3.5. The 55b deletion mutant acquired normal tolerance to benzyl alcohol induced sedation. The tolerance assay shows that *slo*$^{\Delta 55b}$ flies acquired tolerance to benzyl alcohol. The tolerance was also detected by 7 d after the first exposure, but disappeared by 14 days. CS wild type was utilized as a control showing tolerance with normal duration. On the day of treatment, age-matched female flies were either drug sedated or mock sedated. On the day of assay, all the flies were sedated completely with anesthetic benzyl alcohol, the recovery process was monitored and the recovery curves were plotted. The curve shows the percentage of recovered flies from their first sedation (blue) and the second (red) drug exposure over time. The statistical significance between the two recovery curves was determined by log-rank test. $*P \leq 0.05$.

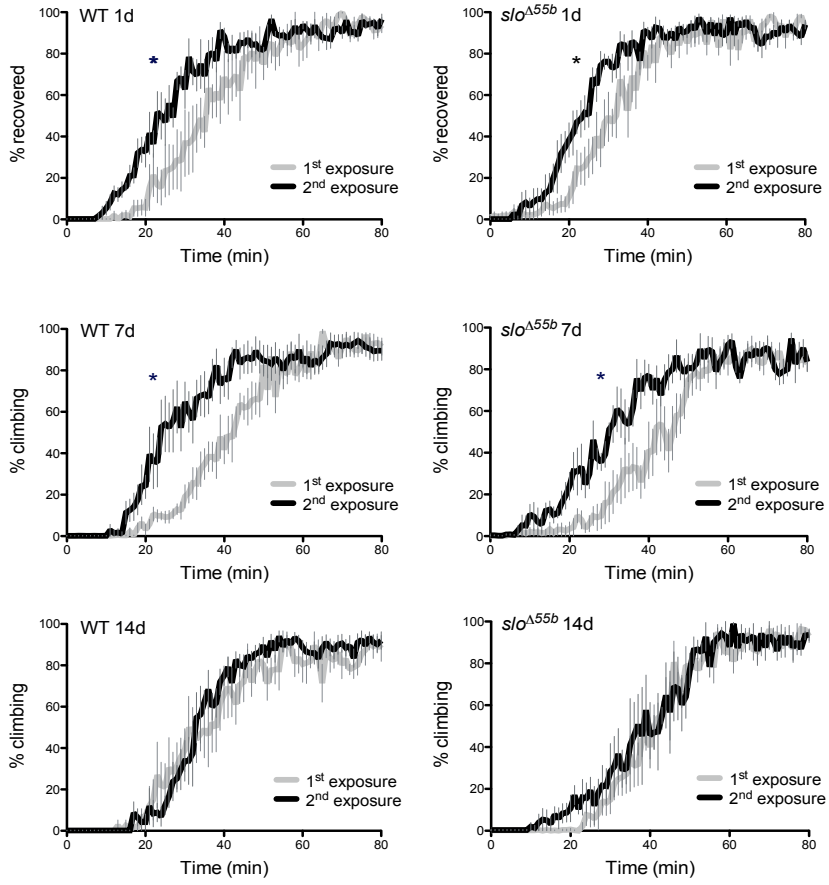

Figure 3.6. Drug sedation caused similar electrophysiological changes in *slo*$^{\Delta 55b}$ and wild type flies. A) Drug sedation increased following frequency. B) Drug sedation enhanced seizure susceptibility in both lines. Electroconvulsive stimuli of varying voltages ranging 5-50 V were utilized to determine seizure susceptibility, which is represented by the minimum stimulus voltage to trigger seizure. The average stimulus voltages in wild type and *slo*$^{\Delta 55b}$ measured one day after BA sedation. BA sedation reduced stimulus voltage in both stocks. Unpaired *t*-test, n = 5~9, $*P \leq 0.05$. Error bars represent SEM.

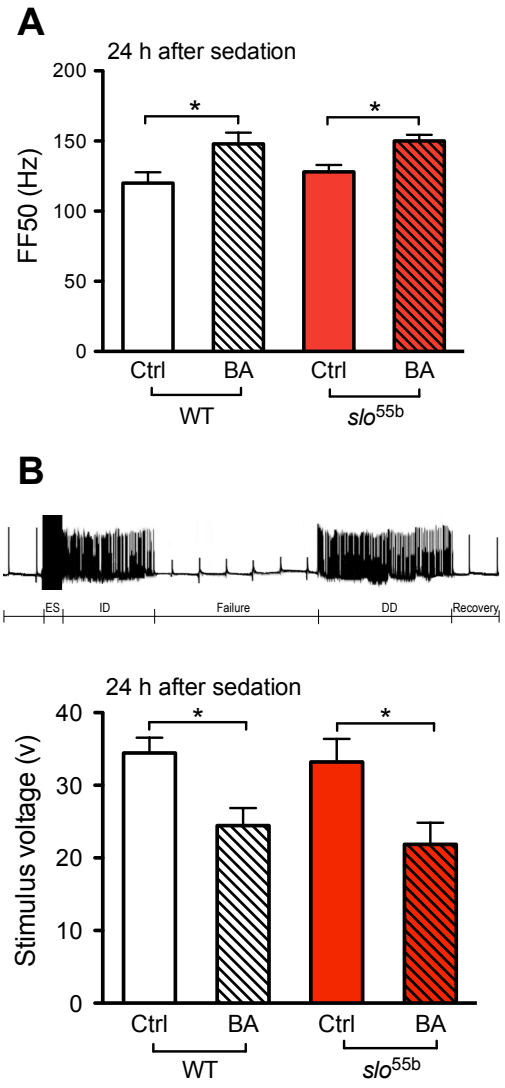

Figure 3.7. The *slo*$^{\Delta 55b}$ mutation did not affect all the locomotor activities. A) The *slo*$^{\Delta 55b}$ mutant exhibited enhanced walking distance compared to CS wild type and *slo*$^{\Delta 6b}$ in a 10 min free walking test. B) The *slo*$^{\Delta 55b}$ flies showed normal climbing ability. Flies that climbed beyond 10 cm within 10 sec were considered as passing the climbing assay. Over 95% of CS and *slo*$^{\Delta 55b}$ flies passed the climbing test, whereas only 30% of the loss-of-function mutant *slo*^{4} stock passed it. C) The *slo*$^{\Delta 55b}$ mutation did not affect flight capacity. Flies were dropped into a 15 × 62 cm pipette jar at the top. The falling flies flew toward the wall and were stuck in the mineral oil pre-coated on the wall, and the distance from the top was measured. Wild type and *slo*$^{\Delta 55b}$ animals fly well, and most of them are found within 10 cm to the top. In contrast *slo*^{4} flies flew poorly and were evenly distributed along the wall. D) Rhythmic activity of CS, *slo*$^{\Delta 55b}$ and *slo*^{4} flies. Recently eclosed flies were entrained in LD for 3 days before being transferred to DD and monitored for 6 days. Both CS and *slo*$^{\Delta 55b}$ flies demonstrated rhythmic oscillation in activity, while *slo*^{4} was behaviorally arhythmic. One-way ANOVA with Dunnett's post hoc test was used to determine the statistical significance. Error bars represent SEM. *$P \leq 0.05$; **$P \leq 0.01$.

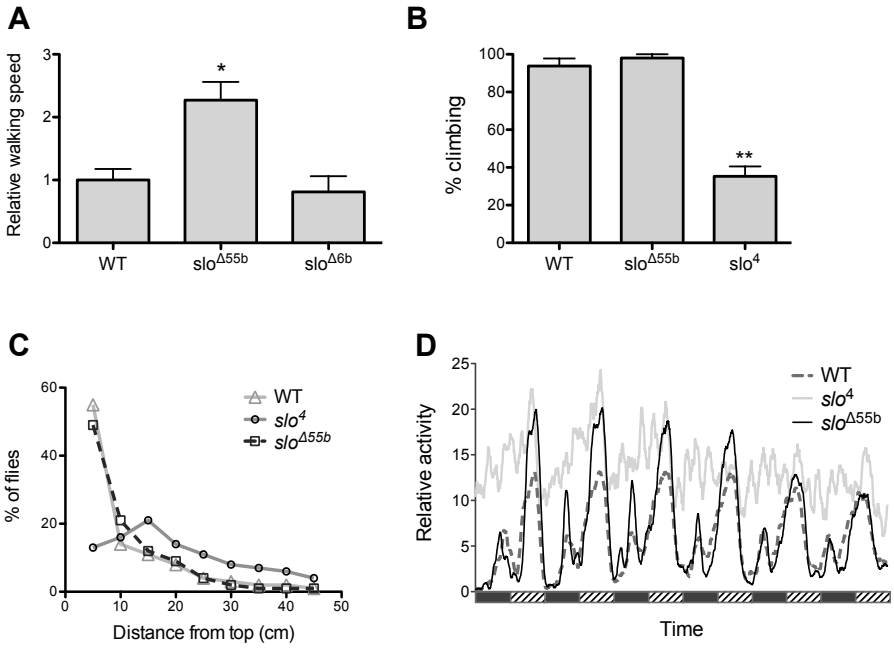

Figure 3.8. Sequence analysis of the 55b element. The binding sites of transcription factors within the 55b element were identified using TRANSFAC database[118]. Transfactor binding sites are: AP-1, Activator Protein-1; BR-C, Broad-Complex; E2F, Dl, Dorsal; Oct-1, Octamer binding factor 1; SBF, Silencer-binding factor; StuAp, the *Aspergillus nidulans* Stunted protein; TGIF, TG-interacting factor. The score describes the quality of the match that ranges from 0 to 1.

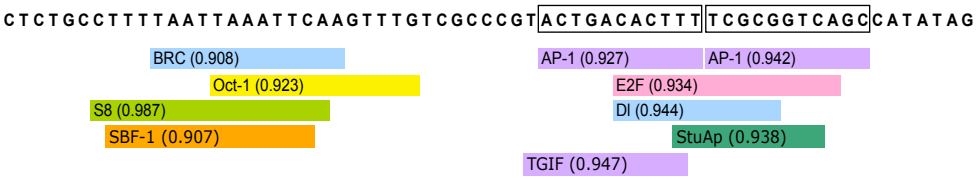

METHODS

Fly stocks

Drosophila stocks were Canton S (wild type), *slo*^{4} and *slo*$^{\Delta 55b}$. Flies were raised on standard cornmeal medium in a 12:12 light:dark cycle at 22°C. Newly eclosed flies collected during an interval of 2 days were studied 3-5 days after eclosion.

Ends-out gene targeting of the 55b element

The 55b element of *slo* was ablated using ends-out gene targeting method developed by Golic and coworkers[88]. At first, the two homologous sequences flanking the *slo* 55b element were amplified by PCR using Canton S genomic DNA as the template together with a proofreading *PfuTurbo* DNA polymerase (Stratagene CA). More specifically, primers 5'-GCGGCCGCCTCGGTGGTTTAGCCAGTA-3' and 5'-GCGGCCGCGCCAAGACAAGGCGAATTCAA-3' were used in the PCR to amplify and add *Not*I sites to both ends of a 3.1-kb DNA fragment upstream of the 55b element, while primers 5'-GGCGCGCCAAATGCCCGTATAGTCATA-3' and 5'-GGCGCGC CTAAAGACGCCCAGACAAATG-3' were designed to amplify and add *Asc*I termini to a 3-kb DNA fragment downstream of 55b. These two fragments were then inserted with the same orientation into their corresponding sites that flank the *white*$^{+}$ gene in the ends-out vector pW25[95]. This construct, also called the donor construct, was introduced into the *white*$^{-}$ fly by standard *P* element germline transformation. All the insertion lines are mapped for the location of the donor transgene, and lines with the donor transgene on

the first or the second chromosome were utilized to induce gene targeting.

To induce targeting, donor insertion lines are crossed to the *P{hsp70FLP}P{hsp70I-SceI}* strain (Bloomington # 6934), and the progeny were heat-shocked at 38°C for one hour during their first three days of development to induce transgenic FLP and I-SceI which worked on their corresponding recognition sites in the donor sequence. The donor sequence was hopped out from its insertion site in a circular form under the action of FLP recombinase, and was linearized after I-sceI digestion. These changes allow pairing and crossover between the homologous donor fragment and the targeted 55b region. Thus that 55b was replaced by the $white^{+}$ from the donor sequence. Virgin females with $white^{+}$ and *P{hsp70FLP}P{hsp70I-SceI}* are collected and crossed to male FLP flies (Bloomington # 6938), and the progeny are screened for solid red eyes. The $white^{+}$ gene was mapped to identify targeted events in which $white^{+}$ was relocated to the target chromosome 3. And Southern blotting was carried out to further confirm targeted events occurred exactly in the designed position. Finally, the targeted strain was crossed to *P{Cre}* line (Bloomington # 1501) to remove the $white^{+}$ maker and obtain the 55b deletion mutant $slo^{\Delta 55b}$. The female $slo^{\Delta 55b}$ fly was backcrossed to male Canton S for six generations.

Southern blotting analysis

Southern blot analyses were performed to verify the ends-out targeting events using a DIG kit (Roche Diagnostics, IN) as recommended by the manufacturer. Genomic DNA was prepared from flies carrying the targeted allele and wild type, followed by

overnight digestion with *Hind*III (NEB, MA), separated by agarose gel electrophoresis and transferred to nylon membranes as described[96]. The probe DNA in use was the 3.1-kb upstream homologous fragment of the 55b element. The blot was hybridized to the digoxigenin (DIG) labeled probe and was detected by DIG antibody and chemiluminescence signal.

Benzyl alcohol exposure and tolerance assay

Benzyl alcohol exposure and tolerance assay were performed as described in Chapter 2.

Locomotor activity analysis

Mobility analysis

A total of 12 age-matched female flies were monitored for mobility in a 12-well cell culture plate (well diameter 35 mm, 5 mm high), with each animal in a separate well. Humidified air was delivered through the plate to prevent dryness. After 5 minutes of equilibration, the activity of the flies was recorded in a 10-min video using a computer-controlled web camera place above the plate. The quantification of locomotor activity (in walking speed) by video-tracking was performed as described[119]. Experiments were performed at the same time of day to screen out the influence of circadian rhythms. Flies tested were CS, $slo^{\Delta 55b}$ and $slo^{\Delta 6b}$. Each assay was repeated three times and a One-way ANOVA with Dunnett's post hoc test was used to determine the statistical significance.

Climbing assay, flight assay, Sticky-feet behavioral test and Circadian analysis

The climbing assay, flight assay, sticky-feet behavioral test and circadian rhythm analysis were conducted as described in Chapter 2.

Quantitative RT-PCR analysis

RNA was extracted from heads or the whole body. The quantitive RT-PCR was conducted as described in Chapter 2. The primers used are shown as follows: *slo* exon C1 forward primer 5'-AAACAAAGCTAAATAAGTTGTGAAAGGA-3'; *slo* exon C1 reverse primer 5'-GATAGTTGTTCGTTCTTTTGAATTTGA-3'; *slo* exon C2 forward primer 5'-GCTATTTATAATAGACGGGCCAAGTT-3'; *slo* exon C2 reverse primer 5'-GGAAATCCGAAAGATACGAATGAT-3'; *Cyp1* forward primer 5'-ACCAACCACAA CGGCACTG-3; *Cyp1* reverse primer 5'-TGCTTCAGCTCGAAGTTCTCATC-3'.

Chromatin immunoprecipitation assay

The chromatin immunoprecipitation (ChromIP) assays were performed as described in Chapter 2.

Electrophysiology analysis

Seizure susceptibility and following frequency of the GF pathway were determined as described in Chapter 2.

Chapter 4: Histone acetylation in tolerance

INTRODUCTION

In Drosophila, the *slo* gene encodes the BK-type voltage- and Ca^{2+}-activated K^+ channel that is involved in the acquisition of functional tolerance to anesthetic drug induced sedation. Tolerance is defined as the reduced responsiveness to an effect of a drug caused by prior drug exposure[1]. It has been shown that neural *slo* expression is necessary for the development of drug-induced rapid tolerance. A single sedating dose of the anesthetic benzyl alcohol or ethanol induces the expression of *slo* in the nervous system. Moreover, mutations ablating neural *slo* expression also block tolerance, while activating a *slo* transgene that expresses a neural splice variant phenocopies tolerance[13,46].

The Drosophila *slo* gene is regulated by alternative promoter activation and alternative mRNA splicing, which lead to the functional diversity of BK channels. The *slo* gene has a complex 7 kb control region, containing at least five transcriptional promoters that mediate developmental and tissue-specific expression, including neural specific promoters C0 and C1, the midgut promoters C1b and C1c, and the muscle promoter C2 that regulates expression in the muscle and tracheal cells[27]. The *slo* gene also contains five alternative splicing sites[31]. Theoretically, activation of *slo* expression through such regulation can give rise to over 1000 distinct peptides[31]. Presumably, alternative splicing allows cells to customize BK channels by fine-tuning conductance and calcium sensitivity to meet their particular needs.

A large number of evolutionarily conserved DNA elements and protein binding motifs have been identified in the transcriptional regulatory region of *slo*. The DNA elements 6b and 55b are short non-core promoter DNA elements recently identified by sequence comparison between the twelve Drosophila species whose genome has been sequenced[27,103]. The *slo* regulatory region contains two putative cAMP responsive element (CRE) binding sites and a putative AP-1 binding site within the 55b element[68]. The CRE sites and AP-1 sites have similar consensus sequences, and their specific recognizing proteins, c-jun and CREB, have been shown to be able to dimerize and bind to an AP-1/CRE-like binding site[108].

Recently it was shown that benzyl alcohol exposure induces dynamic spatiotemporal changes of histone H4 acetylation across the *slo* control region. Four hours after drug sedation, an acetylation spike is observed over the 55b DNA element. Two hours later, enhanced histone H4 acetylation has been observed at the 6b element and across the two neural promoters (C0 and C1). During this time, neural *slo* message abundance becomes elevated and behavioral tolerance can first be detected. Twenty-four hours after sedation, *slo* message level decreases and H4 acetylation is only observed at the 6b element. By 48 hr, both histone acetylation level and *slo* message abundance have returned to baseline[68].

Inducing histone acetylation with a universal histone deacetylase inhibitor, sodium butyrate, causes hyperacetylation across the *slo* transcriptional control region, induces *slo* transcription and phenocopies tolerance. The CREB transcription factor has been shown

to be involved in these drug-induced changes. Benzyl alcohol sedation enhances the occupancy of activated CREB in the *slo* regulatory region, while activation of a CREB dominant-negative transgene blocks hyperacetylation at *slo* regulatory regions, prevents *slo* message induction and ablates tolerance[68,69].

The enhancement of histone acetylation by sodium butyrate is not confined to the *slo* control region but also occurs elsewhere in the genome. While a functional *slo* allele is required for sodium butyrate-induced resistance[68], this does not exclude the possibility that the hyperacetylation across the *slo* regulatory region may not reflect changes that are required for or that cause drug-dependent induction of *slo*. Because of a lack of direct evidence linking the state of histone acetylation across the *slo* control region to *slo* induction and the acquisition of tolerance, I wished to specifically manipulate acetylation within the *slo* transcriptional control region and to determine the effect on *slo* transcription and the production of functional tolerance to benzyl alcohol sedation. To achieve this goal, I tethered histone acetylation modifiers (an HDAC and a HAT) adjacent to the 6b or 55b elements of the *slo* control region in order to artificially reduce or enhance acetylation at the sites. These two DNA elements were chosen because their hyperacetylation status is specifically altered following benzyl alcohol sedation[68]. Tethering was performed by expressing a GAL4DBD-HDAC or GAL4DBD-HAT fusion protein in flies in which a UAS sequence was inserted adjacent to either 6b or 55b. The Gal4DBD domain is the DNA binding domain (DBD) of the yeast Gal4 transcription factor. This DBD specifically binds to the UAS[120].

RESULTS

To study the effect of localized histone acetylation at the 6b element and the 55b element in the *slo* regulatory region, histone acetylation modifiers were docked at these elements respectively through a binary Gal4-UAS expression system (Fig. 4.1). This system is composed of two components: the DNA-binding domain of the yeast transcription activator protein Gal4 and a short DNA sequence named upstream activation sequence (UAS), to which Gal4 binds specifically. More specifically, a single copy of the UAS was inserted 5' of the 6b and 55b elements by homologous recombination to generate the slo^{6bUAS} and slo^{55bUAS} mutations. Southern blot analysis was carried out to identify strains in which targeting had correctly occurred (Fig. 4.2). The slo^{6bUAS} and slo^{55bUAS} stocks were individually crossed to stocks carrying three different heat shock inducible Gal4 transgenes. They are the $Gal4^{DBD}$-HDAC, $Gal4^{DBD}$-HAT and a $Gal4^{DBD}$ transgenes. The $Gal4^{DBD}$-HDAC transgene expresses a hybrid Gal4 transcription factor in which the GAL4 DNA binding domain (DBD) is fused to a HDAC domain from transcription factor Rpd3/HDAC1. The $Gal4^{DBD}$-HAT transgene expresses a hybrid Gal4 protein in which the DBD domain is fused to the HAT domain from transcription factor Chameau/HAT1. The $Gal4^{DBD}$ transgene expresses a transcription factor that contains only the Gal4 DNA binding domain (but not HDAC or HAT domain). $Gal4^{DBD}$ was used as a control for the effect of binding an enzymatically-inactive protein at the UAS sites. Expression of these transgenes is driven by a heat-inducible hsp70 promoter. Offspring

from the crosses contain both the slo^{UAS} allele and the inducible Gal4 derivatives.

Following heat induction, the modified Gal4 protein should bind to the inserted UAS from where the tethered HAT or HDAC domain can modify the local histone acetylation state. In this manner we should be able to determine whether acetylation at these positions is sufficient for *slo* induction. In addition, we should be able to determine whether acetylation at these positions is necessary for the response of *slo* to benzyl alcohol sedation. A heat pulse is used to activate the hsp70 promoter that drives expression of the Gal4-derived transgenes. Using this two-part system, the histone modifiers will be tied to the 6b element or the 55b element in order to locally change the histone acetylation level (Fig 4.1).

I also obtained ideal control animals for all the UAS knock-in lines from the genetic crosses to induce homologous recombination. These control lines were isolated when homologous recombination took place downstream of the UAS sequence of the donor. Therefore the control lines, slo^{6bL} and slo^{55bL}, have the same genetic background as the UAS knock-in lines, except for the absence of the UAS motif.

HS-GAL4^{DBD}*-HDAC;* slo^{6bUAS} females acquired tolerance to benzyl alcohol as long as the *HS-GAL4*^{DBD}*-HDAC* transgene was not activated (Fig. 4.3A). Moreover, resistance to benzyl alcohol was unchanged in animals after heat shock induction of the HDAC expressing transgene (Fig. 4.3B). However, activation of the HDAC transgene interfered with the capacity of flies to acquire tolerance. Not only did the animals not acquire

tolerance, but they instead showed sensitization to benzyl alcohol sedation when the HDAC transgene was activated 24 h before the first benzyl alcohol exposure (left-most panel of Fig. 4.3C). Tolerance was also blocked if the activating heat shock occurred 24 h after the first drug exposure (left-most panel of Fig. 4.3D). In contrast, the *HS-GAL4^{DBD}-HDAC; slo^{6bL}* control animals acquired tolerance to drug sedation whether the HS was delivered 24 h before benzyl alcohol sedation or 24 h after benzyl alcohol sedation (right-most panels of Fig. 4.3C & D, respectively).

In a parallel series of experiments using *HS-GAL4^{DBD}-HDAC; slo^{55bUAS}* females I observed that activating the HDAC transgene 24 h before the first drug exposure blocked tolerance (Fig. 4.4C) but did not cause sensitization as with *slo^{6bUAS}*. However, activating it after the 24 after the first drug treatment had no effect on tolerance acquisition (Fig. 4.4D). This latter result is in contrast to the *slo^{6bUAS}* experiment (see above).

These data showed that tethering a HDAC adjacent to *slo* control elements blocked tolerance to benzyl alcohol. The only difference between the UAS knock-in lines and the controls is the insertion of a UAS motif adjacent to either the 6b or the 55b DNA elements, and only activating the HDAC transgene in the UAS knock-in lines blocked tolerance. I also noticed the repressing effect of HDAC was stronger when the HDAC transgene was induced before a drug exposure that has been shown to induce histone acetylation, suggesting that docking an HDAC at specific DNA elements (6b and 55b) of *slo* control region represses drug-induced *slo* activation.

The *HS-GAL4^{DBD}-HAT; slo^{6bUAS}* stock developed tolerance to benzyl alcohol when

the HAT transgene was not activated (Fig. 4.5A). Heat shock induction of HAT expression had no effect on benzyl alcohol resistance or tolerance (Fig. 4.5B-D). The same results were observed in *HS-GAL4^{DBD}-HAT; slo^{55bUAS}* animals (Fig. 4.6). Thus, tethering a Gal4-HAT at either 6b or 55b had no effect on the capacity of flies to acquire benzyl alcohol tolerance.

I also measured neural *slo* message abundance in the two-part system (Fig. 4.7). Total RNA was prepared 6 h after the first drug exposure and quantitated by real-time RT-PCR using C1 primers that specifically recognize neural transcript variants. Benzyl alcohol did not increase *slo* message abundance in *HS-GAL4^{DBD}-HDAC; slo^{6bUAS}* when the HDAC was activated by a heat shock treatment (Fig. 4.7A), however, the drug-induced *slo* expression was detected in *HS-GAL4^{DBD}-HDAC; slo^{6bL}* control animals (Fig. 4.7B). In contrast, activating the HAT increased *slo* abundance in both *HS-GAL4^{DBD}-HAT; slo^{6bUAS}* and its control. Similar results were obtained in *HS-GAL4^{DBD}-HDAC; slo^{55bUAS}* and *HS-GAL4^{DBD}-HAT; slo^{55UAS}* (Fig. 4.8).

To confirm that the ablation of tolerance by the Gal4-HDAC fusion protein was due to the HDAC activity and was not merely a product of the physical binding of a GAL4^{DBD} to specific *slo* DNA elements I used the HS-GAL4^{DBD} transgene. The derived *HS-GAL4^{DBD}; slo^{55bUAS}* animals were subjected to a heat shock treatment to induce the GAL4^{DBD} that binds to the UAS motif adjacent to the 55b element. Twenty-four hours later, the animals received the first benzyl alcohol sedation, followed by the tolerance assay. The total RNA was prepared 6 h after the first drug exposure and quantitated by

real time RT-PCR using C1 primers that recognize the neural transcript variants. I found that both the *HS-GAL4^{DBD}; slo^{55bUAS}* stock and its control line acquired tolerance to benzyl alcohol after the activation of the GAL4^{DBD}, and the *slo* message in both lines was induced (Fig. 4.9).

DISCUSSION

The induction of the *slo* gene has been shown to be important for the development of anesthetic drug tolerance[13,46], Changes in histone H4 acetylation across the *slo* transcription regulatory region have been correlated with benzyl alcohol induction of *slo* expression and functional tolerance. Moreover, administration of a universal HDAC inhibitor, sodium butyrate, leads to hyperacetylation at the 6b area of *slo* control region, induces of *slo* expression and leads to a phenotype similar to tolerance[68]. This evidence suggests that histone acetylation is involved in *slo* induction and the generation of tolerance. However, it is not clear that histone acetylation within *slo* is necessary for the acquisition of tolerance. To further evaluate the role of histone acetylation I used a two-part system that ties histone modifiers adjacent to the conserved DNA elements 6b or 55b of the *slo* gene. Tethering of an HDAC adjacent to either 6b or at 55b blocked tolerance. However, the effect of the HDAC at 6b appeared to be stronger because animals not only failed to acquire tolerance but also showed drug sensitization following a single benzyl alcohol sensitization. This observation suggests that the 6b element is more important in the production of benzyl alcohol tolerance. In concordance with this hypothesis are the results using the 6b knockout allele (Chapter 2) and the 55b knockout allele (Chapter 3).

Transcriptional regulation in eukaryotes is strongly influenced by the post-translational modification of histones. Histone acetylation is the best understood modifications that has been shown to correlate with gene activity: hyperacetylation with a HAT usually causes an increase in gene expression, while an HDAC results in hypoacetylation that is generally correlated with transcriptional inactivation, heterochromatin and silenced genomic areas[121,122].

It has been previously proposed that an HDAC is chronically positioned in the vicinity of the 6b element. The basis for this supposition is that the administration of a universal HDAC inhibitor causes hyperacetylation at the 6b region which also results in the induction of *slo*[68]. This suggests that an HDAC at the 6b DNA element inhibits basal expression of *slo*. In this model, after benzyl alcohol exposure, the HDAC dissociates from the 6b element resulting in *slo* induction. I propose that the Gal4-HDAC artificially positioned at the 6b element cannot be released after drug exposure, and that this blocks *slo* induction and prevents tolerance.

The HDAC transgene used in this study is an Rpd3 allele that has been shown to successfully modify chromatin in Drosophila follicle cells[120]. To date, six different Drosophila HDACs have been identified. These are Rpd3, HDAC3, HDAC4, HDAC6-S, HDAC6-L, and Sir2[123]. None of these HDACs exhibit any DNA binding activity, thus corepressor proteins with DNA-binding domains are thought to be involved in forming HDAC complexes to position the histone modifier to specific genes[124]. In their native form, some HDACs, including Rpd3/HDAC1, are only active within a complex, and a

complex may contain more than one HDAC[125].

It is interesting that the tethering of the RPD3 HDAC domain (Gal4^{DBD}-HDAC) at either 6b or 55b does not affect basal expression of *slo* nor does it affect benzyl alcohol sensitivity. Only after benzyl alcohol sedation is the effect of the tethered HDAC observed.

There are two hypotheses that could account for this behavior. The first hypothesis is that the effect the HDAC is only detectable when its substrate, acetylated histones, increase in concentration. Perhaps, the affinity of the active site for its substrate (Km) is insufficient to support deacetylation. After benzyl alcohol sedation, the acetylation level climbs and raises the local substrate concentration to a level that permits enzyme activity.

A counter hypothesis is that the tethered HDAC is being actively regulated in response to benzyl alcohol sedation. Perhaps, the activation of the Rpd3 HDAC domain depends on its cofactor proteins and that these respond to benzyl alcohol sedation.

In this study, the heat-inducible GAL4^{DBD}:HAT transgene had no effect on drug resistance or tolerance. The HAT transgene in use is a *chameau* allele that has been shown to enhance DNA replication origin activity *in vivo*[120]. The Drosophila Chameau belongs to the MYST HAT family (named after its members MOZ, Ybf2/Sas3, Sas2, and Tip60) and is homologous to the human HAT HBO1. MYST HATs have been shown to activate gene transcription and DNA repair, but they are also involved in transcription silencing[126]. Chameau has been shown to promote H4 acetylation at AP-1 target sites and

activate AP-1 dependent transcription[127]. While modification of histone acetylation is usually linked to transcriptional activation, recent evidence also suggests that Chameau mediated histone acetylation is required for the maintenance of Hox gene repression[128]. Like HDACs, most HATs exist as components of multisubunit complexes, and their substrate preference and gene-specific localization are affected by the cofactors in the same complex[129]. Lacking the essential co-activators for the Chameau HAT in this preparation might have prevented the formation of a functional HAT complex.

Figure 4.1. The scheme to tether chromatin modifiers to the 6b element in *slo* control region. One copy of UAS, the Gal4 binding motif, was inserted at the 5' of the 6b element to generate a slo^{6bUAS} mutation. Then a Gal4 fusion transgene that contains a heat-inducible hsp70 promoter (red box) driving expression of the GAL4 DNA binding domain (DBD) (blue box) fused to HDAC (yellow box) was introduced to the slo^{6bUAS} allele through genetic crossing. Heat-induced expression in progeny with both alleles results in binding of GAL4:HDAC to the UAS motif adjacent to the 6b element. Similarly, other chromatin modifiers can be docked to the 6b element by using specific Gal4 fusion transgene. This strategy is also applicable to the modification of the 55b element.

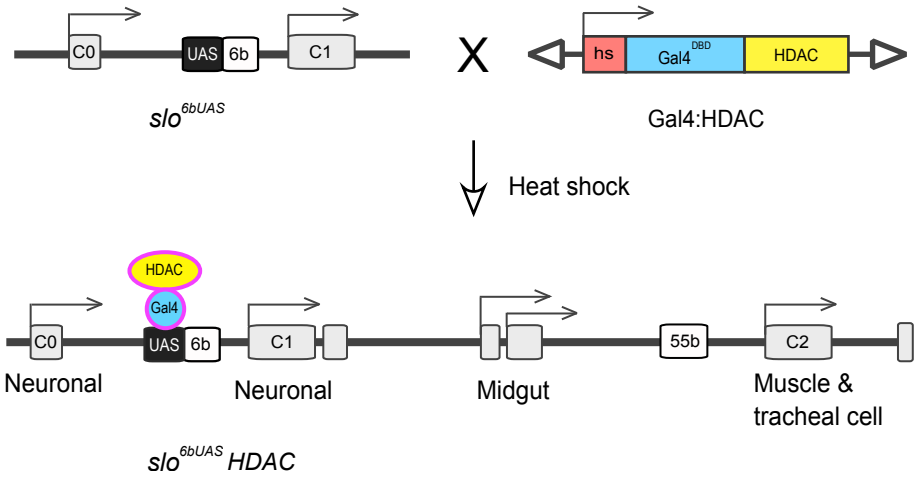

Figure 4.2. Southern analysis of knock-in alleles. A) Southern analysis of *slo*^{6bUAS}. Genomic DNA was digested with *Hind*III and detected using a probe made of the 3'-homologous fragment. DNA from wild type shows a 5.6-kb fragment; homologous targeted alleles showing a 10.4-kb band; and heterozygous targeted allele shows two bands. B) Southern blot analysis of *slo*^{55bUAS}. Genomic DNA was digested with *Hind*III and detected using a probe made of the 3'-homologous fragment. DNA from wild type shows a 5.7-kb fragment; DNA from homologous targeted alleles show a 10.4-kb band; DNA from a heterozygous targeted allele shows two bands.

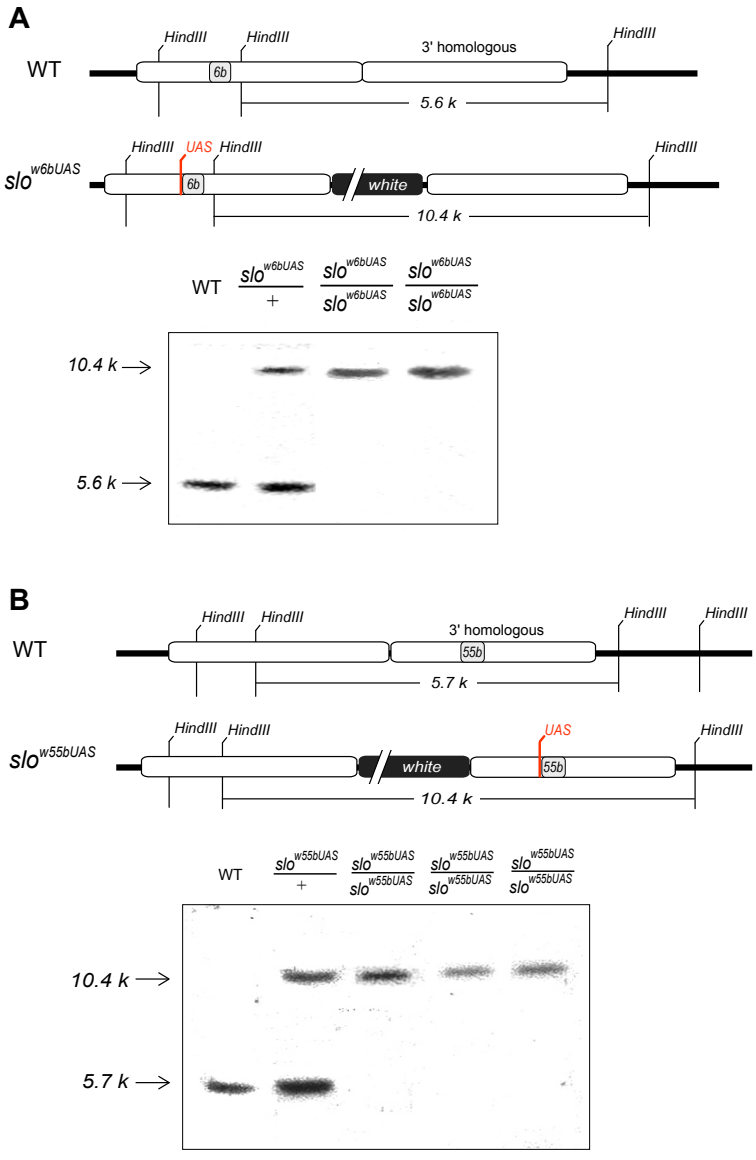

Figure 4.3. Tethering HDAC at the 6b element blocked tolerance. A) *HS-GAL4^{DBD}-HDAC; slo^{6bUAS}* and its control *HS-GAL4^{DBD}-HDAC; slo^{6bL}* acquired tolerance to BA when HDAC was not activated. B) Docking HDAC at 6b region did not affect drug resistance in both lines. C) Docking HDAC at 6b region before drug treatment sensitized the fly to sedation. D) Tethering HDAC at 6b after the first drug exposure blocked tolerance. However, the heat shock treatment in both C and D did not affect tolerance in the control line.

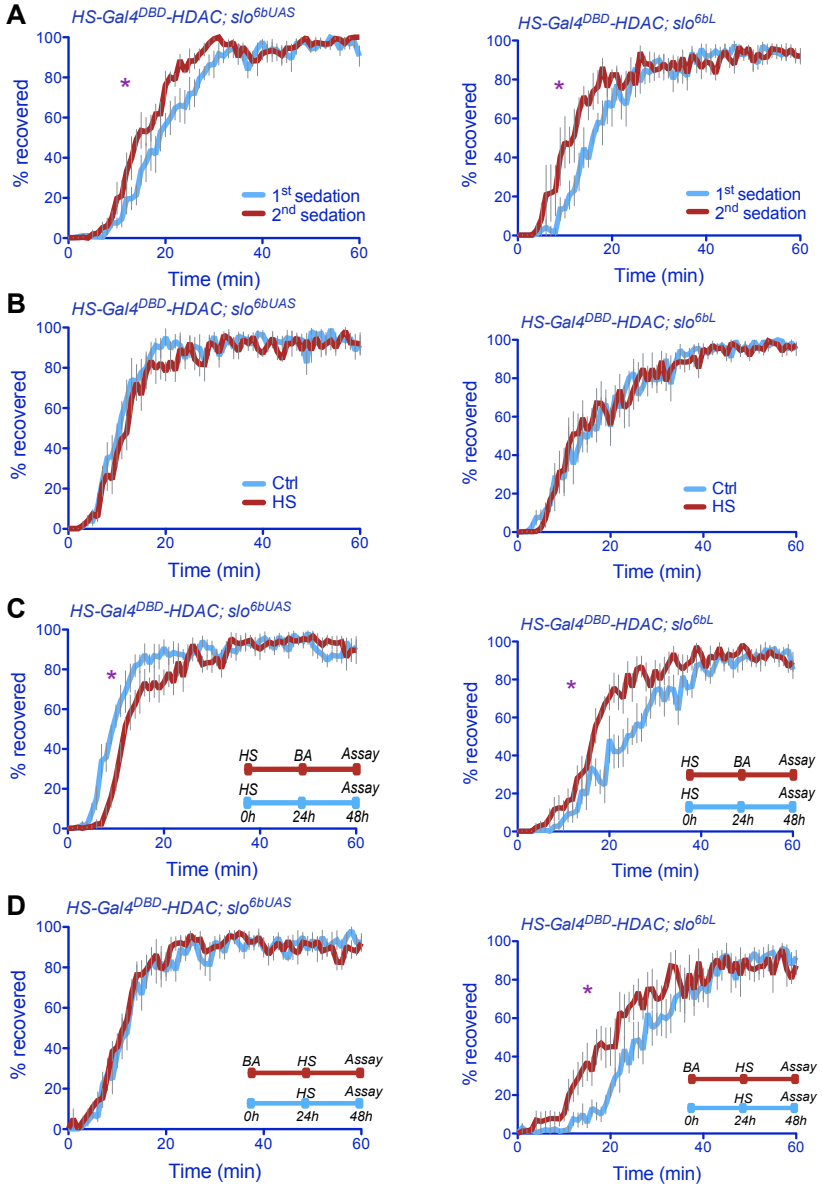

Figure 4.4. Tethering HDAC at the 55b element blocked tolerance. A) HS-GAL4^{DBD}-HDAC; *slo*^{55bUAS} and its control line HS-GAL4^{DBD}-HDAC; *slo*^{55bL} acquired tolerance to BA when HDAC was not activated. B) Docking HDAC at 55b region did not affect drug resistance. C) Docking HDAC at 55b region before drug treatment blocked tolerance. D) Tethering HDAC at 55b after the first drug exposure blocked tolerance. However, the heat shock treatment in both C and D did not affect tolerance in the control line.

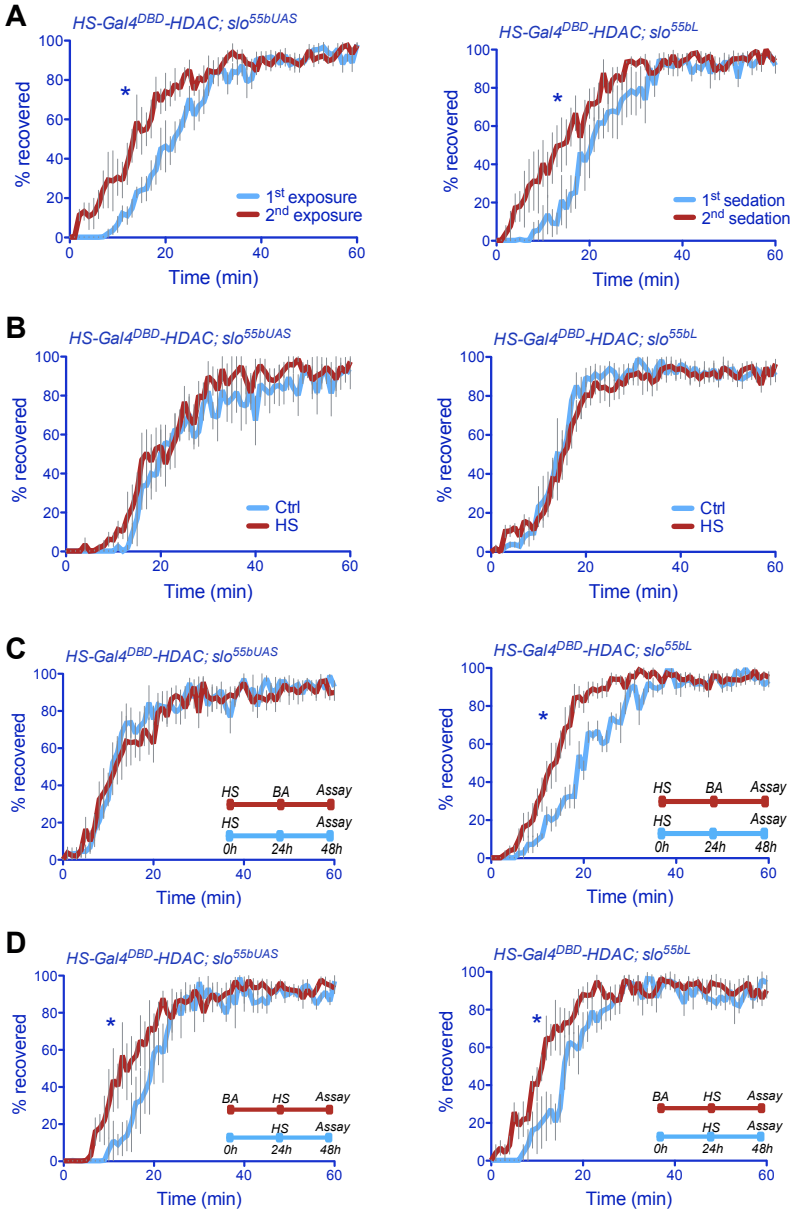

Figure 4.5. Tethering HAT at the 6b element had no effect on drug resistance or tolerance. A) *HS-GAL4^{DBD}-HAT; slo^{6bUAS}* acquired tolerance to BA when HAT was not activated. B) Tethering of Hat at 6b region did not affect drug resistance. C) Docking of HAT at 6b region before the first drug exposure no effect on tolerance. D) Tethering HAT at 6b after the first drug exposure had no effect on tolerance.

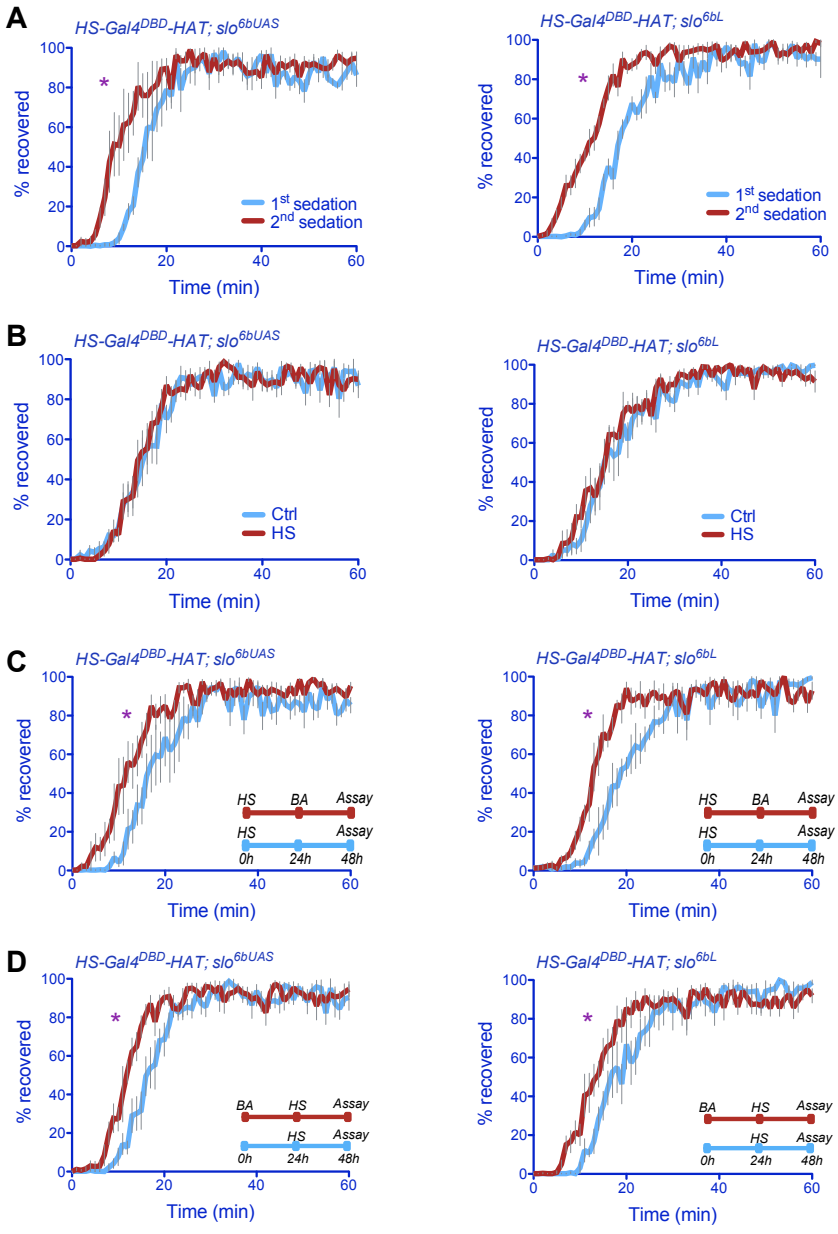

Figure 4.6. Tethering HAT at the 55b element had no effect on drug resistance or tolerance. A) *HS-GAL4^{DBD}-HAT; slo^{55bUAS}* acquired tolerance to BA when HAT was not activated. B) Tethering of Hat at 55b region did not affect drug resistance. C) Docking of HAT at 55b region before the first drug exposure no effect on tolerance. D) Tethering HAT at 55b after the first drug exposure had no effect on tolerance.

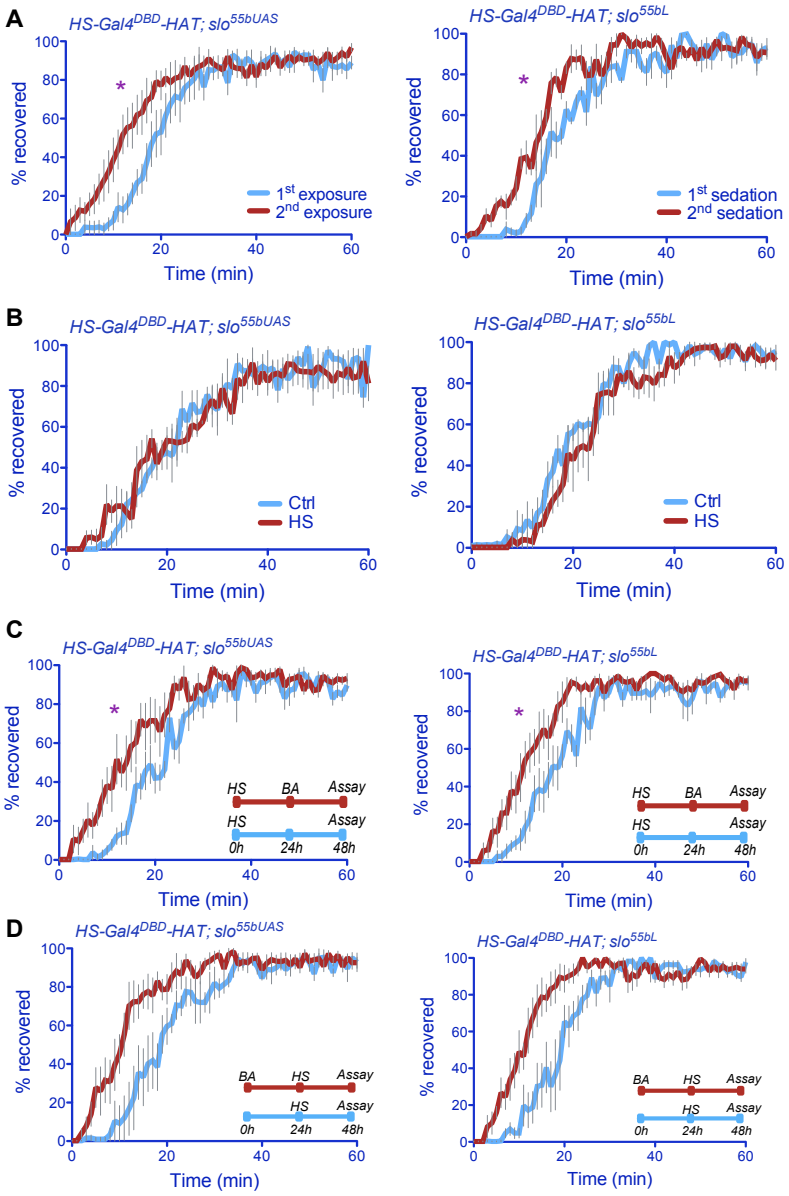

Figure 4.7. The *slo* message abundance in *HS-GAL4^{DBD}-HDAC; slo^{6bUAS}*. Animals were subjected to heat shock at 37°C for 1 h to induce the histone modifier transgene, and a benzyl alcohol sedation 24 h later. RNA was prepared 6 h after sedation. A) Benzyl alcohol did not increase *slo* message in *HS-GAL4^{DBD}-HDAC; slo^{6bUAS}* when HDAC was activated. B) Drug induced *slo* message in *GAL4^{DBD}-HDAC; slo^{6bL}* control animals. C, D) Docking of HAT at 55b region increase *slo* abundance in both *HS-GAL4^{DBD}-HAT; slo^{6bUAS}* and its control. Student's *t*-test, $*P \leq 0.05$. Error bars represent SEM.

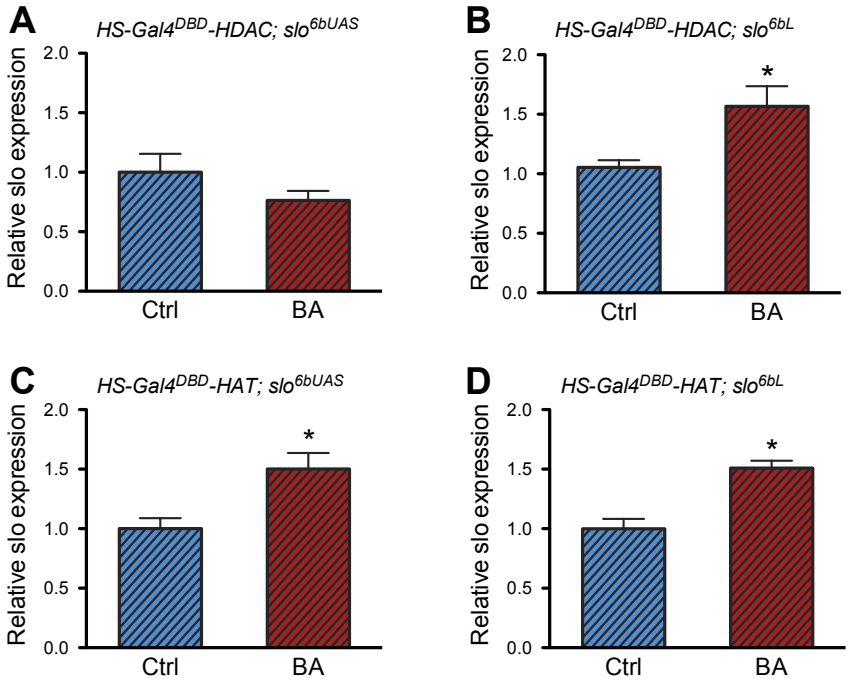

Figure 4.8. The *slo* message abundance in *HS-GAL4^{DBD}-HDAC; slo^{55bUAS}*. Animals were subjected to heat shock at 37°C for 1 h to induce the histone modifier transgene, and a benzyl alcohol sedation 24 h later. RNA was prepared 6 h after sedation. A) Benzyl alcohol did not increase *slo* message in *HS-GAL4^{DBD}-HDAC; slo^{55bUAS}* when HDAC was activated. B) Drug induced *slo* message in *GAL4^{DBD}-HDAC; slo^{55bL}* control animals. C, D) Docking of HAT at 55b region increase *slo* abundance in both *HS-GAL4^{DBD}-HAT; slo^{55bUAS}* and its control. Student's *t*-test, $*P \leq 0.05$. Error bars represent SEM.

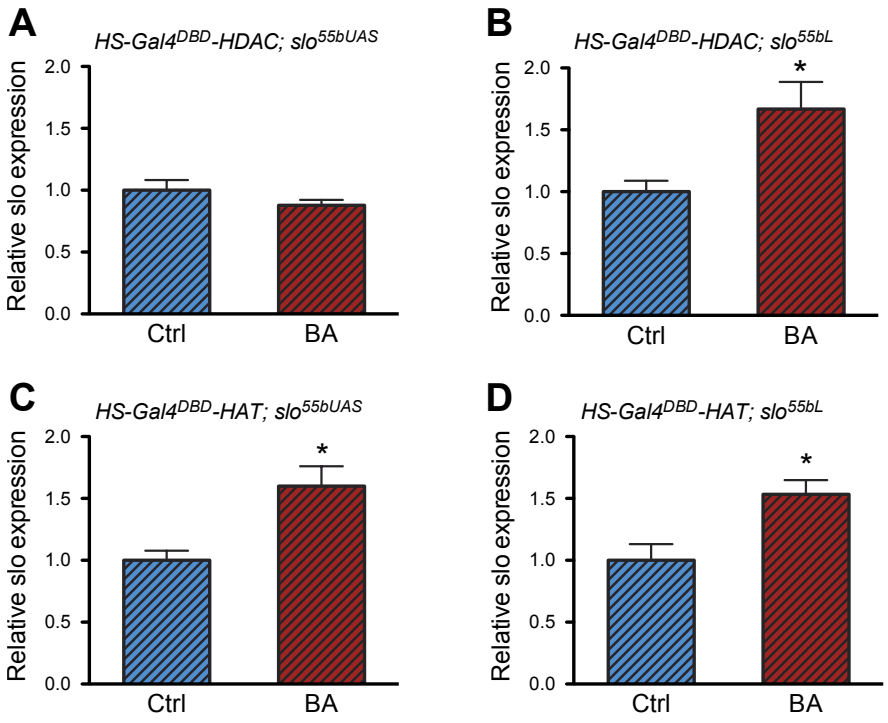

Figure 4.9. Tethering GAL4^{DBD} at the 55b element alone had no effect on tolerance. To investigate if GAL4^{DBD} also blocked *slo* induction and tolerance, *HS-GAL4^{DBD}*; *slo^{55bUAS}* animals were subjected to heat shock at 37°C for 1 h to induce GAL4^{DBD} that binds to the UAS motif adjacent to the 55b element. Twenty-three hours later, the animals received the first benzyl alcohol sedation, followed by tolerance assay one day later. RNA was prepared 6 h after the first drug exposure and quantitated by real time PCR using C1 primers that recognize the neural transcript variants. A) The *HS-GAL4^{DBD}*; *slo^{55bUAS}* stock and its control line acquired tolerance to benzyl alcohol after activating GAL4^{DBD}. B) The *slo* messages in both lines were induced. C&D) *slo* message was significantly induced in both lines.

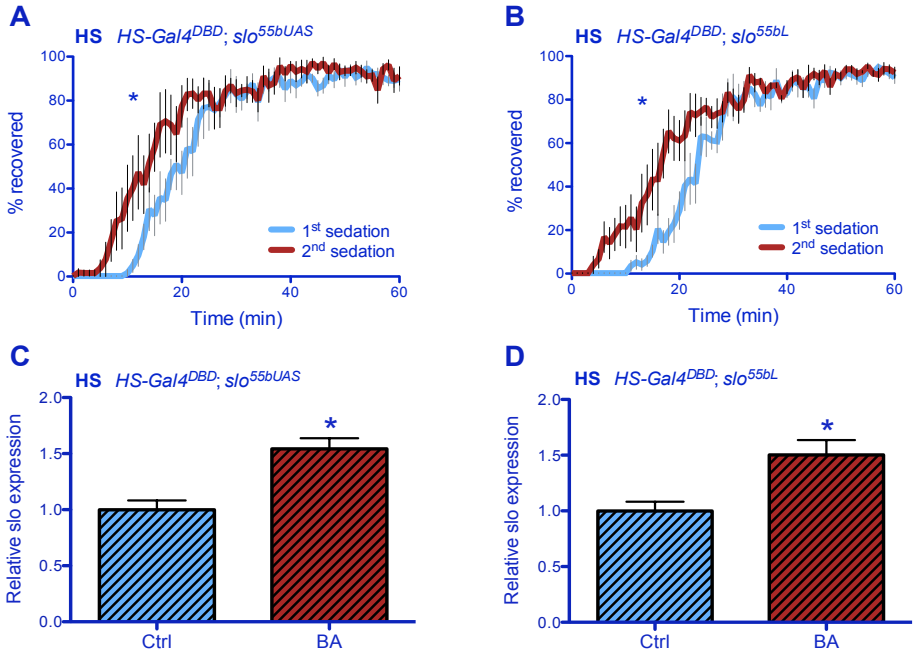

METHODS

Fly stocks

Flies were raised on standard cornmeal food and kept at 22°C in a 12:12 hrs light:dark cycle. Flies that emerged from pupae were collected over a 2-day period, transferred to fresh food, and studied three days later. Drosophila stocks were wild type CS, slo^{6bUAS}, slo^{55bUAS}, *hsf4*, $Gal4^{DBD}$, $Gal4^{DBD}$*:HAT* and $Gal4^{DBD}$*:HDAC*. The last three strains were from B. Calvi. *hsf4* is a temperature-sensitive allele from the Bloomington stock center (Bloomington IN). Adults homozygous for *hsf4* develop normally at permissive temperature (25°C and below) but not at 29°C or higher temperature[130].

Generation of slo^{6bUAS} and slo^{55bUAS} knock-in mutants

To generate the slo^{6bUAS} allele, a copy of the UAS sequence was inserted to the 5' end of the 6b DNA element in *slo* regulatory region using ends-out gene targeting strategy[88]. At first, the 5' homologous sequence containing a UAS next to the 6b element and the 3' homologous sequence were amplified by PCR using Canton S genomic DNA as the template and a proofreading *PfuTurbo* DNA polymerase (Stratagene CA). More specifically, primers 5'-GCGGCCGCACCACAAGTTCCCCAAAAC-3' and 5'-CGTATTTAAATTCTCAGTTCTCG-3' were used to amplify and add *Not*I and *Swa*I termini to the 5' end and the 3' end, respectively, to a 1 kb fragment upstream of the 6b element; primers 5'-TTTAAACGGAGTACTGTCCTCCGAACGGCGAGAATAGTGC TGATTTTG-3' and 5'-TAGCTTTGTTTGCCCACGA-3' were used to amplify and add a *Dra*I and a UAS site to the 5' end of a 0.4 kb fragment with the 6b located at the 5' end;

primers 5'-AATTAATTACCGCGTTCGTC-3' and 5'-ACTAGTGCATGCTCGCAAA GCAAACACACTC-3' were used in the PCR to amplify and add the *Sph*I and the *Spe*I sites to the 3' end of a 2.3 kb DNA fragment downstream of the 6b element. These three fragments were digested with corresponding restriction enzymes and ligated to form a 3.5 kb fragment before being inserted into the polylinker at 5' of *white*$^{+}$ gene marker in the ends-out vector pW25[95], between the *Not*I site and the *Sph*I site. While primers 5'-GGCGCGCCATTACAAATTAACACCCAGTTGTG-3' and 5'-CCTAGGCGAATTC GAAAAGCGTTAGC-3' were designed to amplify and add *Asc*I terminal to the 5' end, and add *Avr*II terminal to the 3' end of a 3 kb DNA fragment into the polylinker to the 3' end of *white*$^{+}$ gene in the vector. This donor construct was introduced into the *white*^{1118} fly by standard *P* element germline transformation. All the insertion lines were mapped for the location of the donor transgene, and lines with the donor transgene on the first or the second chromosome were utilized to induce gene targeting. The target gene *slo* is located on the third chromosome.

To induce targeting, donor insertion lines are crossed to the *P{hsp70FLP}P{hsp70I-SceI}* strain (Bloomington # 6934), and the progeny were heat-shocked at 38°C for one hour during their first three days of development to induce transgenic FLP and I-SceI that acted on their corresponding recognition sites in the ends-out vector. The donor fragment, including two pieces of homologous fragments and a *white*$^{+}$ in between, was hopped out from its original insertion site in a circular form under the action of FLP recombinase, and a double-strand break was introduced to linearize the

donor by restriction enzyme I-sceI. These changes allow pairing and crossover between the homologous fragments of donor and the targeted chromosomal 6b region. Thus that 6b was replaced by the *white*$^{+}$ from the donor sequence. Virgin females with *white*$^{+}$ and *P{hsp70FLP}P{hsp70I-SceI}* are collected and crossed to male FLP flies (Bloomington # 6938), and the progeny are screened for solid red eyes. The *white*$^{+}$ gene was mapped to identify targeted events in which *white*$^{+}$ was relocated to the target chromosome 3. And Southern blotting was carried out to further confirm targeted events occurred exactly in the designed position, and the targeted alleles were sequenced to confirm if they carry the UAS motif. Finally, the targeted strain was crossed to *P{Cre}* line (Bloomington # 1501) to remove the *white*$^{+}$ maker and obtain the UAS knock-in mutant *slo*^{6bUAS}. When the homologous recombination took place downstream of the UAS sequence in the donor, the control line *slo*^{6bL} was obtained that contains all the chromosomal background as the knock-in line, except for the UAS motif.

The *slo*^{55bUAS} allele was generated using the same strategy except that a UAS motif was inserted at the 5' end of the 55b DNA element. To build the donor construct, primers 5'-GCGGCCGCCAGGATACGCAGATACCCAGATAC-3' and 5'-GCATGCAATTGG ATTGAATTTAGAAGT-3' were used to amplify and a *Not*I site to the 5' end and a *Sph*I site to the 3' end, respectively, of a 3.2 kb fragment upstream of the 55b element. The fragment was inserted into the polylinker to the 5' end of *white*$^{+}$ in pW25. Primers 5'-GGCGCGCCTTGTGAGTGTGTTTGCTTTGC-3' and 5'-TTAATTAAAAGGCAGAG CGCCACGGAGGACAGTACTCCGAGACAAGGCGAATTCAATTGGGTATTGG-3'

were used to amplify and add an *Asc*I site to the 5' end, and add a copy of UAS sequence to the 3' end of a 1.2 kb fragment adjacent to the 5' end of the 55b element; primers 5'-CCTGCCGTTGTCTCTTCTTC-3' and 5'-CTGCAGCCTAGGCGAATTCGAAAAGC GTTAGC-3' were used to amplify and add an *Avr*II site to the 3' end of a 2 kb DNA fragment with the 55b element at the 5' end. The two fragments were digested and ligated to form a 3.2 kb fragment that was inserted into the polylinker to the 3' end of $white^{+}$ in the pW25 vector, between the *Asc*I site and *Avr*II site.

The slo^{6bUAS} and slo^{55bUAS} lines were crossed to stocks expressing histone acetylation modifiers ($Gal4^{DBD}$-HDAC and $Gal4^{DBD}$-HAT) to tether the histone acetyaltion modifying protein to either the 6b element or the 55b element. The derived double mutants were subjected to the benzyl alcohol exposure and tolerance assay.

Southern blotting analysis

Southern blot analyses were performed to verify the knock-in targeting events using a DIG kit (Roche Diagnostics, IN) as recommended by the manufacturer. Genomic DNA was prepared from flies carrying the targeted allele and wild type, followed by overnight digestion with *Hind*III (NEB, MA), separated by agarose gel electrophoresis and transferred to nylon membranes as described[96]. The probe DNA in use was the 3' homologous fragment of donor construct. The blot was hybridized to the digoxigenin (DIG) labeled probe and was detected by DIG antibody and chemiluminescence signal.

Benzyl alcohol exposure and tolerance assay

The benzyl alcohol exposure and tolerance assay were conducted as described in Chapter 2. To activate the heat-inducible Hdac/Hat transgene, the animals were subjected to a 60 min heat shock at 37°C 24 h before the first drug exposure, and 48 h before the tolerance assay. Alternatively, heat shock was conducted 24 h after the first drug exposure, and 24 h before the tolerance assay.

Quantitative RT-PCR analysis

Animals were subjected to heat shock at 37°C for 1 h to induce the histone modifier transgene (HDAC or HAT), and a benzyl alcohol sedation 24 h later. RNA was prepared from fly body 6 h after the first sedation. The quantitive RT-PCR was conducted as described in Chapter 2.

Chapter 5: Conclusions and future directions

SUMMARY AND CONCLUSIONS

Drug tolerance and withdrawal are insidious responses to drugs of abuse; the first increases drug consumption while the second punishes abstention. These two endophenotypes of addiction are thought have a common origin in the homeostatic adaptations triggered to counter the drug effects. The very adaptations that cause drug tolerance by reducing the response to the drug also generate symptoms of withdrawal after drug clearance. Drosophila generate functional tolerance to benzyl alcohol sedation by increasing neural expression of the *slo* BK channel gene. While this homeostatic response counters the effects of the anesthetic, the persistence of the response after drug clearance produces a withdrawal phenotype-an increase in the susceptibility to seizures[53].

Benzyl alcohol induces histone acetylation across the *slo* control region, and enhanced histone acetylation has been detected over two highly conserved DNA regulatory elements–6b and 55b. To investigate the function of these two elements, I generated individual knock-out mutants through Ends-Out gene targeting. Both of the deletions affected the epigenetic profile and the animal's behavior. The 6b deletion caused the animal to overreact to benzyl alcohol. It significantly enhanced drug-induced *slo* expression but did not affect basal *slo* expression. The deletion of 6b prolonged the duration of tolerance. In wild type flies tolerance only lasts about one week, however, the 6b deletion mutant showed a persistent tolerance that lasts at least a month. It also increased the physiological response to drug sedation. The ablation of 55b element did

not affect the ability to acquire tolerance, nor the effect of drug sedation on *slo* induction. However, the 55b mutant did show increased basal muscle expression and an increase in locomotor activity. Thus the 6b element has been identified as a drug-responsive negative regulator of the *slo* neural expression and the 55b element has been identified as a regulator of basal *slo* muscle expression.

To manipulate the endogenous acetylation level over 6b and 55b elements, I built another two mutants that have a UAS sequence next to each element. These UAS mutants were crossed to a transgenic fly carrying a heat shock promoter driven $GAL4^{DBD}$-HDAC (GAL4 DNA binding domain linked histone deacetylase) or $GAL4^{DBD}$-HAT (GAL4 DNA binding domain linked histone acetylase). The derived double mutants were heat-shocked to induce the expression of HDAC or HAT, and tested for the ability to acquire drug tolerance. I found that activation of a HDAC transgene blocked *slo* induction and the ability to acquire functional tolerance. Therefore, the local histone acetylation status across *slo* promoter region plays an important role in the activation of *slo* and the development of tolerance.

FUTURE DIRECTIONS

To further explore how the 6b element regulates *slo* expression and drug responses.

In this study, the 6b DNA element is characterized as a repressive regulator of *slo* expression after benzyl alcohol sedation. By controlling neural *slo* expression, it also alters multiple drug responses, such as tolerance and withdrawal syndromes. The mutation increased the magnitude of the neural *slo* induction after benzyl alcohol

sedation, but the duration was not prolonged. The 6b deletion mutant also showed extremely prolonged tolerance (28 days), while the behavioral changes in withdrawal phenotypes did not show abnormally long persistence.

How can I reconcile the difference in the duration of *slo* expression, tolerance, and the withdrawal phenotypes in the 6b mutant? It is possible that tolerance and the withdrawal phenotypes arise from different structures in the brain. In this scenario, the time-course of the $slo^{\Delta 6b}$ expression in the neurons that produce tolerance would be longer than in the neural structures that produce the withdrawal phenotype. If this is the case, then one must also account for why long-lasting *slo* induction was not observed in $slo^{\Delta 6b}$. This might occur if tolerance is produced by a small brain region whose persistent induction cannot be detected in our whole brain mRNA assays. To resolve these issues, future studies should focus on measuring brain specific levels of *slo* expression in the nervous system after drug exposure. Unfortunately, Drosophila *in situ* hybridization does not have either sufficient sensitivity or a signal-to-noise ratio that makes it useful for this purpose. Furthermore, I do not have an appropriate Drosophila-specific BK channel antibody to trace the dynamic change of *slo* expression in the nervous system after drug sedation. A more modern solution to solve the lack of SLO-specific antibodies would be to epitope-tag the BK channel gene (in the slod6b background) as a way to provide a traceable *slo* protein.

To study the role of transcription factor HSF on tolerance.

A putative HSE, the binding site of transcription factor HSF (heat shock factor), has been identified in the 6b DNA element[68]. HSF stays in an inactive state in unstressed

cells and becomes activated in response to stress. HSF and the stress pathway protect mammals and flies against the stressor and many other insults, such as ethanol intoxication[131,132]. In flies, a brief heat pulse results in a reduction in *slo* expression[13]. I hypothesize that the transcription factor HSF might play a role in drug-induced *slo* activation and the development of tolerance (see Chapter 2, discussion).

To test this hypothesis, I used a temperature sensitive *hsf4* allele to determine if HSF is involved in producing tolerance. In the assay, female *hsf4* and wild type flies were kept at 18°C after eclosion. On day 3, flies were transferred to a 30°C incubator (with a light-dark 12:12 cycle) for 30 min to inactivate the HSF transcription factor. This was immediately followed by benzyl alcohol sedation or mock sedation. These animals were allowed to recover from sedation at 30°C. Twenty-two hours (at 30°C) after the first benzyl alcohol exposure, flies were incubated at 18°C for 30 min to reduce the net effect of heat on the neural activity. One and a half hours later (24 hours post benzyl alcohol exposure), flies were subjected to the tolerance assay at room temperature. In parallel, the *hsf4* and wild type flies that had been maintained at 18°C were also tested for the capacity to acquire tolerance. The *slo* message abundance in these animals was also quantified.

As shown in Fig. 5.1 and Fig. 5.2, the homozygous *hsf4* mutant acquired tolerance at the permissive temperature (18°C), and the *slo* gene was induced after sedation. While at the restrictive temperature (30°C), the *hsf4* mutation blocked tolerance and benzyl alcohol-induced *slo* induction. In contrast, the wild type CS flies were able to develop tolerance and induce *slo* expression after sedation at either temperature (18°C and 30°C).

These results suggest that HSF is required for the drug-induced *slo* activation and the development of tolerance. Future studies should be directed to examine whether the HSF transcription factor binds within the *slo* control region (especially the 6b element). Identification of another transcription factor that helps to mediate *slo*-dependent drug tolerance will greatly enrich our understanding of this drug response.

Figure 5.1. The *hsf4* mutation blocked rapid tolerance to benzyl alcohol sedation. *Hsf4* is a temperature sensitive mutant of the transcription factor HSF. At the permissive temperature (18°C) both the mutant and CS wild type flies acquired tolerance (A, B). At the restrictive temperature (30°C), the disruption of HSF blocked tolerance in the mutant (C), while the CS animals still acquired tolerance (D).

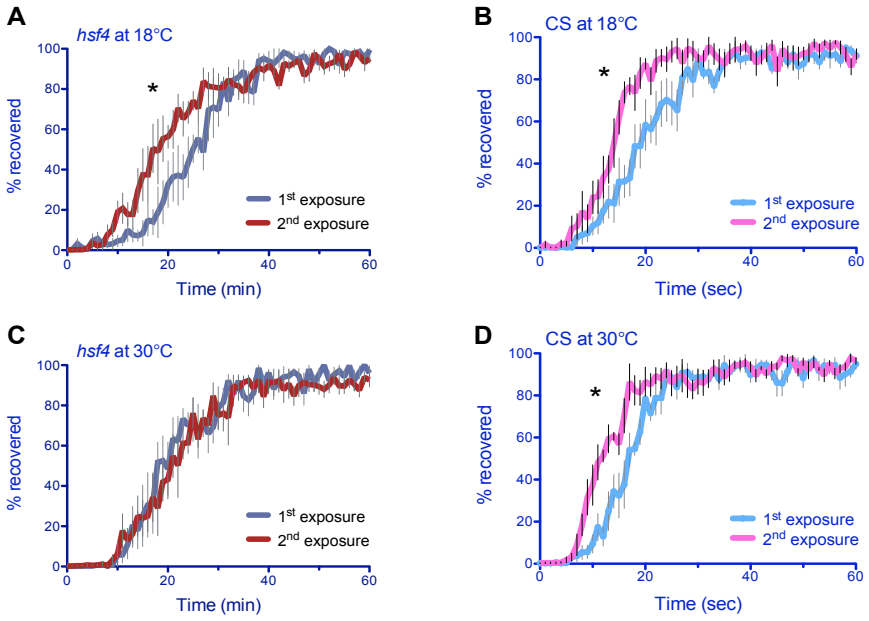

Figure 5.2. The *hsf4* mutation blocked benzyl alcohol induced *slo* transcriptional activation. Benzyl alcohol induced *slo* transcription at 18°C in both the ts mutant line (A) and the CS control line (B). At 30°C, *slo* expression in the *hsf4* mutant was not induced by the drug (C), while CS still showed *slo* induction (D).

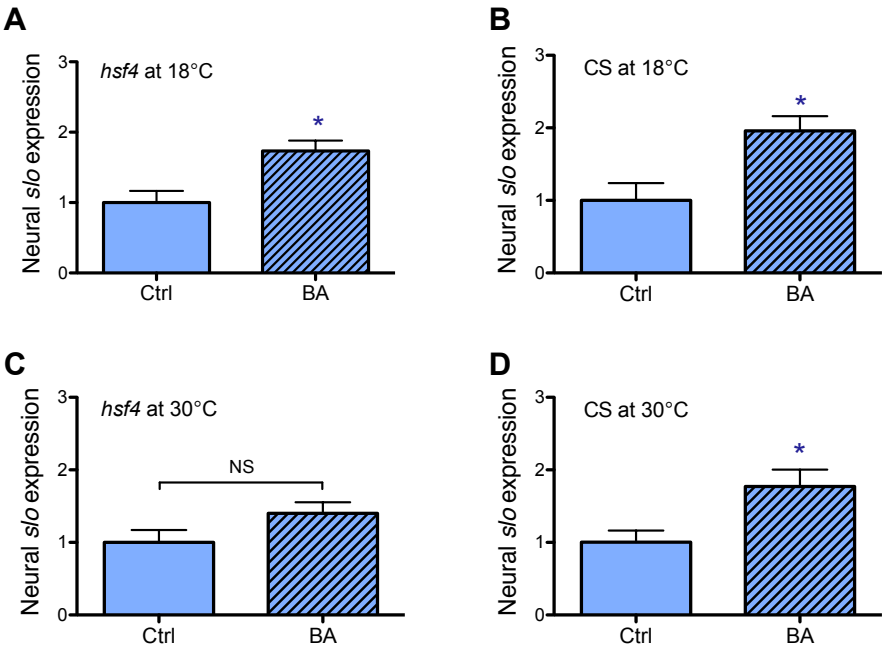

References

1. Sellers, E. M. Addictive drugs: disposition, tolerance, and dependence interrelationships. *Drug Metab Rev* **8**, 5-11 (1978).
2. Littleton, J. & Little, H. Current concepts of ethanol dependence. *Addiction* **89**, 1397-1412 (1994).
3. Koob, G. F. & Nestler, E. J. The neurobiology of drug addiction. *J Neuropsychiatry Clin Neurosci* **9**, 482-497 (1997).
4. Goeders, N. E. The impact of stress on addiction. *Eur Neuropsychopharmacol* **13**, 435-441 (2003).
5. Julien, R. M. *A primer of drug action (primer of drug actons: a concise, nontechnical guide to the actions, uses, and side effects of psychoactive drugs* (New York: Worth Publishers Inc, 2004).
6. Danaei, G. et al. The preventable causes of death in the United States: comparative risk assessment of dietary, lifestyle, and metabolic risk factors. *PLoS Med* **6**, e1000058 (2009).
7. Harwood, H. Updating estimates of the economic costs of alcohol abuse in the United States: estimates, update methods and data. Report prepared by the Lewin Group for the National Institute on Alcohol Abuse and Alcoholism. (2000).
8. McCloskey, S. E., Gershanik, J. J., Lertora, J. J., White, L. & George, W. J. Toxicity of benzyl alcohol in adult and neonatal mice. *J Pharm Sci* **75**, 702-705 (1986).
9. Macht, D. I. A pharmacological and therapeutic study of benzyl alcohol as a local anesthetic. *J Pharmacol Exp Ther* **11**, 263-279 (1918).
10. Wilson, L. & Martin, S. Benzyl alcohol as an alternative local anesthetic. *Ann Emerg Med* **33**, 495-499 (1999).
11. Minogue, S. C. & Sun, D. A. Bacteriostatic saline containing benzyl alcohol decreases the pain associated with the injection of propofol. *Anesth Analg* **100**, 683-6, table of contents (2005).
12. Kimura, E. T., Darby, T. D., Krause, R. A. & Brondyk, H. D. Parenteral toxicity studies with benzyl alcohol. *Toxicol Appl Pharmacol* **18**, 60-68 (1971).
13. Ghezzi, A., Al-Hasan, Y. M., Larios, L. E., Bohm, R. A. & Atkinson, N. S. slo K(+) channel gene regulation mediates rapid drug tolerance. *Proc Natl Acad Sci U S A* **101**, 17276-17281 (2004).
14. Latorre, R., Morera, F. J. & Zaelzer, C. Allosteric interactions and the modular nature of the voltage- and Ca2+-activated (BK) channel. *J Physiol* **588**, 3141-3148 (2010).
15. Knaus, H. G. et al. Distribution of high-conductance Ca(2+)-activated K+ channels in rat brain: targeting to axons and nerve terminals. *J Neurosci* **16**, 955-963 (1996).
16. Marrion, N. V. & Tavalin, S. J. Selective activation of Ca2+-activated K+ channels by co-localized Ca2+ channels in hippocampal neurons. *Nature* **395**, 900-905 (1998).
17. Jiang, Y., Pico, A., Cadene, M., Chait, B. T. & MacKinnon, R. Structure of the RCK domain from the E. coli K+ channel and demonstration of its presence in the human BK channel. *Neuron* **29**, 593-601 (2001).
18. Yuan, P., Leonetti, M. D., Pico, A. R., Hsiung, Y. & MacKinnon, R. Structure of

the human BK channel Ca2+-activation apparatus at 3.0 A resolution. *Science* **329**, 182-186 (2010).
19. Nelson, A. B., Krispel, C. M., Sekirnjak, C. & du Lac, S. Long-lasting increases in intrinsic excitability triggered by inhibition. *Neuron* **40**, 609-620 (2003).
20. Brayden, J. E. & Nelson, M. T. Regulation of arterial tone by activation of calcium-dependent potassium channels. *Science* **256**, 532-535 (1992).
21. Petkov, G. V. et al. Beta1-subunit of the Ca2+-activated K+ channel regulates contractile activity of mouse urinary bladder smooth muscle. *J Physiol* **537**, 443-452 (2001).
22. Hu, H. et al. Presynaptic Ca2+-activated K+ channels in glutamatergic hippocampal terminals and their role in spike repolarization and regulation of transmitter release. *J Neurosci* **21**, 9585-9597 (2001).
23. Pyott, S. J., Glowatzki, E., Trimmer, J. S. & Aldrich, R. W. Extrasynaptic localization of inactivating calcium-activated potassium channels in mouse inner hair cells. *J Neurosci* **24**, 9469-9474 (2004).
24. Knott, T. K., Dopico, A. M., Dayanithi, G., Lemos, J. & Treistman, S. N. Integrated channel plasticity contributes to alcohol tolerance in neurohypophysial terminals. *Mol Pharmacol* **62**, 135-142 (2002).
25. Atkinson, N. S., Robertson, G. A. & Ganetzky, B. A component of calcium-activated potassium channels encoded by the Drosophila slo locus. *Science* **253**, 551-555 (1991).
26. Adelman, J. P. et al. Calcium-activated potassium channels expressed from cloned complementary DNAs. *Neuron* **9**, 209-216 (1992).
27. Bohm, R. A., Wang, B., Brenner, R. & Atkinson, N. S. Transcriptional control of Ca(2+)-activated K(+) channel expression: identification of a second, evolutionarily conserved, neuronal promoter. *J Exp Biol* **203**, 693-704 (2000).
28. Becker, M. N., Brenner, R. & Atkinson, N. S. Tissue-specific expression of a Drosophila calcium-activated potassium channel. *J Neurosci* **15**, 6250-6259 (1995).
29. Brenner, R., Thomas, T. O., Becker, M. N. & Atkinson, N. S. Tissue-specific expression of a Ca(2+)-activated K+ channel is controlled by multiple upstream regulatory elements. *J Neurosci* **16**, 1827-1835 (1996).
30. Brenner, R. & Atkinson, N. S. Calcium-activated potassium channel gene expression in the midgut of Drosophila. *Comp Biochem Physiol B Biochem Mol Biol* **118**, 411-420 (1997).
31. Yu, J. Y., Upadhyaya, A. B. & Atkinson, N. S. Tissue-specific alternative splicing of BK channel transcripts in Drosophila. *Genes Brain Behav* **5**, 329-339 (2006).
32. Lagrutta, A., Shen, K. Z., North, R. A. & Adelman, J. P. Functional differences among alternatively spliced variants of Slowpoke, a Drosophila calcium-activated potassium channel. *J Biol Chem* **269**, 20347-20351 (1994).
33. Tanaka, Y. et al. Beta1-subunit of MaxiK channel in smooth muscle: a key molecule which tunes muscle mechanical activity. *J Pharmacol Sci* **94**, 339-347 (2004).
34. Uebele, V. N. et al. Cloning and functional expression of two families of beta-subunits of the large conductance calcium-activated K+ channel. *J Biol Chem* **275**, 23211-23218 (2000).
35. Brenner, R., Jegla, T. J., Wickenden, A., Liu, Y. & Aldrich, R. W. Cloning and functional characterization of novel large conductance calcium-activated potassium channel beta subunits, hKCNMB3 and hKCNMB4. *J Biol Chem* **275**, 6453-6461

(2000).
36. Schopperle, W. M. et al. Slob, a novel protein that interacts with the Slowpoke calcium-dependent potassium channel. *Neuron* **20**, 565-573 (1998).
37. Ma, H., Zhang, J. & Levitan, I. B. Slob, a Slowpoke channel-binding protein, modulates synaptic transmission. *J Gen Physiol* **137**, 225-238 (2011).
38. Tian, L. et al. Alternative splicing switches potassium channel sensitivity to protein phosphorylation. *J Biol Chem* **276**, 7717-7720 (2001).
39. Schubert, R. & Nelson, M. T. Protein kinases: tuners of the BKCa channel in smooth muscle. *Trends Pharmacol Sci* **22**, 505-512 (2001).
40. Liu, J., Asuncion-Chin, M., Liu, P. & Dopico, A. M. CaM kinase II phosphorylation of slo Thr107 regulates activity and ethanol responses of BK channels. *Nat Neurosci* **9**, 41-49 (2006).
41. Alioua, A. et al. Coupling of c-Src to large conductance voltage- and Ca2+-activated K+ channels as a new mechanism of agonist-induced vasoconstriction. *Proc Natl Acad Sci U S A* **99**, 14560-14565 (2002).
42. Dopico, A. M., Anantharam, V. & Treistman, S. N. Ethanol increases the activity of Ca(++)-dependent K+ (mslo) channels: functional interaction with cytosolic Ca++. *J Pharmacol Exp Ther* **284**, 258-268 (1998).
43. Davies, A. G. et al. A central role of the BK potassium channel in behavioral responses to ethanol in C. elegans. *Cell* **115**, 655-666 (2003).
44. Dopico, A. M., Widmer, H., Wang, G., Lemos, J. R. & Treistman, S. N. Rat supraoptic magnocellular neurones show distinct large conductance, Ca2+-activated K+ channel subtypes in cell bodies versus nerve endings. *J Physiol* **519 Pt 1**, 101-114 (1999).
45. Pietrzykowski, A. Z. et al. Alcohol tolerance in large-conductance, calcium-activated potassium channels of CNS terminals is intrinsic and includes two components: decreased ethanol potentiation and decreased channel density. *J Neurosci* **24**, 8322-8332 (2004).
46. Cowmeadow, R. B., Krishnan, H. R. & Atkinson, N. S. The slowpoke gene is necessary for rapid ethanol tolerance in Drosophila. *Alcohol Clin Exp Res* **29**, 1777-1786 (2005).
47. Cowmeadow, R. B. et al. Ethanol tolerance caused by slowpoke induction in Drosophila. *Alcohol Clin Exp Res* **30**, 745-753 (2006).
48. Warbington, L., Hillman, T., Adams, C. & Stern, M. Reduced transmitter release conferred by mutations in the slowpoke-encoded Ca2(+)-activated K+ channel gene of Drosophila. *Invert Neurosci* **2**, 51-60 (1996).
49. Lovell, P. V. & McCobb, D. P. Pituitary control of BK potassium channel function and intrinsic firing properties of adrenal chromaffin cells. *J Neurosci* **21**, 3429-3442 (2001).
50. Pattillo, J. M. et al. Contribution of presynaptic calcium-activated potassium currents to transmitter release regulation in cultured Xenopus nerve-muscle synapses. *Neuroscience* **102**, 229-240 (2001).
51. Van Goor, F., Li, Y. X. & Stojilkovic, S. S. Paradoxical role of large-conductance calcium-activated K+ (BK) channels in controlling action potential-driven Ca2+ entry in anterior pituitary cells. *J Neurosci* **21**, 5902-5915 (2001).
52. Brenner, R. et al. BK channel beta4 subunit reduces dentate gyrus excitability and protects against temporal lobe seizures. *Nat Neurosci* **8**, 1752-1759 (2005).
53. Ghezzi, A., Pohl, J. B., Wang, Y. & Atkinson, N. S. BK channels play a counter-

adaptive role in drug tolerance and dependence. *Proc Natl Acad Sci U S A* **107**, 16360-16365 (2010).
54. Levenson, J. M. & Sweatt, J. D. Epigenetic mechanisms in memory formation. *Nat Rev Neurosci* **6**, 108-118 (2005).
55. Bird, A. Perceptions of epigenetics. *Nature* **447**, 396-398 (2007).
56. Kouzarides, T. Chromatin modifications and their function. *Cell* **128**, 693-705 (2007).
57. Weaver, R. F. *Molecular biology* (Mcgraw-Hill, New York, 2007).
58. Dhalluin, C. et al. Structure and ligand of a histone acetyltransferase bromodomain. *Nature* **399**, 491-496 (1999).
59. Jacobson, R. H., Ladurner, A. G., King, D. S. & Tjian, R. Structure and function of a human TAFII250 double bromodomain module. *Science* **288**, 1422-1425 (2000).
60. Kurdistani, S. K., Tavazoie, S. & Grunstein, M. Mapping global histone acetylation patterns to gene expression. *Cell* **117**, 721-733 (2004).
61. Pokholok, D. K. et al. Genome-wide map of nucleosome acetylation and methylation in yeast. *Cell* **122**, 517-527 (2005).
62. Li, B., Carey, M. & Workman, J. L. The role of chromatin during transcription. *Cell* **128**, 707-719 (2007).
63. Vakoc, C. R., Mandat, S. A., Olenchock, B. A. & Blobel, G. A. Histone H3 lysine 9 methylation and HP1gamma are associated with transcription elongation through mammalian chromatin. *Mol Cell* **19**, 381-391 (2005).
64. Peters, A. H. et al. Partitioning and plasticity of repressive histone methylation states in mammalian chromatin. *Mol Cell* **12**, 1577-1589 (2003).
65. Mahadevan, L. C., Willis, A. C. & Barratt, M. J. Rapid histone H3 phosphorylation in response to growth factors, phorbol esters, okadaic acid, and protein synthesis inhibitors. *Cell* **65**, 775-783 (1991).
66. Kumar, A. et al. Chromatin remodeling is a key mechanism underlying cocaine-induced plasticity in striatum. *Neuron* **48**, 303-314 (2005).
67. Levine, A. A. et al. CREB-binding protein controls response to cocaine by acetylating histones at the fosB promoter in the mouse striatum. *Proc Natl Acad Sci U S A* **102**, 19186-19191 (2005).
68. Wang, Y., Krishnan, H. R., Ghezzi, A., Yin, J. C. & Atkinson, N. S. Drug-induced epigenetic changes produce drug tolerance. *PLoS Biol* **5**, 2342-2353 (2007).
69. Wang, Y., Ghezzi, A., Yin, J. C. & Atkinson, N. S. CREB regulation of BK channel gene expression underlies rapid drug tolerance. *Genes Brain Behav* **8**, 369-376 (2009).
70. Adams, M. D. et al. The genome sequence of Drosophila melanogaster. *Science* **287**, 2185-2195 (2000).
71. Lloyd, T. E. et al. A genome-wide search for synaptic vesicle cycle proteins in Drosophila. *Neuron* **26**, 45-50 (2000).
72. Littleton, J. T. & Ganetzky, B. Ion channels and synaptic organization: analysis of the Drosophila genome. *Neuron* **26**, 35-43 (2000).
73. Rubin, G. M. et al. Comparative genomics of the eukaryotes. *Science* **287**, 2204-2215 (2000).
74. Bell, A. J., McBride, S. M. & Dockendorff, T. C. Flies as the ointment: Drosophila modeling to enhance drug discovery. *Fly (Austin)* **3**, 39-49 (2009).
75. Mackay, T. F. & Anholt, R. R. Of flies and man: Drosophila as a model for human complex traits. *Annu Rev Genomics Hum Genet* **7**, 339-367 (2006).

76. Sokolowski, M. B. Drosophila: genetics meets behaviour. *Nat Rev Genet* **2**, 879-890 (2001).
77. Pick, S. & Strauss, R. Goal-driven behavioral adaptations in gap-climbing Drosophila. *Curr Biol* **15**, 1473-1478 (2005).
78. Tinette, S., Zhang, L. & Robichon, A. Cooperation between Drosophila flies in searching behavior. *Genes Brain Behav* **3**, 39-50 (2004).
79. Koob, G. F. & Le, M., Michel. *Neurobiology of addiction* (Elsevier Academic Press, Amsterdam ; Boston, 2006).
80. Martin, W. R. XVI. A homeostatic and redundancy theory of tolerance to and dependence on narcotic analgesics. *Res Publ Assoc Res Nerv Ment Dis* **46**, 206-225 (1968).
81. Del Re, A. M., Dopico, A. M. & Woodward, J. J. Effects of the abused inhalant toluene on ethanol-sensitive potassium channels expressed in oocytes. *Brain Res* **1087**, 75-82 (2006).
82. Crowder, C. M. Ethanol targets: a BK channel cocktail in C. elegans. *Trends Neurosci* **27**, 579-582 (2004).
83. Dopico, A. M., Lemos, J. R. & Treistman, S. N. Ethanol increases the activity of large conductance, Ca(2+)-activated K+ channels in isolated neurohypophysial terminals. *Mol Pharmacol* **49**, 40-48 (1996).
84. Pietrzykowski, A. Z. et al. Posttranscriptional regulation of BK channel splice variant stability by miR-9 underlies neuroadaptation to alcohol. *Neuron* **59**, 274-287 (2008).
85. Alhasan, Y. M. Mechanisms of benzyl alcohol tolerance in Drosophila melanogaster. (2009).
86. Fry, C. J. & Farnham, P. J. Context-dependent transcriptional regulation. *J Biol Chem* **274**, 29583-29586 (1999).
87. Heintzman, N. D. et al. Distinct and predictive chromatin signatures of transcriptional promoters and enhancers in the human genome. *Nat Genet* **39**, 311-318 (2007).
88. Gong, W. J. & Golic, K. G. Ends-out, or replacement, gene targeting in Drosophila. *Proc Natl Acad Sci U S A* **100**, 2556-2561 (2003).
89. Ceriani, M. F. et al. Genome-wide expression analysis in Drosophila reveals genes controlling circadian behavior. *J Neurosci* **22**, 9305-9319 (2002).
90. Zeng, L. H., Rensing, N. R. & Wong, M. The mammalian target of rapamycin signaling pathway mediates epileptogenesis in a model of temporal lobe epilepsy. *J Neurosci* **29**, 6964-6972 (2009).
91. Etherington, J. M. Emergency management of acute alcohol problems. Part 1: Uncomplicated withdrawal. *Can Fam Physician* **42**, 2186-2190 (1996).
92. Atkinson, N. S. et al. Molecular separation of two behavioral phenotypes by a mutation affecting the promoters of a Ca-activated K channel. *J Neurosci* **20**, 2988-2993 (2000).
93. Spencer, V. A. & Davie, J. R. Role of covalent modifications of histones in regulating gene expression. *Gene* **240**, 1-12 (1999).
94. Fritah, S. et al. Heat-shock factor 1 controls genome-wide acetylation in heat-shocked cells. *Mol Biol Cell* **20**, 4976-4984 (2009).
95. Gong, W. J. & Golic, K. G. Genomic deletions of the Drosophila melanogaster Hsp70 genes. *Genetics* **168**, 1467-1476 (2004).
96. Ausubel, F. M. *Current protocols in molecular biology* (J. Wiley, Hoboken, NJ,

2001).
97. Ramazani, R. B., Krishnan, H. R., Bergeson, S. E. & Atkinson, N. S. Computer automated movement detection for the analysis of behavior. *J Neurosci Methods* **162**, 171-179 (2007).
98. Bland, J. M. & Altman, D. G. The logrank test. *BMJ* **328**, 1073 (2004).
99. Bewick, V., Cheek, L. & Ball, J. Statistics review 12: survival analysis. *Crit Care* **8**, 389-394 (2004).
100. Feany, M. B. & Bender, W. W. A Drosophila model of Parkinson's disease. *Nature* **404**, 394-398 (2000).
101. Brenner, R. et al. Complementation of physiological and behavioral defects by a slowpoke Ca(2+) -activated K(+) channel transgene. *J Neurochem* **75**, 1310-1319 (2000).
102. Levine, J. D., Funes, P., Dowse, H. B. & Hall, J. C. Signal analysis of behavioral and molecular cycles. *BMC Neurosci* **3**, 1 (2002).
103. Chang, W. M. et al. Muscle-specific transcriptional regulation of the slowpoke Ca(2+)-activated K(+) channel gene. *J Biol Chem* **275**, 3991-3998 (2000).
104. Crepaldi, L. & Riccio, A. Chromatin learns to behave. *Epigenetics* **4**, 23-26 (2009).
105. Renthal, W. & Nestler, E. J. Histone acetylation in drug addiction. *Semin Cell Dev Biol* **20**, 387-394 (2009).
106. Rong, Y. S. & Golic, K. G. Gene targeting by homologous recombination in Drosophila. *Science* **288**, 2013-2018 (2000).
107. Schuckit, M. A. & Smith, T. L. The relationships of a family history of alcohol dependence, a low level of response to alcohol and six domains of life functioning to the development of alcohol use disorders. *J Stud Alcohol* **61**, 827-835 (2000).
108. Newell, C. L., Deisseroth, A. B. & Lopez-Berestein, G. Interaction of nuclear proteins with an AP-1/CRE-like promoter sequence in the human TNF-alpha gene. *J Leukoc Biol* **56**, 27-35 (1994).
109. Wotton, D., Lo, R. S., Swaby, L. A. & Massague, J. Multiple modes of repression by the Smad transcriptional corepressor TGIF. *J Biol Chem* **274**, 37105-37110 (1999).
110. Wotton, D., Lo, R. S., Lee, S. & Massague, J. A Smad transcriptional corepressor. *Cell* **97**, 29-39 (1999).
111. Dutton, J. R., Johns, S. & Miller, B. L. StuAp is a sequence-specific transcription factor that regulates developmental complexity in Aspergillus nidulans. *EMBO J* **16**, 5710-5721 (1997).
112. Karin, M., Liu, Z. & Zandi, E. AP-1 function and regulation. *Curr Opin Cell Biol* **9**, 240-246 (1997).
113. Arias, J. et al. Activation of cAMP and mitogen responsive genes relies on a common nuclear factor. *Nature* **370**, 226-229 (1994).
114. Kwok, R. P. et al. Nuclear protein CBP is a coactivator for the transcription factor CREB. *Nature* **370**, 223-226 (1994).
115. Hai, T. & Curran, T. Cross-family dimerization of transcription factors Fos/Jun and ATF/CREB alters DNA binding specificity. *Proc Natl Acad Sci U S A* **88**, 3720-3724 (1991).
116. Masquilier, D. & Sassone-Corsi, P. Transcriptional cross-talk: nuclear factors CREM and CREB bind to AP-1 sites and inhibit activation by Jun. *J Biol Chem* **267**, 22460-22466 (1992).
117. Bannister, A. J. & Kouzarides, T. The CBP co-activator is a histone

acetyltransferase. *Nature* **384**, 641-643 (1996).
118. Wingender, E., Dietze, P., Karas, H. & Knuppel, R. TRANSFAC: a database on transcription factors and their DNA binding sites. *Nucleic Acids Res* **24**, 238-241 (1996).
119. Khurana, S., Li, W. K. & Atkinson, N. S. Image enhancement for tracking the translucent larvae of Drosophila melanogaster. *PLoS One* **5**, e15259 (2010).
120. Aggarwal, B. D. & Calvi, B. R. Chromatin regulates origin activity in Drosophila follicle cells. *Nature* **430**, 372-376 (2004).
121. Turner, B. M. Histone acetylation and an epigenetic code. *Bioessays* **22**, 836-845 (2000).
122. Workman, J. L. & Kingston, R. E. Alteration of nucleosome structure as a mechanism of transcriptional regulation. *Annu Rev Biochem* **67**, 545-579 (1998).
123. Cho, Y., Griswold, A., Campbell, C. & Min, K. T. Individual histone deacetylases in Drosophila modulate transcription of distinct genes. *Genomics* **86**, 606-617 (2005).
124. Mottus, R., Sobel, R. E. & Grigliatti, T. A. Mutational analysis of a histone deacetylase in Drosophila melanogaster: missense mutations suppress gene silencing associated with position effect variegation. *Genetics* **154**, 657-668 (2000).
125. de Ruijter, A. J., van Gennip, A. H., Caron, H. N., Kemp, S. & van Kuilenburg, A. B. Histone deacetylases (HDACs): characterization of the classical HDAC family. *Biochem J* **370**, 737-749 (2003).
126. Voss, A. K. & Thomas, T. MYST family histone acetyltransferases take center stage in stem cells and development. *Bioessays* **31**, 1050-1061 (2009).
127. Miotto, B. et al. Chameau HAT and DRpd3 HDAC function as antagonistic cofactors of JNK/AP-1-dependent transcription during Drosophila metamorphosis. *Genes Dev* **20**, 101-112 (2006).
128. Grienenberger, A. et al. The MYST domain acetyltransferase Chameau functions in epigenetic mechanisms of transcriptional repression. *Curr Biol* **12**, 762-766 (2002).
129. Carrozza, M. J., Utley, R. T., Workman, J. L. & Cote, J. The diverse functions of histone acetyltransferase complexes. *Trends Genet* **19**, 321-329 (2003).
130. Jedlicka, P., Mortin, M. A. & Wu, C. Multiple functions of Drosophila heat shock transcription factor in vivo. *EMBO J* **16**, 2452-2462 (1997).
131. Hahn, G. M., Shiu, E. C. & Auger, E. A. Mammalian stress proteins HSP70 and HSP28 coinduced by nicotine and either ethanol or heat. *Mol Cell Biol* **11**, 6034-6040 (1991).
132. Scholz, H., Franz, M. & Heberlein, U. The hangover gene defines a stress pathway required for ethanol tolerance development. *Nature* **436**, 845-847 (2005).